USING MATHEMATICAL MODELS TO UNDERSTAND THE IMPACT OF CLIMATE CHANGE ON TICK-BORNE INFECTIONS ACROSS SCOTLAND

ADRIAN J. WORTON

Doctor of Philosophy

Department of Computing Science and Mathematics

University of Stirling

September 2016

DECLARATION

I, Adrian J. Worton, hereby declare that this work has not been submitted for any other degree at this University or any other institution and that, except where reference is made to the work of other authors, the material presented is original.

September 2016

ABSTRACT

Ticks are of global interest as the pathogens they spread can cause diseases that are of importance to both human health and economies. In Scotland, the most populous tick species is the sheep tick *Ixodes ricinus*, which is the vector of pathogens causing diseases such as Lyme borreliosis and Louping-ill. Recently, both the density and spread of *I. ricinus* ticks have grown across much of Europe, including Scotland, increasing disease risk. Due to the nature of the tick lifecycle they are particularly dependent on environmental factors, including temperature and habitat type. Because of this, the recent increase in tick-borne disease risk is believed to be linked to climate change. Many mathematical models have been used to explore the interactions between ticks and factors within their environments; this thesis begins by presenting a thorough review of previous modelling of tick and tick-borne pathogen dynamics, identifying current knowledge gaps. The main body of this thesis introduces an original mathematical modelling framework with the aim to further our understanding of the impact of climate change on tick-borne disease risk. This modelling framework takes into account how key environmental factors influence the *I. ricinus* lifecycle, and is used to create predictions of how *I. ricinus* density and disease risk will change across Scotland under future climate warming scenarios. These predictions are mapped using Geographical Information System software to give a clear spatial representation of the model predictions. It was found that as temperatures increase, so to do *I. ricinus* densities, as well as Louping-ill and Lyme borreliosis risk. These

results give a strong indication of the disease risk implications of any changes to the Scottish environment, and so have the potential to inform policy-making. Additionally, the models identify areas of possible future research.

ACKNOWLEDGEMENTS

Firstly, I must thank Rachel and Lucy for their supervision. You've been great to work with, and I am very grateful for your time and insights. In particular, I am indebted to you for helping me get this thesis finished on time.

I am also grateful to the University of Stirling and the James Hutton Institute for providing the funding for this project. In particular, I would like to thank the staff of the Department of Computing Science and Mathematics at Stirling for the excellent services and support they have provided.

It would have been impossible to have undertaken a project such as this without being able to share the experience with people in the same boat. Therefore, I'd like to thank all the fellow PhD students I have befriended during the last four years. I'd particularly like to thank Brian, Paul and Iona (I know how competitive you can be, so please note that I purely listed you based on surname alphabetical order) for all the laughs. Hopefully I can share my experiences to help you when you are submitting your theses. I'd like to give an additional thanks to Paul for being an incredible office-mate. I have no idea where I'd be without your endless help.

I'd like to thank all my friends and family for their support during this project. In particular, it would be impossible to ask for more supportive parents, I hope you realise how much I have needed you during the last four years.

Finally, my largest thanks goes to Fiona. I cannot imagine how I'd have tackled the home leg of my thesis without you. Quack.

TABLE OF CONTENTS

LIST OF FIGURES

LIST OF TABLES

1

INTRODUCTION

Mathematical models have long been used to help understand systems that occur in the real world, in fields such as computer science and psychology, and for topics such as economic forecasting and fluid dynamics. Modelling techniques can allow existing empirical data to be used to create predictions for scenarios which it is not possible to observe, such as cases where ethical regulations prevent experimentation, or for predictions of the future. Modelling can also be a faster alternative to empirical studies in urgent situations.

Mathematical biology is a field that has grown over recent years as improving modelling techniques have allowed for a broader range of biological systems to be investigated more realistically. This field often requires mathematicians and biologists to collaborate in order to develop models that are based on both sound mathematical principles and accurate biological information. However, there must always be a compromise; no biological system is so simple that a mathematical model can hope to represent every mechanism that influences it. Therefore, whilst mathematical models can be informative, caution must always be taken with any model predictions as they will always have inbuilt assumptions.

A large field within mathematical biology is disease modelling, where mathematical models are used to gain insights into the dynamics of infection. Through such modelling it can be possible to identify mechanisms within the system that are important for controlling infectious disease spread. Increasingly used in conjunction with disease modelling, Geographical Information Systems (GIS) are systems which record and display a wide range of geographical data in map form. These can be extremely useful in disease modelling as they allow the environmental factors that may influence the spread of an infection to be used to predict which regions are likely to have the highest disease risk.

This thesis focuses on tick-borne diseases, which are of significant economic and public health interest worldwide. As ticks feed on almost any terrestrial vertebrate of a sufficient size, they can transmit a wide variety of pathogens, many of which cause serious disease. Therefore, ticks are one of the most important vectors of disease-causing pathogens in Europe (Gilbert, 2013). Ticks are particularly dependent on their environments (James et al., 2013), and therefore it is important to understand the effect climate change will have on the geographical range and dynamics of ticks and the pathogens they spread. Whilst many studies have mathematically modelled tick and tick-borne disease dynamics, few have used environmental data to make predictions of the effect climate change will have. Therefore, this thesis develops a modelling framework which combines a dynamic mathematical model of ticks and the pathogens they spread with environmental data and GIS mapping software in order to create predictive maps of future tick-borne disease risk across Scotland. Such an approach is novel and will bring new perspective to our understanding of how disease risk may be influenced by climate change.

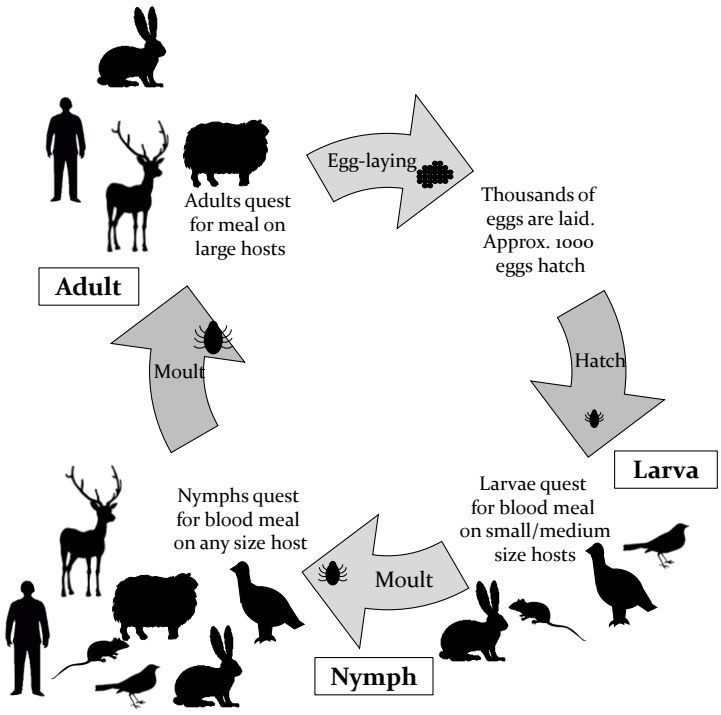

Figure 1.1: Lifecycle schematic for the sheep tick *Ixodes ricinus*. Silhouettes indicate possible hosts, but not all.

This chapter presents an overview of the biological background used to inform the modelling work undertaken within this thesis, as well as explaining the significance of ticks and the pathogens they spread. Additionally, the aims of the thesis are given to provide a guide to the motivation of this work. However, specific biological details of the pathogens modelled in this thesis will be given at the start of the relevant chapters.

1.1 BIOLOGICAL BACKGROUND AND SIGNIFICANCE

1.1.1 *Tick lifecycle*

Ticks are arachnids that are widely distributed across the world, particularly in warm, humid climates. Across the northern hemisphere, the two families of

ticks found are soft-bodied ticks (*Argasidae*) and hard-bodied ticks (*Ixodidae*), with hundreds of species of each known (Randolph, 2004). The work within this thesis will focus on the sheep tick (*Ixodes ricinus* L.), which is the species most commonly found in Scotland and is the main vector for multiple significant pathogens (explored in section 1.1.2).

The lifecycle of *Ixodid* ticks is split into three active stages, or instars: larva, nymph and adult. At each stage a tick must find a suitable host to draw a blood meal from. Generally, adult ticks require a large mammalian host such as sheep or deer, whilst other stages will feed on any host, including small mammals and birds (Gray, 1998; Gilbert, 2016a). After feeding, ticks will drop off the host and bury themselves in the ground vegetation layers, where larvae and nymphs moult into the next instar and adult ticks reproduce, with females laying a clutch of thousands of eggs, before dying. Although ticks in cool climates such as Scotland are thought to usually feed once per year, in warmer climates or warmer years some ticks are able to moult into the next instar within the same year and therefore feed twice in the same season (Randolph et al., 2002). An overview of the tick lifecycle is shown in figure 1.1.

In order to find a blood meal ticks climb to the top of blades of grass or similar plants and hold their front two legs out in anticipation of latching onto a potential host. This behaviour is known as questing. Once a tick has found a suitable host it will find an appropriate area of the animal to feed, favouring areas where it is harder to be removed by the host (for example around the ears or neck), where it will stay for approximately a week. *Ixodid* ticks are unable to walk far horizontally; therefore the spatial movement and distribution of ticks is primarily driven by the movement of their hosts.

As ticks are cold-blooded they require sufficient warmth in order to provide the energy for them to quest. Therefore, in cool climates such as Scotland the time of year when ticks are most active is between spring and autumn.

An environment-dependent model of tick dynamics is developed in chapter 3 to predict the impact climate change has on tick density across Scotland.

1.1.2 *Tick-borne diseases*

Ticks are the primary vector of a wide range of pathogens that cause infectious diseases throughout the world, with a heavy impact on human, livestock and wildlife health. Within Britain ticks are known to spread pathogens which cause zoonotic diseases such as Bartonellosis, Ehrlichiosis and Anaplasmosis, which can all cause serious health problems for both humans and animals (BADA UK, 2016). However, this thesis will focus on two tick-borne diseases: Louping-ill and Lyme borreliosis.

Louping-ill is a disease caused by a flavivirus which primarily affects sheep (*Ovis aries*) and red grouse (*Lagopus lagopus scoticus*), and there have been cases of serious illness in humans (Davidson et al., 1991). The name derives from the old Scottish word 'loup', which describes the leaping motion of infected sheep; more importantly, the disease can kill infected livestock, and is therefore of great importance in rural communities. Whilst a treatment vaccine for sheep has been developed, no such protection exists for grouse. As grouse are highly susceptible to the disease, with 78% mortality observed in laboratory trials (Reid, 1975), the modelling work on Louping-ill in this thesis will focus on the threat to grouse caused by the disease. Louping-ill is caused by the pathogen Louping-ill virus (LIV), which is transmitted to grouse from *I. ricinus* ticks. However, as grouse generally do not feed adult ticks, a system which allows ticks and therefore LIV

to persist will require mammalian hosts to be present, such as red deer (*Cervus elaphus*) or mountain hares (*Lepus timidus*) (Hudson, 1992) that are essential hosts for adult female *I. ricinus* ticks. There has been plenty of previous modelling of LIV systems (reviewed in chapter 2), with good parameterisation. This makes it an ideal system to use when developing a new modelling system, as done in chapter 4.

Lyme borreliosis (commonly known as Lyme disease) is named after the town Old Lyme in Connecticut, where there was a spate of cases in the 1970s (Gray, 1998). In the UK and throughout Europe it is the most common tick-borne disease in humans. Within Scotland there has been an almost 10-fold increase in Lyme borreliosis cases from 2000-2010 (Health Protection Scotland, 2016). Infection with Lyme borreliosis can cause complications of the brain, skin and joints (Tilly et al., 2008). Lyme disease is caused by the complex of spirochete bacteria *Borrelia burgdorferi* sensu lato, which, like LIV, is most commonly transmitted by *I. ricinus* ticks. *B. burgdorferi* s.l. tends to be most prevalent in wooded areas, as it is maintained by small mammals and birds, which are competent transmission hosts (Gray, 1998). Due to the increasing risk Lyme borreliosis poses to public health, this is a very relevant policy issue at the moment. Therefore, Lyme borreliosis is used as a case study in chapter 5, as predicting the impact of climate change on disease risk is likely to be one of the most practical uses of the modelling framework developed in this thesis.

1.1.3 *The influence of climate change*

Climate change is recognised as one of, if not the single, greatest threats to human life in the world today. Global temperatures have risen consistently since the 1960s, with 2015 the warmest full year recorded to date (NASA/GISS, 2016). This rise

has been linked to large-scale changes, such as rising sea levels and habitat loss for many species. Such rising temperatures have also led to an increase in extreme weather events (Hansen et al., 2012), which further destabilise communities and habitats. The Intergovernmental Panel on Climate Change predict that "the net damage costs of climate change are likely to be significant and to increase over time" (IPCC, 2007).

Like all free-living terrestrial arthropods, ticks are strongly affected by their environment. Firstly, ticks need the appropriate vegetation to provide cover when moulting (James et al., 2013). Secondly, like all arthropods, their activity is affected by temperature, such that they require sufficient warmth to provide the energy to quest for meals (Gilbert et al., 2014). Thirdly, the humidity of a tick's environment has to be high enough to prevent desiccation (James et al., 2013). Finally, ticks require enough hosts present to provide blood meals for all three stages of the tick lifecycle (Randolph, 2004). As tick survival and activity are influenced by climate, it is likely that so too are the pathogens they carry. Therefore, in order to predict future tick-borne disease risk, we have to understand how climate change will affect ticks and tick-borne pathogen prevalence. In this thesis therefore a novel combined modelling approach is developed whereby mathematical models utilising coupled differential equations are combined with GIS mapping tools to predict the impact of climate change on (a) tick population dynamics (chapter 3), (b) LIV risk (chapter 4) and (c) *B. burgdorferi* s.l. risk (chapter 5).

1.2 AIMS AND LAYOUT OF THE THESIS

This thesis aims to predict the effect climate change has on tick-borne disease risk across Scotland, specifically that of Louping-ill and Lyme borreliosis. To achieve this, an entirely original modelling approach is developed, dependent

on environmental factors, in order to study the predicted changes in disease risk under a variety of climate warming scenarios. The model predictions are coupled with GIS data for Scotland in order to create risk maps for each of these future scenarios. The model is then extended into a modelling framework to allow it to be adapted for further tick-borne pathogen systems. Combining dynamic tick-borne disease modelling with GIS mapping is a novel approach and one which can be very useful in giving a spatial representation for the model predictions.

Chapter 2 of this thesis reviews previous mathematical modelling in the field of tick and tick-borne pathogen dynamics. This is important to provide the background for the modelling work undertaken in this thesis, as well as to highlight the knowledge gaps that this thesis aims to fill. The majority of the previous mathematical modelling of ticks and tick-borne pathogens is covered by the paper Norman et al. (2015), of which the author of this thesis is a co-author. The importance of Norman et al. (2015) in relation to this thesis is considered, highlighting the studies which are particularly influential in the modelling work undertaken. In addition, models not covered by Norman et al. (2015) which influence this thesis are reviewed.

Chapter 3 presents an original model for the *I. ricinus* lifecycle. This model is dependent on environmental factors (namely temperature, host density and habitat), and the model is used to make predictions of tick densities across Scotland under various climate warming scenarios. GIS mapping software is used to give a visual representation of the model predictions. Creating this model is important for providing the foundation upon which the later pathogen models can be built.

Chapter 4 expands the tick lifecycle model to include pathogen and transmission host dynamics for LIV. This is used to make predictions of LIV risk for a variety of climate warming scenarios. The influence of habitat and host density on the model is also considered. The model created in this chapter is important in demonstrating that the novel methods developed in the previous chapter can be used to predict disease risk. GIS mapping software is used to create predictive disease risk maps across Scotland in order to spatially visualise the model predictions, in a novel combination of LIV modelling with GIS tools.

Chapter 5 investigates how the LIV model can be adapted into a modelling framework for other tick-borne pathogen systems. To achieve this, the LIV model is generalised to create basic models. These are then augmented by identifying the appropriate modelling required in order to include further mechanisms which can be added to the basic models. To demonstrate that the framework can be applied to a new pathogen system, a model is created to represent *B. burgdorferi* s.l. dynamics, which uses available parameter data to create predictions of how climate warming will influence disease risk.

Chapter 6 discusses the predictions from the models in the thesis, how they relate to the aims, and their global context. The limitations of the modelling framework created are discussed, along with what future work can be undertook to address these.

Appendix A presents the methodology behind the application of the models within this thesis. Particularly, the focus is on how the models utilise GIS data, and how climate warming predictions were applied across Scotland.

Appendix B provides the full code used to run the models within this thesis.

2

PREVIOUS MODELLING

Over the last couple of decades the number of studies modelling tick and tick-borne pathogen systems has been steadily increasing. However, no comprehensive review of such modelling work has been undertaken in recent years. Such an analysis is timely as it allows for the current state of tick-borne pathogen modelling to be assessed. Therefore, this chapter presents a review of previous mathematical models of tick and tick-borne pathogen systems. Reviewing these studies is important in understanding the techniques developed so far, as well as highlighting knowledge gaps. Additionally, this chapter aims to highlight those studies which have an influence over the modelling methods used within this thesis.

Much of this is covered in the paper by Norman et al. (2015), of which the author of this thesis is a co-author. Therefore, that paper is presented in section 2.1, with section 2.2 highlighting the parts of it which are of particular relevance to this thesis. Section 2.3 reviews models which are not covered by Norman et al. (2015).

2.1 PAST AND FUTURE PERSPECTIVES ON MATHEMATICAL MODELS OF TICK-BORNE PATHOGENS (NORMAN ET AL. 2015)

Norman, R.A., Worton, A.J., Gilbert, L. (2015). Past and future perspectives on mathematical models of tick-borne pathogens. Parasitology pp 1-10.

2.1.1 *Summary*

Ticks are vectors of pathogens which are important both with respect to human health and economically. They have a complex life cycle requiring several blood meals throughout their life. These blood meals take place on different individual hosts and potentially on different host species. Their life cycle is also dependent on environmental conditions such as the temperature and habitat type. Mathematical models have been used for more than 30 years to help us understand how tick dynamics are dependent on these environmental factors and host availability. In this paper, we review models of tick dynamics and summarise the main results. This summary is split into two parts, one which looks at tick dynamics and one which looks at tick-borne pathogens. In general, the models of tick dynamics are used to determine when the peak in tick densities is likely to occur in the year and how that changes with environmental conditions. The models of tick-borne pathogens focus more on the conditions under which the pathogen can persist and how host population densities might be manipulated to control these pathogens. In the final section of the paper, we identify gaps in the current knowledge and future modelling approaches. These include spatial models linked to environmental information and Geographic Information System (GIS) maps, and development of new modelling techniques which model tick densities per host more explicitly.

2.1.2 *Introduction*

Ticks are the most important vectors of zoonotic disease-causing pathogens in Europe (Gilbert, 2013), transmitting the tick-borne encephalitis (TBE) complex of viruses, *Anaplasma phagocytophyllum*, *Babesia* and *Rickettsia* species and *Borrelia burgdorferi* sensu lato, the complex of bacteria that cause Lyme borreliosis, amongst others (BADA UK, 2016). *Ixodes ricinus* L. ticks are particularly implicated in pathogen transmission because they are almost ubiquitous across Europe and are generalist feeders, which allows for pathogen transmission among different host species. *Ixodes ricinus* are increasing in number and range in many parts of Northern Europe (reviewed by Medlock et al. 2013).

In any given geographical region tick population dynamics are dependent on a number of biotic and abiotic factors including the density of different host species, and other factors that influence survival and activity such as temperature and humidity and vegetation types, the latter of which provide habitats for different hosts and create different microclimates (James et al., 2013).

Mathematical models have been used extensively to predict the dynamics of tick populations under different conditions including climate change. However, high tick densities do not necessarily mean high prevalence or risk of tick-borne pathogens, since this is dependent not only ticks but also competent transmission hosts. Therefore, models have also been used to predict the tick-borne pathogen dynamics and the theoretical effectiveness of different tick-borne pathogen control methods under different environmental or management scenarios. In this paper, we will review the use of those models for different systems, summarise the key results in different contexts and discuss possible future directions of mathematical modelling of tick-borne pathogens.

2.1.3 *Mathematical models of tick population dynamics*

Although there are a number of different tick species globally this review will focus on *I. ricinus* and we will specify when we cite any papers which refer to other species.

The *I. ricinus* life cycle develops from the egg, through two immature stages (larvae and nymph) to the adult stage. Each immature stage requires a blood meal from a suitable vertebrate host before developing to the next stage and the adult female requires a blood meal before producing eggs. Adult females feed primarily on large mammals such as deer, sheep or hares whilst the immature stages can also feed on smaller vertebrates such as mice, voles and birds (e.g. Gray 1998). The *I. ricinus* life cycle usually takes 3–4 years to complete (Randolph, 2004).

In winter ticks often enter behavioural diapause induced by cold and/or short day length (Randolph et al. 2002; but see Gray 1987). Therefore, tick activity is highly seasonal with ticks in Northern Europe being active mainly between spring and autumn when temperatures are warm enough (Lindgren et al., 2000). Activity is inhibited by cold temperatures but increases with temperature up to a limit (12–20 °C depending on population e.g. Gilbert et al. 2014; Tomkins et al. 2014). Tick host-seeking (questing) activity can also be inhibited by low relative humidity or high saturation deficits (this is a function of relative humidity and temperature and gives an estimate of the drying power of the air; Perret et al. 2000). After feeding, ticks also become inactive due to physiological diapause while they develop into the next stage (Randolph et al., 2002).

One of the first mathematical models developed to describe tick population dynamics was published in 1981 (Gardiner et al., 1981). This study used empirical data from experiments to predict how tick development times depend on temper-

ature. They did not put this into a formal predictive modelling framework but they did try to determine functional relationships between development time and different measures of temperature (i.e. air and soil temperature). In particular, they looked at how experimentally predicted development times estimated in the laboratory translated to the field where temperature fluctuations are much less predictable. They found that soil temperatures recorded at a depth of 50mm are useful predictors for larval and nymphal development phases. In terms of egg development time they found that air temperatures are useful for predicting the development time of eggs laid in the spring but soil temperature is a better predictor for those laid in autumn. They suggested that this might be because during diapause eggs may be conditioned to develop according to the temperature of their environment rather than air temperature.

Mount and Haile (1989) developed a computer simulation model of the American dog tick *Dermacentor variabilis* (Say). This model simulated the effects of environmental variables such as ambient temperature, habitat and host density on American dog tick population dynamics. They validated the model by comparing its predictions with empirical data from Virginia, Maryland and Massachusetts. The authors concluded that the model produced acceptable values for equilibrium population densities and seasonal activity patterns and went on to extend this model to include Rocky Mountain spotted fever dynamics (Cooksey et al., 1990).

Over the last 40 years Sarah Randolph and collaborators have written a large number of papers on tick biology and population dynamics. These are largely empirical; however, there are also some which model tick population dynamics. The first of these came in 1997 (Randolph and Rogers, 1997) where they presented a simulation model of the African tick *Rhipicephalus appendiculatus*. This simulation model incorporated temperature-dependent rates of egg production and develop-

ment, climate-driven density-independent mortality rates and density-dependent regulation of both nymphs and adults. The model successfully described both the seasonality and annual range of variation in numbers of each tick stage observed at each of four test sites in Uganda, Burundi and South Africa.

In 2002, Randolph et al. (2002) used empirical data on tick counts, various microclimatic factors and fat contents of ticks to create a population model explaining seasonality of *I. ricinus* in the UK. This study showed large variation in questing activity between years, but the date of questing (i.e. host-seeking activity) in 1 year was used to predict the start of questing for the next stage the following year, with reasonable accuracy. This was an important paper that also found evidence of two cohorts of ticks within a life stage within a season. Those nymphs with higher relative fat contents had emerged and become active more recently than those with lower fat contents. The suggestion was that spring-questing nymphs had overwintered, having fed as larvae the previous late summer or autumn; meanwhile autumn-questing nymphs had fed as larvae in the spring of the same calendar year.

More recently, Dobson et al. (2011) used a stage-classified Leslie matrix model to break the tick life cycle into the key parts, with a particular focus on two types of diapause: developmental and behavioural, with the latter being important in determining how many times a year an individual tick might feed. This model was then used by Dobson and Randolph (2011) to make long-term predictions of the effects of host densities, climate and acaricide treatment of hosts on tick populations.

In 2005, Ogden et al. (2005) developed a model of *Ixodes scapularis* Say (1821) in which tick development rates were modelled as temperature-dependent time delays. Time spent in egg and engorged tick states and questing activities were

all temperature dependent. The parameters were estimated using data taken from Ogden et al. (2004). The model was validated using data from Ontario and Maryland and in both cases the observed seasonal activity patterns were predicted by the model. The models were then used to predict theoretical geographical limits for the establishment of *I. scapularis* in Canada. The model predicted that the temperature conditions which are suitable for the tick are wider than the existing distribution, implying that there is potential for spread.

An age-structured stochastic model was used to describe the dynamics of tick populations by Hancock et al. (2011). They focused on the effect of temperature on the development between each stage of the tick life cycle, i.e. from egg to larva, larva to nymph, nymph to adult and adult laying eggs. This model also introduced pathogen dynamics into the model. This allowed the model to predict that, if a pathogen is introduced into the system, it is most likely to persist if it is introduced at a time of year of peak tick questing.

A completely different approach was adopted by Schwarz et al. (2009) who used statistical methods to identify the relationship between vegetation and tick distribution. *I. ricinus* tick count data were correlated with plant communities, and the resulting relationship was used to predict *I. ricinus* distribution across the German nature reserve Siebengebirge, using GIS. A similar process was undertaken by Braga (2012) to identify the associations between habitat, host densities, temperature and other climatic factors on observed tick abundance at sites across Scotland. The resulting output was used to predict tick abundance over all of Scotland according to GIS-based environmental data, and visualised as a series of raster maps showing predicted tick abundance. The key parameters in this basic algorithm were then altered in accordance with environmental change

projections (climate change and woodland expansion), to produce predictions of future tick abundance over Scotland due to environmental change scenarios.

Jore et al. (2011) also used a statistical method to investigate *I. ricinus* tick dynamics. A principle component analysis provided a model which explained 67% of the variation in past *I. ricinus* densities in Norway. The study suggests that *I. ricinus* have expanded northwards since 1983.

Summary

For almost 35 years mathematical models of tick dynamics have been developed. The models have largely focused on the impact of environmental factors on these dynamics. Field observations show that tick life stages emerge at different points in the season and peak at different times in different geographical regions. In some areas, we can have bimodal tick dynamics within a year (e.g. Tagliapietra et al. 2011) and in other areas there is only one peak. The models described above have been able to replicate the observed tick dynamics for particular geographical areas, tick species and environmental conditions. However, it is clear that in order to be able to predict tick dynamics we would need to have key pieces of information about the environment (and particularly the temperature) in which they live.

Lorenz et al. (2014) explicitly looked at the extrapolation of landscape model results based on one area or time to other spatial or temporal systems for Lyme disease and *I. scapularis* and concluded that models based on measures of vegetation, habitat patch characteristics and herbaceous land-cover emerged as effective predictors of observed disease and vector distribution. These would

therefore be important characteristics of an area to measure in order to predict these distributions.

2.1.4 *Mathematical models of tick-borne pathogen dynamics*

Modelling of tick-borne pathogens has focussed on a small number of pathogens which are important for human or animal health and welfare. The three main systems which have been modelled extensively are Louping ill virus (LIV), western tick-borne encephalitis virus (TBEV) and *B. burgdorferi* sensu lato, the causative agent of Lyme disease. This section will focus largely on LIV since this pathogen has the largest body of modelling work and it is the area of expertise of the authors. It also illustrates many of the biological features which need to be incorporated into models and so is a good case study for models of other system.

In general, transmission of these pathogens can occur in three ways (although also see Park et al. 2001 discussed below for LIV). The most common form of transmission occurs when susceptible ticks feed on infected hosts who have virus in their bloodstream (viraemic hosts) and pick up the virus. These ticks then moult into their next developmental stage and when they take their next blood meal then they can pass the pathogen onto a susceptible host, this will be a different individual and can also be a different host species (Labuda and Nuttall, 2004). The second method is vertical transmission; for some pathogens infection is passed from adult ticks to eggs and onto larvae (Labuda and Nuttall, 2004). Finally, for some hosts and some pathogens there can be non-viraemic or co-feeding transmission in which susceptible ticks feeding near to infectious ticks can pick up infection without the host having a viraemic response (Jones et al., 1987).

2.1.4.1 *Louping-ill virus*

A large number of increasingly complex models have been used to help us understand LIV, which is the western-most variant of Western TBEV. LIV is transmitted by *I. ricinus* and causes disease in livestock, especially sheep *Ovus aries*, as well as red grouse, *Lagopus lagopus scoticus*, a valuable game bird. A vaccine has been developed for livestock but not for red grouse that are highly susceptible to the disease, with 78% mortality rates in experimentally infected birds in the laboratory (Reid, 1975). The hosts and transmission cycle of this complex virus system has been recently reviewed (Gilbert, 2016b), but mathematical models can be extremely useful in helping to identify gaps in our biological knowledge of the system, identifying the relative importance of different host species hosts, and predicting the effectiveness of potential control strategies.

The first mathematical model of LIV was presented by Hudson et al. (1995), where a series of coupled ordinary differential equations describing LIV on red grouse moorland was presented. This model explored the interactions between ticks and red grouse and their role in the dynamics of LIV. The model predicted that grouse alone cannot support a tick population since very few adult ticks feed on grouse, therefore other hosts are required to complete the tick life cycle. Within this model the alternative hosts were mountain hares *Lepus timidus*, although similar later studies examined the role of red deer *Cervus elaphus* (Gilbert et al., 2001; Norman et al., 2004) and sheep (Porter et al., 2011). Hudson et al. (1995) also calculated a formula for the conditions for persistence of both ticks and LIV. For tick persistence a sufficient number of hosts (or combination of host types) which can feed all stages of ticks are required, while LIV persistence also requires a competent LIV transmission host (red grouse in this model) to make up a sufficient proportion of the total tick hosts. This means that, in order

for the pathogen to persist one needs enough tick hosts to maintain the tick population, with a sufficient number of these being pathogen-transmitting hosts. This threshold formula comes from the basic reproductive rate or number, R_0, which is a concept used widely in epidemic models. When $R_0 > 1$ then the pathogen persists and when $R_0 < 1$ the pathogen dies out.

Some more complex later LIV models have also predicted an eventual 'dilution effect' where pathogen prevalence declines if there are too many non-pathogen-transmitting tick hosts (hosts which do not transmit the pathogen such as deer) compared with competent transmission hosts which causes potential pathogen-transmitting bites to be 'wasted' and the effect of the pathogen to be diluted (Norman et al., 1999; Gilbert et al., 2001).

Sheep are known to produce a LIV viraemia after infection, and are known to be competent transmission hosts. However, the role of lambs is less well understood; if ewes have been bitten by infected ticks, their young lambs acquire immunity from the virus from drinking the colostrum from their mothers in the first few days or weeks of life. However, as the lambs age this immunity wanes, leaving them at risk of contracting LIV. Thus, lambs could potentially have a role as a reservoir host. Therefore, another differential equation model was created to understand the role that lambs may play as a reservoir of LIV. The model predicted that, whilst in theory large numbers of lambs could act as a reservoir for the virus, it is more likely that, in most situations, these numbers are probably small (Laurenson et al., 2000).

Laurenson et al. (2003) examined the impact of near-eradication of mountain hares on tick burdens and LIV seroprevalence in red grouse, using both empirical data and differential equation models. The models compared the scenario where mountain hares simply act as tick amplifying hosts to a scenario where hares were

both tick hosts and non-viraemic transmission hosts. It was found that the model which included non-viraemic transmission produced predictions that fitted the data better than the simpler model did. Laboratory experiments had already identified mountain hares as competent transmission hosts (through supporting non-viraemic transmission between co-feeding ticks) in the laboratory (Nuttall and Jones, 1991; Jones et al., 1997). In addition, models have shown that non-viraemic transmission via co-feeding may allow the virus to persist more readily than it would otherwise have done, and allow the virus to persist even in the absence of viraemic hosts if the level of non-viraemic transmission is high enough (Norman et al., 2004). However, the Laurenson et al. (2003) study was important in demonstrating that mountain hares can be LIV reservoir hosts in the field. There were large management repercussions to this research, as many grouse moor managers over Scotland began large-scale culls of mountain hares, leading to political issues (reviewed by Harrison et al. 2010; Gilbert 2016b). Models again had political impact by providing evidence against culling mountain hares: while the Laurenson et al. (2003) system included only red grouse and mountain hares, most areas in Scotland managed for grouse hunting also have deer. Therefore, Gilbert et al. (2001) modelled a three-host system, including deer as well as red grouse and mountain hares. Importantly, this three-host model predicted that LIV would always persist in the presence of even low densities of deer, even if all mountain hares were culled. This was because red grouse are transmission hosts for the virus while deer, although not competent transmission hosts, are important hosts for all stages of tick, so together both virus and tick life cycles can be maintained. This Gilbert et al. (2001) model has been crucial in the arguments against large-scale mountain hare culls (Harrison et al., 2010; Gilbert, 2016b).

Mathematical models have also been used in helping identify which pathogen control methods could be theoretically most effective in LIV control. Porter et al. (2011) developed models to predict the effectiveness of using acaricide-treated sheep as a tool to control ticks and LIV in red grouse. The model predicted that the presence of deer limits the effectiveness of such a strategy, but for certain conditions the use of acaricide on sheep could theoretically be a viable method for controlling ticks and LIV providing that high numbers of sheep are treated and acaricide efficacy remains high, while deer densities must be very low (Porter et al., 2011). Due to this predicted adverse impact of deer on the success of treating sheep to control ticks and LIV, and because deer are known to maintain high tick population densities in Scotland and move ticks between habitats (Ruiz-Fons and Gilbert, 2010; Jones et al., 2011; Gilbert et al., 2012), models were then developed to test the theoretical effectiveness of acaricide-treated deer on controlling ticks and LIV (Porter et al., 2013a). The model predicted that treating deer could control ticks and LIV if high acaricide efficacies were maintained and if a large proportion of the deer population was treated. Furthermore, effectiveness was improved if there were only low densities of deer. However, although the model predicted that this control method is theoretically plausible, it is unlikely that the conditions could be met in practical terms, in wild deer. Therefore, using an age-structured differential equation model, including splitting the grouse life cycle to represent the different behaviour between chicks and adults, Porter et al. (2013b) investigated whether acaricide treatment of the grouse themselves could help reduce ticks in the environment and LIV in the grouse population. Again, this was theoretically possible, but in the presence of deer, high acaricide efficacies were required and high proportions of the grouse population treated, were needed for successful control. This is due to the deer amplifying the tick

population. These types of models can therefore be of use in decision-making by land managers for choosing disease control options, such as whether to try a certain control method or not depending on the situation in a specific area, taking into account any practical difficulties.

It is generally assumed that LIV is transmitted through ticks biting their hosts, and model parameterisation generally reflects this assumption. However, red grouse chicks frequently eat invertebrates, including ticks (Park et al., 2001). This is a potentially important route of transmission: it has been suggested that 73–98% of LIV infection in red grouse in their first year could stem from ingestion (Gilbert et al., 2004). Introducing this infection route to LIV modelling has an interesting effect: when using the standard method for calculating the basic reproduction number for the persistence of LIV, then the algebraic results and numerical simulations do not match. The standard method of analysis causes virus persistence to be underestimated, as the ingestion of infected ticks causes a feedback loop where the virus can persist with seemingly insufficient hosts (Porter et al., 2011). This phenomenon requires further investigation, as it may indicate interesting gaps in our knowledge of the biology of the LIV system as well as an anomaly in the current modelling approach.

In the LIV models described above, there has been no explicit spatial component to the models. However, Watts et al. (2009) investigated the interaction between neighbouring areas by expanding the previously existing LIV models into a two-patch system with host movement between patches. Comparison with empirical data showed that whilst the one-patch model was a reasonable indicator for tick numbers, it tended to underestimate the prevalence of the LIV. When considering the two-patch model, the results depended largely on finding the appropriate balance of deer movement between the two sites (Watts et al., 2009). Jones et al.

(2011) developed a different type of differential equation model, which explicitly tracked the number of ticks on each host, to predict how deer moving ticks from forest onto moorland might affect ticks and LIV in red grouse on the moorland. The assumption was that ticks are more abundant in forest than on moorland, which is supported by empirical data (Ruiz-Fons and Gilbert, 2010). This model predicted the highest levels of LIV in moorland to occur where it is bordering forest regions, due to higher tick numbers there. Furthermore, this model was important in examining for the first time the impact of landscape heterogeneity on predicted pathogen levels: virus prevalence was predicted to be higher in landscapes that have larger forest patches, and higher landscape fragmentation, which increases the number of borders between the two habitats (Jones et al., 2011).

Summary

The transmission, persistence and dynamics of LIV are complex with many interacting factors to take into account. The focus of the modelling work described above has been on trying to understand the roles that different hosts play in maintaining these dynamics. Hosts can play three possible roles, they can either simply act as tick amplifiers (e.g. deer) or they can both amplify ticks and transmit virus (e.g. sheep for viraemic transmission or hares for non-viraemic transmission) or finally they can transmit the disease but not support the ticks (e.g. grouse). The ability to control the virus in any particular geographical area is highly dependent on the host community structure. In addition there are practical issues involved in trying to control the virus in this system which is made up of mostly wild

hosts. There are both physical difficulties in delivering treatment and legislative difficulties in which treatments are permitted.

2.1.4.2 *Other tick-borne pathogens*

Tick-borne encephalitis

TBE is a neurological disease which is of significant public health interest across mainland Europe (Labuda et al., 1993). It is caused by the TBEV, which is primarily transmitted by *I. ricinus* ticks, where rodents act as the competent host for the virus.

There are two significant ways in which deer can influence TBEV dynamics. Firstly, as deer are the main host which *I. ricinus* adults feed on, their presence, as with LIV, has an amplification effect on tick abundance. Secondly, as deer do not support TBEV transmission, very high deer densities can eventually lead to the dilution effect lowering TBEV levels (again similar to model predictions of LIV).

In both 2003 and 2007, Rosa and co-authors extended the models of Norman et al. (1999) to explicitly include the questing and feeding tick stages and the aggregation of ticks on the hosts (Rosà et al., 2003; Rosà and Pugliese, 2007). They investigated changes in host densities and different infection pathways to determine when the dilution effect might occur. They found the new result that the dilution effect might occur at high densities of disease competent hosts. The authors state that better information on tick demography would be needed before it would be possible to predict whether this effect would happen in the field. However, there is some evidence that this is the case in the TBE system (Perkins, 2003).

In 2012, the same Italian group published a pair of papers taking both an empirical and theoretical approach to understanding the effect of deer density on

tick distributions on rodents and therefore on the risk of TBE in a region; Cagnacci et al. (2012) empirically found a hump-shaped relationship between deer density and ticks feeding on rodents, and a negative relationship between deer density and TBE occurrence. Twinned with this, a model was developed by Bolzoni et al. (2012) to explain these findings. They found hump-shaped relationships between deer density and both the number of ticks feeding on rodents and TBEV prevalence in ticks. For low deer densities this can be explained by the tick amplification effect, for high deer densities the virus dilution mechanism dominates the dynamics. The role of climate change on tick-borne pathogen prevalence was scrutinised by Randolph (2008). In this study, TBEV was used as a case example. A statistical model was used to show that climate change is not enough to explain historical changes in TBE incidence within Europe. An alternative model was presented, showing how the introduction of further factors allowed for a better model fit of the data. Crucially, such a model included socioeconomic factors such as unemployment, agricultural practices and income. Zeman et al. (2010) used GIS analysis to similarly find that heterogeneity in TBE trends cannot be fully explained by geographic and climatic factors. However, they also found that the inclusion of socioeconomic conditions could not satisfactorily explain the anomalies.

Summary

As with Louping ill the persistence and dynamics of TBE are dependent on host densities and deer play a crucial role in this. Some of the papers described above, particularly in the 2003 and 2007 papers, Rosà et al. (2003); Rosà and Pugliese (2007) present general results which could apply to a number of different tick-

borne pathogens and, in particular the results that dilution effects are very dependent on tick demography and density-dependent constraints are true more generally than just for TBE. In most of the models presented here TBE has been a case study of a model which addresses more general questions.

Lyme disease

Borrelia burgdorferi s.l. is the suite of spirochete bacteria which causes Lyme disease. This is a pathogen which has a wildlife reservoir but infects humans in the northern hemisphere (Tilly et al., 2008). Porco (1999) used a time-independent differential equation model to investigate how the prevalence of *B. burgdorferi* s.l. in *I. scapularis* (Say) nymphs is affected by various model parameters. The infectivity of white-footed mice *Peromyscus leucopus* (a key transmission host in the Eastern USA) was predicted to be the parameter which increased *B. burgdorferi* s. l. prevalence the most, whilst a tenfold increase in the density of deer (which do not transmit the pathogen) significantly reduced *B. burgdorferi* s.l. prevalence, suggesting that this is another system where the dilution effect can occur.

Zhang and Zhao (2013) presented a seasonal reaction–diffusion model of Lyme disease, utilising it to study the dynamics of the system in bounded and unbounded spaces. For bounded habitats a threshold for pathogen persistence was predicted, whilst for unbounded habitats they were able to predict the speed of pathogen spread.

In their 2007 paper, Ogden et al. (2007) considered the work of Wilson and Spielman (1985) and hypothesised that the transmission cycles of *B. burgdorferi* s.l. are very efficient in north-eastern North America because the seasonal activity of nymphal and larval *I. scapularis* is asynchronous. They then developed a

simulation model which integrated transmission patterns imposed by seasonal asynchronous nymph and larvae with a model of infection in white footed mice. They parameterised the model for *B. burgdorferi* s.l. and *Anaplasma phagocytophilum* as examples. They found that duration of host infectivity, transmission efficiency to ticks and co-feeding transmission are the major factors determining fitness of pathogens in *I. scapularis* in North America.

The same group then wrote a series of papers looking *I. scapularis* in Canada where is established in some places and emerging in others. In Wu et al. (2013) they developed a temperature driven map of the basic reproductive number for the ticks and found that while the geographical extent of suitable tick habitat is expected to increase with climate warming the rate of invasion will also increase. In a subsequent paper, Ogden et al. (2013) investigated the speed of *B. burgdorferi* s.l. invasion after establishment of ticks. The model showed that the number of immigrating ticks was a key determinant of pathogen invasion and so the authors hypothesised that a 5-year gap would occur between tick and *B. burgdorferi* s.l. invasion in Eastern Canada but a much shorter gap in Central Canada. This was consistent with empirical evidence.

Summary

Borrelia burgdorferi s.l. is another pathogen for which the dilution effect appears to occur. In this case rodents are the main reservoir host and *B. burgdorferi* s.l. is emerging in a number of different areas as the tick hosts expand their range in response to climate change or socioeconomic factors.

2.1.4.3 *More general models of tick-borne pathogen*

More generally, Hartemink et al. (2008) determined ways of characterising the basic reproductive number in a tick-borne pathogen system which has multiple transmission routes using the next generation matrix (e.g. Diekmann et al. 2010). They showed that the complexities of the tick transmission cycle can be overcome by separating the host population into epidemiologically different types of individuals and constructing a matrix of reproduction numbers. They then used field and experimental data to parameterise this next-generation matrix for *B. burgdorferi* s.l. and TBEV.

Dunn et al. (2013) used a general model of tick-borne pathogens to study the basic reproductive number and found that the transmission efficiency to the ticks, the survival rate from feeding larvae to feeding nymphs and the fraction of nymphs to find a competent host are the most important factors in determining R_0.

Another general tick-borne pathogen model was created by Zeman (1997), where reported cases of disease were smoothed over to create risk maps for Lyme disease and TBE in Central Bavaria. This study indicated that *B. burgdorferi* s.l. is wider spread than TBEV, but that both pathogens share the same main foci. Similarly, Hönig et al. (2011) assessed the suitability of various habitats for supporting *I. ricinus* ticks, creating a model with which they were able to create a tick-borne pathogen risk map for South Bohemia, which was compared to clinical cases of TBE for validation. The model suggested that the areas mostly suitable for tick-borne pathogens were along the river valleys. However, when human activity is taken into account, the surroundings of large settlements are equally likely to provide tick-borne pathogen cases.

Another aspect of transmission which is considerably less well understood is the pattern of aggregation of ticks on hosts. Ferreri et al. (2014) analysed a 9-year time series of *I. ricinus* feeding on *Apodemus flavicollis* mice, the reservoir host for TBE in Trentino, Northern Italy. The tail of the distribution of the number of ticks per host was fitted to three theoretical distributions. The impact of these distributions on pathogen transmission was investigated using a stochastic model. Model simulations showed that there were different outcomes of disease spread with different distribution laws amongst ticks and so it is important to have data on these distributions which can vary seasonally.

The models discussed above are not an exhaustive list, but do describe models which help us to understand many of the different complexities of tick-borne pathogen systems, and showcase the diversity of models now being developed for a wide range of end uses.

2.1.5 *Knowledge gaps and future directions*

As we have seen mathematical models have been used for more than 30 years to help to predict tick dynamics and subsequently pathogen dynamics. The models presented here have been used in two ways, firstly to predict when tick densities are at their peak within a year and how that peak varies with environmental factors. Secondly, they have been used to predict pathogen persistence for different combinations of available host species with different transmission competencies. In particular, they have looked at the interaction between tick amplifying hosts and disease-transmitting hosts and how densities of these hosts could be manipulated to control the disease.

One of the problems of these modelling studies is the difficulty in gathering empirical data to validate the model results. This is largely because there is a

great deal of variability between sites in terms of habitat cover, microclimate and host densities. This is not unique to the tick system; it is difficult for a number of reasons to carry out experiments in natural systems. It is also difficult to measure realistic tick densities (e.g. Dobson 2014).

However, most of the models described here have succeeded in doing some type of validation and they provide useful qualitative results.

Future modelling approaches are likely to be focussed in two main areas. One is to look at spatial patterns of tick and disease risk, and in particular to link environmental information in GIS systems to models of tick and pathogen dynamics in a mechanistic way. These models can then be used to predict the impact of climate change on tick and disease risk across a given geographical region. This type of modelling is currently being carried out by the authors for both LIV and Lyme disease in Scotland. The advantage of this type of modelling is that it is generalisable and could be applied to any country with the right type of environmental data available in GIS form. It can also predict risks are going to change over time rather than only looking at the end points as has been done before (e.g. Braga 2012).

If we can identify which areas are going to have significant increases in disease risk, then we can inform policy makers and target control efforts. For example, if we could identify which areas are going to have higher and lower Lyme disease risk then we could target efforts to educate the public on how to avoid being bitten in those high risk areas.

The second direction in which we predict tick modelling will move is to further develop a new modelling technique which was introduced in Jones et al. (2011). In that paper, the authors developed a model which keeps track of the number of hosts with a particular number of ticks on it. This allows us to consider the

distribution of ticks amongst the hosts and the spatial element of the model allowed hosts to be infected in one place and for ticks to drop off them in another area. This allows us to model the movement of ticks which is not possible in the more traditional models. This ability adds to the level of biological realism and allows us to answer questions which it is not normally possible to answer. For example, we would be able to model control more explicitly in terms of how many ticks are lost from an individual host. This approach allows us to relax the intrinsic assumption of most models that all host individuals, and indeed, all tick individual behave in the same average way and to look at distributions of behaviour which should bring further insights into these important systems.

Whilst it is interesting to speculate about future directions in the modelling of tick-borne diseases, it is also likely that future modelling will be developed in response to new insights, either in the current systems, or in emerging diseases which become a problem in the light of climate change, for example. New models or new methods of analysis will have to be developed in order to answer specific questions for particular biological systems.

2.2 Importance of Norman et al. (2015) in relation to this thesis

Whilst early models of parasites, ticks and tick-borne diseases have been extremely influential over subsequent models, it is the recent models that are of primary interest here.

2.2.1 *Tick lifecycle model (chapter 3)*

The model of most interest in chapter 3 is that presented in Dobson et al. (2011) and explored further by Dobson and Randolph (2011). Since the model presented

by Dobson et al. (2011) takes a similar approach to the tick lifecycle model presented in chapter 3 of splitting the tick lifecycle into different states within each tick stage, it is therefore an ideal model to use for comparisons of assumptions and parameterisation of tick dynamics. There are naturally key differences between the modelling approach in Dobson et al. (2011) and those presented within this thesis, most notably the fact that Dobson et al. (2011) use a Leslie matrix modelling method rather than the coupled differential equations which will be presented in this thesis. Therefore, any parameters taken from the Dobson et al. (2011) model are carefully adjusted to reflect the change in modelling type.

Ideas drawn from models which include disease can still help the development of disease-free tick lifecycle model, especially since the interaction between ticks and hosts is often a major focus of disease-focused studies. Hudson et al. (1995), Gilbert et al. (2001), Laurenson et al. (2003), Norman et al. (2004) and Porter (2011) provide examples of how coupled differential equation models can be used to model the interactions between ticks and their hosts and served as a foundation for the modelling approach taken in this thesis. In particular, the method of modelling tick hosts as having heterogeneous effects on the success of instars in feeding influenced the creation of the weekly feeding limits discussed in chapter 3.

As the tick lifecycle model uses GIS mapping software to visualise the changes occurring under different temperature scenarios, models which have a similar output are of interest. Specifically, Schwarz et al. (2009) and Braga (2012) used GIS mapping to display predictions of tick densities across Germany and Scotland respectively. Like chapter 3, these studies looked at the interactions between ticks and their environments. However, in contrast to the tick lifecycle model created in chapter 3, the studies by Schwarz et al. (2009) and Braga (2012) use statistical

methods to make their predictions. Therefore for the long-term predictions made in this thesis, the statistical methods used by Schwarz et al. (2009) and Braga (2012) are not considered.

On a more practical level, Watts et al. (2009) and later Porter (2011) used a method of sensitivity analysis that is useful in quantifying the effect that each parameter has on the associated model, showing both the parameters which have an unduly large effect and a measure of the variability of model output which is explained by each parameter. Therefore, in this thesis this method is used in the analysis of the models in chapters 3, 4 and 5.

2.2.2 *Louping-ill virus model (chapter 4)*

The models which influence the tick lifecycle model presented in chapter 3 are also influential in the Louping-ill virus (LIV) model (chapter 4), since this is built upon the foundations of the tick lifecycle model. Additionally, models which influenced the work in chapter 3 may influence the work in chapter 4 in new ways.

When considering the routes of transmission between tick and host, the models of Hudson et al. (1995) and Norman et al. (1999) were very influential in providing a structure to base the transmission dynamics of the LIV model in chapter 4 on. The study by Gilbert et al. (2001) used a system where red grouse are the competent transmission host present, with red deer and mountain hares are solely tick-carrying hosts, which is the system used in the LIV model. The aforementioned models created by Hudson et al. (1995), Norman et al. (1999) and Gilbert et al. (2001), as well as those created by Porter (2011) all contain mechanisms akin to those in the LIV model, and therefore are useful for parameterisation.

Previous models have used GIS mapping software to display predictive maps of disease risk, as the LIV model does. Models by Zeman (1997), Rizzoli et al. (2004) and Hönig et al. (2011) use this method in studies of systems of *B. burgdorferi* s.l. and TBEV. Whilst these were primarily statistical analyses which looked at pathogens other than LIV in areas other than Scotland, they were useful for providing examples of how disease risk can be displayed geographically.

Part of the focus in chapter 4 is on how the dilution effect (whereby the increased presence of an incompetent transmission host reduces pathogen prevalence as infected tick bites are 'wasted') influences the LIV model output. Therefore, previous models which have displayed the dilution effect are of interest. The first model to study the dilution effect was that created by Norman et al. (1999), whilst later Gilbert et al. (2001) predicted a dilution effect in a host system similar to that in chapter 4. Additionally, the study by Bolzoni et al. (2012) found evidence of a dilution effect of deer on TBEV. The natures of the dilution effect in these models are used in comparison to that found in the LIV model in chapter 4.

2.2.3 *Modelling framework (chapter 5)*

Since chapter 5 expands the LIV model into a modelling framework which can be adapted for a variety of tick-borne disease systems and mechanisms, the models within the review paper which are most relevant to this chapter are those which utilise such mechanisms. For example, when considering the transmission rate, the models used by Gilbert et al. (2001) and Zhang and Zhao (2013) provide examples where the transmission rate from infected nymphs biting susceptible hosts, and uninfected larvae biting infected hosts is set to 100%.

An important mechanism considered within chapter 5 is that of non-viraemic transmission through co-feeding ticks. The models created by Gilbert et al. (2001), Laurenson et al. (2003) and Norman et al. (2004) include co-feeding as a route of transmission, and as such are used when considering how such a mechanism can be incorporated into the modelling framework.

There are a number of models in the thesis by Porter (2011) which include mechanisms considered in chapter 5. There is a model created to investigate the effect of including ingestion of infected ticks by grouse chicks as a route of transmission in a LIV system. The structure of this model is used in this thesis when considering how the modelling framework can be extended to include ingestion. Additionally, Porter (2011) creates models to look at the effect of using acaricide on various tick hosts, namely sheep, red deer and red grouse. These models are influential in chapter 5 when demonstrating what has to be considered when adding such management strategies into a model of a tick-borne pathogen system.

2.3 FURTHER MODELS WHICH INFLUENCE THIS THESIS

The following papers are ones which are influential in the creation of the models within this thesis, but are not outlined by Norman et al. (2015). This section outlines the work done in these studies, and how they influenced this thesis.

Kiffner et al. 2011. This study began with a series of field observations on rodents in south Germany, collecting tick counts and climatic data. These were then combined with a stepwise forward model selection procedure in order to find the best fit. Whilst there was found to be some unexplained variation in tick burdens, the model was able to be used to address various hypotheses. The one of these which is most relevant to this thesis is that evidence was found that the

dilution effect does occur with increasing rodent densities. Therefore this model is of use when the predictions of the LIV model in chapter 4 are considered, in particular the diluting effect of tick-only hosts.

Hartfield et al. 2011. The model presented by Norman et al. (1999) is adapted for *B. burgdorferi* s.l. dynamics. The aim of this is firstly to understand the conditions of the dilution effect in a *B. burgdorferi* s.l. system, and secondly to predict how quickly *B. burgdorferi* s.l. establishes itself following the introduction of deer to the system. As this study partly focuses on the dilution effect, it is of relevance to the exploration of this effect in chapter 4, whilst the parameterisation of the model for *B. burgdorferi* s.l. dynamics is of relevance to the model created in chapter 5.

Li et al. 2016. The model presented in this paper is an agent-based model designed to predict Lyme borreliosis risk across Scotland. The influence of temperature and altitude were considered when making disease risk predictions. For instance, the model predicts that whilst higher altitudes currently experience lower disease risk, with higher temperatures this risk will increase for high altitude areas. Given the nature of this study, it is clear that this study is particularly relevant to the *B. burgdorferi* s.l. case study. This study is used as a comparison for the methods used in chapter 5.

2.4 SUMMARY

This chapter aimed to provide a review of previous mathematical modelling of tick and tick-borne pathogen systems. Through doing this, knowledge gaps can be highlighted and addressed within this thesis. Additionally, the modelling methods used can be an influence on those used in the modelling work carried out later in this thesis.

One of the main areas in future research on tick-borne pathogen systems highlighted as one to be explored was the combination of mechanistic models with environmental information to provide spatial representations of disease risk. This will be addressed through the work in this thesis, firstly by developing a new modelling system for tick dynamics (chapter 3), then by adapting this model for the dynamics of LIV (chapter 4) and *B. burgdorferi* s.l. (chapter 5). Additionally, the studies highlighted in this chapter provide a number of different methods which will be considered when developing and analysing these models.

3

CREATING A NOVEL ENVIRONMENT-DEPENDENT TICK LIFECYCLE MODEL

3.1 INTRODUCTION

The overall aim of this thesis is to develop a modelling framework which can be used to predict the influence climate change will have on tick-borne disease risk. Tick-borne disease risk depends on the density and activity of ticks, as well as the pathogen. Therefore, the first step is to develop an original model for the tick lifecycle, factoring in the environmental aspects which are likely to influence tick density. This model can then be used to predict the changes in tick density across Scotland for future climate warming scenarios. As *Ixodes ricinus* ticks are the most prevalent species of tick across Scotland, this chapter will focus on their dynamics.

Ticks are the most important vectors of zoonotic disease-causing pathogens in Europe, transmitting the tick-borne encephalitis complex of viruses, *Anaplasma phagocytophyllum*, *Babesia* and *Rickettsia* species and *Borrelia burgdorferi* sensu lato, the complex of bacteria that cause Lyme borreliosis, amongst others (BADA UK, 2016). *I. ricinus* ticks are particularly implicated in pathogen transmission because they are almost ubiquitous across Europe and are generalist feeders, which allows

for pathogen transmission among different host species (Gilbert, 2016a). *I. ricinus* are increasing in number and range in many parts of northern Europe (reviewed by Medlock et al. 2013).

As discussed in chapter 1, the *I. ricinus* lifecycle develops from the egg, through two immature stages (larvae and nymph) to the adult stage and usually takes around three years to complete. Each immature stage requires a single blood meal, taking a few days, from a suitable vertebrate host before developing to the next stage and the adult female requires a blood meal before producing eggs. Because *Ixodid* ticks spend the vast majority of their life away from the host in vegetation or the ground, their activity and survival is highly influenced by the surrounding local environment. The activity of *I. ricinus*, like most invertebrates, is inhibited by low temperatures (Gilbert et al., 2014) and they tend not to seek hosts (behaviour known as questing) at low humidities or high saturation deficits in order to avoid desiccation (Randolph et al., 2002). Adult female *I. ricinus* feed primarily on large mammals such as deer, sheep or hares whilst the immature stages can also feed on smaller vertebrates such as mice, voles and birds (e.g. Gray 1998). For forecasting future tick activity or abundance these factors must be therefore taken into account.

In order to make spatially explicit large-scale associations between environmental factors and disease risk parameters, Geographic Information Systems (GIS) have been increasingly used, including modelling the dynamics of ticks and tick-borne diseases (Daniel et al., 2004). Tick-borne disease systems which have been investigated in this way include tick-borne encephalitis virus and *B. burgdorferi* in Bavaria (Zeman 1997; Hönig et al. 2011) and Italy (Rizzoli et al., 2004), as well as predictions of tick populations in Germany (Schwarz et al., 2009) and Scotland (Braga, 2012). These studies primarily used large spatial data sets of

vectors, pathogens or disease incidence coupled with spatial environmental data, and used statistical methods to predict regions of high disease risk. However, to the knowledge of the authors GIS has not been combined with dynamic modelling to predict tick abundance or disease risk. Here, a newly developed dynamic model is presented, based on temperature- and host-dependent seasonal tick dynamics, which is then combined with GIS-based spatial environmental information to predict tick abundance over Scotland, and how abundance will change under climate warming scenarios. Scotland is an ideal country for pioneering this approach as the issue of ticks and tick-borne disease risk is of increasing concern: it has been shown to have increasing tick abundance (Kirby et al., 2004) and reported incidence of Lyme borreliosis has been increasing enormously this century (Health Protection Scotland, 2016). Furthermore, there are data sets available of tick abundance at a large number of sites throughout Scotland, several relevant studies on *I. ricinus* in the Scottish context (e.g. Gilbert 2010, 2013; Gilbert et al. 2014) that can provide locally relevant parameter values, and available national-scale GIS-based environmental information. In addition, Scotland has a highly heterogeneous landscape, with widely varying climates, elevations and habitats for its size, widely varying tick abundances over the country may be predicted.

This chapter aims to develop a novel mechanistic model of the *I. ricinus* lifecycle which can be used to predict the effect climate change has on tick density. This model can then be used as a basic for models of tick-borne pathogen systems, specifically Louping-ill virus (LIV; chapter 4) and *B. burgdorferi* s.l. (chapter 5).

Parameter	Value	Explanation and justification
a_T	628	Average successful birth rate for each adult tick per year. Gray (1981) and Buczek et al. (2014).
b_L	0.047	Natural mortality rate for each tick stage's active state. Dobson et al. (2011).
b_N	0.024	
b_A	0.009	
b_{WL}	0.00995	Natural mortality rate for larvae developing into nymphs during winter. Dobson et al. (2011).
b_{WN}	0.00333	Natural mortality rate for nymphs developing into adults during winter. Dobson et al. (2011).
L_{host}	Varied	Weekly feeding limit for each tick stage and each host. Varies for different habitat types (see table 3.2).
N_{host}	Varied	
A_{host}	Varied	
T_1	5	Temperature (°C) at which ticks begin to emerge from overwintering. Perret et al. (2000).
T_2	9	Temperature (°C) at which all ticks have emerged from overwintering. Perret et al. (2000).

Table 3.1: The definitions, numerical values used and sources of model parameters. All rates are per week unless otherwise stated.

3.2 MODEL DEVELOPMENT

3.2.1 *Model development*

The model consists of a series of differential equations which run across the calendar year, followed by a discrete time step to move onto the next year. This discrete step is taken at the time when temperatures are at their coldest, and therefore when tick activity would be at its lowest. To represent temperature across the year, a simple sine function is used ($T(t)$, where t is the week of the year), starting and ending at the coldest point in the year, and peaking in the middle at the warmest. This function is given by equation 3.1, where a is the minimum temperature and b is the maximum. The remaining values ensure that

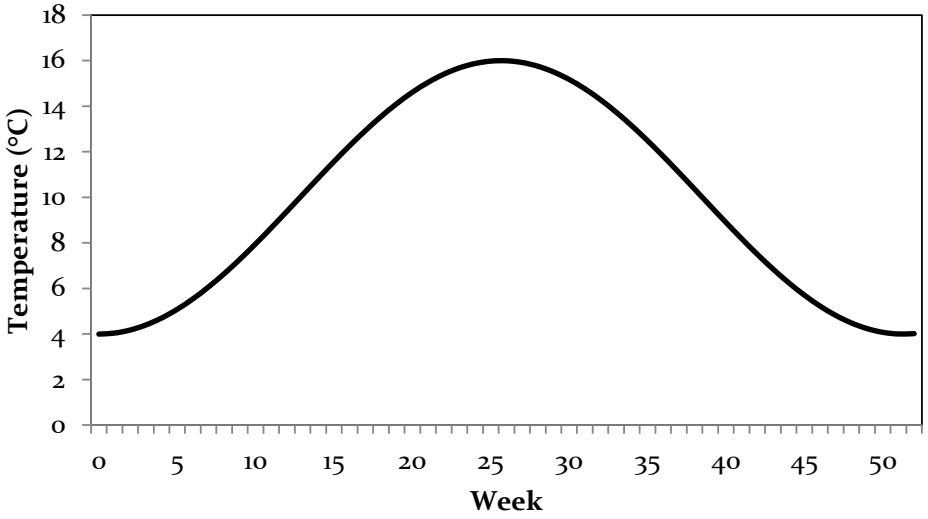

Figure 3.1: An example of the temperature function $T(t)$ across a calendar year. For this demonstrative figure the annual minimum temperature (a) is set to 4 and the annual maximum temperature (b) is set to 16.

the function is at its minimum at weeks 0 and 52, and reaches its peak at week 26. Figure 3.1 shows an example of this function across a calendar year.

$$T(t) = \left(\frac{b-a}{2} \times \sin\left(\frac{t}{2.6\pi} - 0.5\pi\right)\right) + \frac{a+b}{2} \tag{3.1}$$

The tick lifecycle is broken up into three active life stages (larvae, nymph and adult), with each stage split further into one group which has yet to feed that year (termed here as "active" to represent ticks that are available to quest if the conditions are appropriate) and one group that has already fed (which no longer quest and termed here as "developing") (figure 3.2). Whilst ticks feeding twice (i.e. as a larva and then as a nymph or as a nymph and then as an adult) within one season is documented (Randolph et al., 2002), these observations were made south of Scotland in warmer climates where temperature-dependent development

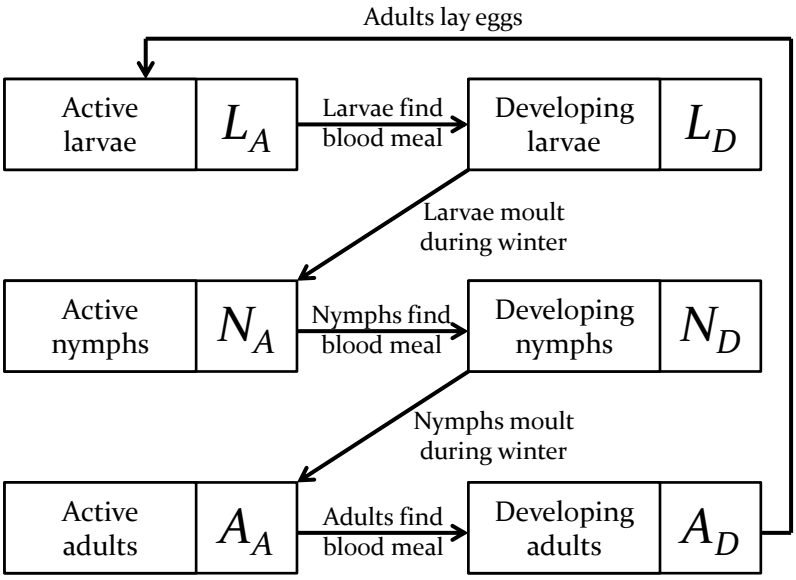

Figure 3.2: Schematic outline of model. Ticks successfully feeding is found through the weekly feeding function $S(x, K)$, whilst progression over winter to the next stage is carried out at the end of each year, as is tick birth. Each class within the model has its own weekly mortality rate, not shown on this schematic.

times are faster. Such behaviour has not been demonstrated in Scotland and, furthermore, as the speed of interstadial development is temperature-dependent (Randolph et al., 2002) it is likely that the colder summers in Scotland would result in only a very small proportion of ticks being able to feed twice per season. Therefore, in the model presented here, all ticks are assumed to feed once per year.

The time unit used by the model is weekly, as this fits with the typical period spent by ticks feeding on a blood host (Randolph, 2004).

3.2.1.1 *Tick feeding*

For ticks of any given stage to find a blood meal, Randolph (2004) identified four key aspects of tick development between stages: entering the stage (i.e. devel-

opment from the previous stage), questing for a meal, successfully feeding on a host, and mortality. These have all been incorporated into the model presented here.

Field studies have suggested that ticks begin questing when weekly temperatures reach 7°C (Perret et al., 2000). Therefore, a function is introduced to the model to represent this behaviour. As tick questing activity becomes negligible during winter in Scotland, a temperature boundary (T_1) is set in the model, below which all active ticks are assumed to not be questing as they are overwintering. A second temperature boundary (T_2) is set, above which all active ticks are available to quest, having emerged from overwintering. Due to individual variation in real life, it is likely that some ticks do quest below 7°C; this temperature will be when enough ticks had emerged to be noticed in empirical studies. Therefore, for the model it is assumed that there is variation in individual emergence around a mean of 7°C, and so T1 is set to 5°C and T2 is set to 9°C. Between these two temperature boundaries it is assumed there is a linear progression as ticks gradually become available to quest. The equation for the function which describes the pattern of emergence from overwintering between these two temperatures is given by equation 3.2.

$$F(t) = \begin{cases} 0 & T(t) \leqslant T_1, \\ \frac{T(t)-T_1}{T_2-T_1} & T_1 < T(t) \leqslant T_2, \\ 1 & T_2 < T(t) \end{cases} \tag{3.2}$$

Note that ticks which have emerged from the winter are not necessarily questing at every time point. They have a limited amount of energy and so need to quest

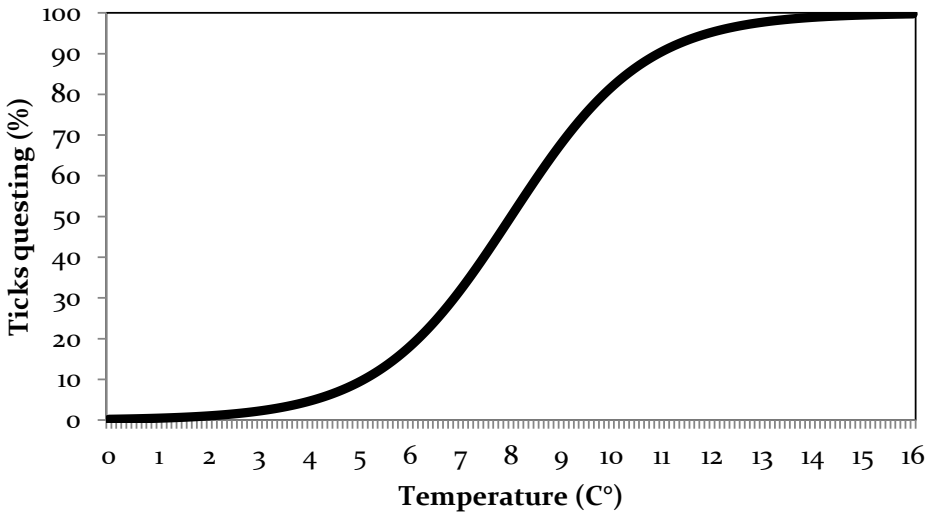

Figure 3.3: Percentage of active ticks assumed to be questing, $P(t)$, for temperatures between 0 and 16°C. The function is based on empirical data from Gilbert et al. (2014).

in appropriate conditions. Therefore, a questing function $P(t)$ is introduced to the model, which describes ticks within the active state questing for a host. This questing function is based on data from experiments conducted by Gilbert et al. (2014), who determined the proportion of potentially active, emerged ticks which were questing at different temperatures. For ticks collected in Scotland, they found that the vast majority of ticks began questing between 6°C and 12°C, with almost 100% questing at 15°C. Equation 3.3 approximates the results from Gilbert et al. (2014), and figure 3.3 shows this function for temperatures between 0 and 16°C.

$$P(t) = \frac{1}{1 + exp\left[\frac{3}{4}(8 - T(t))\right]} \tag{3.3}$$

The probability of a tick finding a host is assumed to be directly proportional to the density of each host species present at a particular site. It is also assumed that the number of ticks which find a meal in a given time period increases with the number of ticks which are questing up to a threshold limit which depends on how many hosts are available. This also acts as the density dependence within the model, rather than at birth. For comparison, Gilbert et al. (2001) apply density dependence at birth, as higher tick densities would be expected to result in more intensive grooming and greater competition for blood meals. However, both of these elements will more directly affect the tick lifecycle at the feeding stage rather than at birth.

Therefore, the upper limit for the number of ticks which can feed in a given week has to be estimated. This weekly feeding limit is calculated by using available data to estimate the number of ticks each host type can carry at each time step, which is then multiplied by the density of each host species present (table 3.2). The density-dependent relationship given by equation 3.4 is then used to model the number of ticks which find a host in a given week, where x is the number of ticks of a given stage which are questing, w and r are constants which determine the shape of the curve and K is the weekly feeding limit discussed above. When running the model, K is referred to as L_{host}, N_{host} or A_{host} when it is the weekly feeding limit for larvae, nymphs and adults respectively. Equation 3.4 is an adaptation of the solution of the logistic equation and satisfies the assumptions discussed above.

$$S(x, K) = \frac{wK}{w + (K - w)exp(rx)} - w \tag{3.4}$$

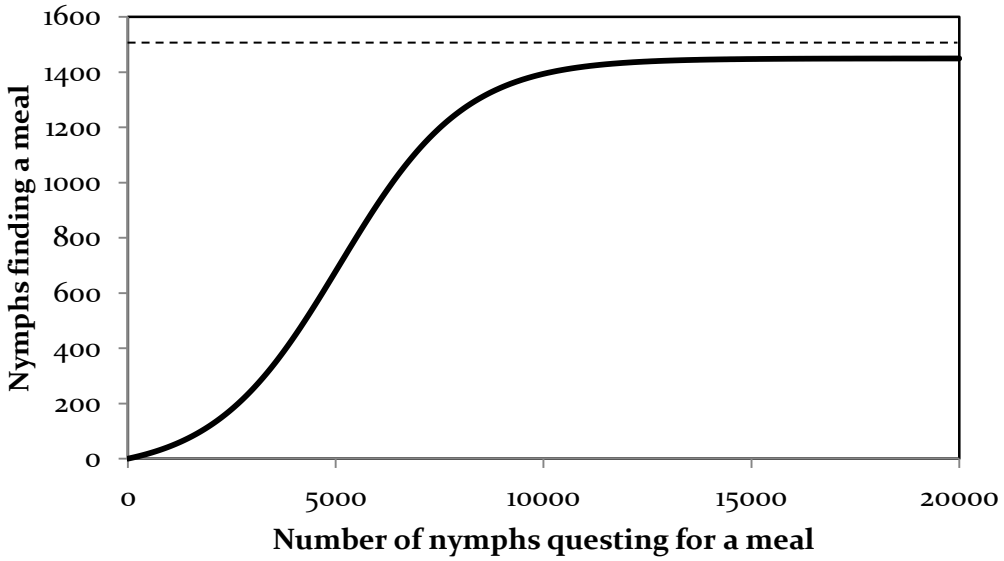

Figure 3.4: An example of the feeding function $S(x, K)$, where x is the number of ticks per km² questing and K is the weekly feeding limit, which for the purposes of this demonstrative graph is set to 1500 (dashed line).

There are no available data which can be used to parameterise this function further, therefore it is arbitrarily estimated that in order for 95% of questing ticks to find a meal, $8K$ ticks per km² need to be questing. To achieve this, w is set as 50, whilst r is given by equation 3.5. An example of this function is shown in figure 3.4.

$$r = \frac{\ln\left[\frac{w}{19(K-w)}\right]}{8K} \tag{3.5}$$

Mortality rates for questing ticks are given as 0.0068, 0.0034 and 0.00136 per day for larvae, nymphs and adults respectively by Dobson et al. (2011). The questing tick class used by Dobson et al. (2011) corresponds to the active tick class used within the model presented in this chapter. However, as the model developed

by Dobson et al. (2011) uses a daily time unit, these parameters were modified to reflect the weekly time unit used within the models within this chapter. The weekly mortality rates were found using the formula in equation 3.6, with values of 0.047, 0.024 and 0.009 per week for larvae, nymphs and adults respectively.

$$mortality_{week} = 1 - (1 - mortality_{day})^7 \tag{3.6}$$

All ticks which have not fed by the end of the year are assumed to have died. Additionally, all adults are removed from the model at the end of each year, assumed to have reached the end of their lifespan.

Worked example of tick feeding mechanism

This section will demonstrate a worked example of the feeding mechanism in the model in order to make clear the processes involved in running the model. The numbers used within this example are purely for demonstrative purposes, and are not necessarily used when making model predictions. This example will focus on nymph feeding dynamics at a single point in time, but the principle is identical for larvae and adults.

The minimum (a) and maximum (b) temperatures for the example are 2°C and 10°C respectively, and it takes place during week 18 (t). The active nymph density ($N_A(t)$) is 10000 per km². Present in the area are two hosts, labelled Host A and Host B. Each individual of species Host A can feed up to 5 nymphs in a given week whilst each individual of species Host B can feed up to 20 nymphs in

a given week. The densities of Hosts A and B are 110 per km² and 16 per km² respectively.

To begin with, a, b and t are substituted into the $T(t)$ function in equation 3.1 to calculate a temperature value for that week of 8.3659°C. Using this temperature in the $F(t)$ function set out by equation 3.2 gives a value of 0.8415. This means that at this temperature 84.15% of ticks have emerged from overwintering. Using the temperature in the $P(t)$ function set out by equation 3.3 gives a value of 0.5682. This means that at this temperature 56.82% of emerged ticks quest for a blood meal in the model. Multiplying both of these percentages by the active nymph density gives the density of nymphs questing for a meal as 2390.54.

The weekly feeding limit for nymphs (N_{host}) is given by calculating the total number of available blood meals in a given week. To find this, the nymph capacity of Host A is multiplied by its density to give 550. The same is done for Host B, giving 320. These are then summed to get a value for N_{host} of 870. Therefore 2390.54 and 870 are the arguments of the $S(x, K)$ function set out by equation 3.4, giving a value of 610.285. This is the nymphs per km² which have successfully fed and move into the developing nymph class ($N_D(t)$) at that time. The remaining nymphs either stay in the active nymph class, or are removed through the weekly mortality rate.

3.2.1.2 *Tick interstadial development*

As ticks which have successfully fed are assumed not to feed a second time that year, all fed ticks stay in the developing class until the end of the year, at which point they progress to the active class of the next instar. As the model's developing class is equivalent to the behavioural diapause category in the paper presented by Dobson et al. (2011), the relevant mortality rates are used, scaled to reflect

weekly mortality using equation 3.6. Therefore, the mortality rates of 0.001428 and 0.000476 per day used by Dobson et al. (2011) are changed to mortality rates 0.00995 and 0.00333 per week for larvae and nymphs respectively.

3.2.1.3 *Tick birth*

As larvae will have hatched by the start of the tick activity season in early spring, all births within the model occur at the start of each year before ticks are active. In a study of ticks collected in Ireland, Gray (1981) investigated the fecundity of *I. ricinus* ticks. From the results of this study, an estimate of 1400 eggs laid per female is taken. This is multiplied by the 89.6% hatching success found by Buczek et al. (2014) to get 1254 successful births, which is then halved to represent a 1:1 adult sex ratio (as used by Dobson et al. 2011) to get a total number of larvae born per adult as 628.

3.2.1.4 *Host densities and tick burdens on hosts*

In order to provide a value for the number of blood meals available to questing ticks in a given week (L_{host}, N_{host} or A_{host} depending on the instar), the density of each tick host is required, along with an estimation of the capacity of each species to host each instar of tick, referred to as the tick burden. Ideally, an estimation of the maximum number of ticks a host can feed would be used. However, this information is difficult to find for all hosts, therefore, the average is used. Whilst this will be below the maximum, potentially by a large amount, it should still keep the influence each individual host has on the tick lifecycle relative.

Parameter	PB	RG	MH	ReD	RoD	SM
Tick burdens on each host species.						
Larva	3.11	15	63.7	15.18	10.78	1.61
Nymph	0.25	4	37.4	70.41	23.9	0.04
Adult	0	0	11.4	81.25	29.82	0
Density of each host species in each habitat (per km²).						
Blanket bog	0	0	8	1	0	0
Heather moorland	0	0, 50, 100	8	0, 5, 15	0	0
Montane	0	20	16	0.1	0	0
Mixed woodland	70	0	0	0	4	8500
Conifer plantation	35	0	0	0	2	4250

Table 3.2: The values used in the model for ticks feeding per individual host each week on each host species and densities (per km²) of each host species in each habitat category included within the model. The acronyms at the head of each column refer to an individual host group: PB = passerine bird; RG = red grouse; MH = mountain hare; ReD = red deer; RoD = roe deer; SM = small mammals.

The density of each host type is found for the different habitats within the model: blanket bog, heather moorland, montane, mixed woodland and conifer plantation. Urban areas and prime agricultural land were not considered in the model, as these areas are considered to have extremely low tick densities (Gilbert unpublished data) and, probably as a consequence, there is no information associating tick abundance to environmental factors in these areas. The uplands of Scotland are highly managed landscapes, so host densities are a direct result of the management objectives of the land holding unit (Wightman and Tingay, 2015). Of particular importance to the model is the fact that some areas of heather moorland are managed specifically to maximise densities of red grouse, since they are valuable gamebirds. Red grouse managers maintain very low deer densities in order to keep tick numbers low (Wightman and Tingay, 2015). Conversely, other areas of heather moorland aim to maintain high deer densities for commercial red deer hunting, and these areas therefore tend to have few red grouse. Other

upland areas of Scotland are less specialised and maintain a mix of game at intermediate densities. Therefore, heather moorland areas in the model were categorised into three host community groups:

- High grouse densities, no deer
- Low grouse densities, low deer densities
- No grouse, high deer densities

The full details of how the heather areas in the model were split into these categories are presented in appendix A.

Red grouse (*Lagopus lagopus scoticus*)

Gilbert (unpublished) found that the average tick counts on red grouse are approximately 15 larvae and 4 nymphs per grouse, with no adult ticks found. These data were collected in peak tick questing months.

For heather moorland habitats, high and low red grouse density estimates are required for the three classifications of heather habitat. A typical high density of grouse on moorland is estimated to be 100 per km² (Hudson, 1992), with the low density taken to be 50 per km². Red grouse are not generally present on montane habitats; however rock ptarmigan (*Lagopus muta*), a member of the grouse family, are (Gilbert, 2016a). In the absence of official population data on the density of ptarmigan in montane areas an estimate of 20 per km² is used, as ptarmigan density is estimated to be lower than typical grouse densities. Members of the grouse family are generally not found on any of the other habitats within the model; therefore their density for blanket bog, mixed woodland and conifer plantation is set to 0.

Red deer (*Cervus elpahus*)

Gilbert (unpublished) found that during April-October, the time at which most ticks would be expected to feed, the average count of adult ticks upon red deer at any one time was 81.25. Using the ratios of larvae and nymphs to adults found on red deer by Mysterud et al. (2014), the larval and nymphal burdens of red deer were estimated to be 15.18 and 70.41 respectively.

The Deer Management Group data, which was used to separate the heather habitats, was studied in order to derive estimates for a low and a high deer density on heather. From this, a low deer density of 5 per km², and a high deer density of 15 per km² were used. An index of red deer abundance by habitat type (Pérez-Barbería et al., 2013) was used to estimate red deer density within the model for the remaining habitats. From this, densities of 1 per km² for blanket bog, and 0.1 per km² for montane were estimated.

Mountain hares (*Lepus timidus*)

Tick counts on mountain hares allowed the tick burdens of mountain hares to be estimated as 63.7 for larvae, 37.4 for nymphs and 11.4 for adults (Laurenson unpublished).

Mountain hare density for blanket bog and heather moorland was estimated to be 8 per km² (Gilbert unpublished), whilst for montane habitats it was estimated to be 16 per km², due to the increased abundance of mountain hares at higher altitudes (estimated from Gilbert 2010).

Roe deer (*Capreolus capreolus*)

Kiffner et al. (2010) estimated the burdens of each tick instar on roe deer in central Europe from a long-term study of counts on shot roe deer, finding averages of 10.78, 23.90 and 29.82 for larvae, nymphs and adults respectively.

Roe deer densities were interpreted from the results found by Burbaite and Csányi (2009), who suggested a UK-wide density of 3 per km². Since this is a broad nation-wide estimate, a density of 4 per km² is used for mixed woodland (their preferred habitat), and 2 per km² for conifer plantation. Roe deer are assumed in the model not to be present in other habitats, as they generally do not favour these in real life.

Small mammals

For simplicity, the numerous small mammals which can act as tick hosts, especially in woodland habitats, are merged into one host group. This is reasonable as the species within the group are present in the same habitat types (mixed woodland and conifer plantation) and carry similar numbers of ticks (primarily carrying larvae, and never carrying adults). Gilbert et al. (2000) identified field voles (*Microtus agrestis*), common shrews (*Sorex araneus*), wood mice (*Apodemus sylvaticus*) and bank voles (*Myodes glareolus*) as potentially important hosts for ticks. By counting caught specimens, the mean tick burdens of each species was also found, which are shown in table 3.3.

The densities of small mammals were required to find the overall tick burden parameters for the small mammal group. Using a variety of sources for mixed

Species	Average density (per km²)	Total tick burden (per host)
Bank vole	1200	1.4
Common shrew	400	0.4
Field vole	400	1.2
Wood mouse	6500	1.8
Overall	**8500**	**1.64**

Table 3.3: The densities of the four small mammal species identified as important to tick persistence, and their tick burden per individual. The tick burdens are larvae and nymphs combined, as adults do not feed on the species listed. The overall tick burden is weighted by the density of each species, and split according to the 98:2 ratio of larvae to nymphs found by Gilbert et al. (2000).

woodland density, bank voles were approximated at 1200 per km² (Amori et al., 2008), field voles at 400 per km² (Sherratt, 2008), common shrews at 400 per km² and wood mice at 6500 per km² (Harris et al., 1995), therefore the total density for the small mammal group is 8500 per km². The density for conifer plantation is taken as half of the mixed woodland density, at 4250 per km². By finding the average tick burden for the small mammal group, weighted by density, a value of 1.64 is found. Using the larva-to-nymph ratio of 98:2 found in Gilbert et al. (2000), larval and nymphal burdens of 1.61 and 0.03 were obtained.

Passerine birds

As with small mammals, passerine birds are merged into one host group and parameterised as a whole. Again, as with small mammals, the birds within this host group have similar densities across the habitats within the model, and carry similar numbers of ticks. James et al. (2011) indexed the importance of various passerine bird species in supporting tick life and *B. burgdorferi* in Scotland. For both measures the most important five species were song thrushes

Species	Average density (per km²)	Larval burden (per host)	Nymphal burden (per host)
Blackbird	10.5	11.11	0.37
Chaffinch	40	0.86	0.04
Dunnock	11.5	2.56	0.69
Greenfinch	4	0.37	0.05
Song thrush	4	9.00	1.00
Overall	**70**	**3.11**	**0.25**

Table 3.4: The densities of the five passerine bird species identified as important to tick persistence, and their larval and nymphal burdens (adults were not found on the species listed). The overall tick burdens are weighted by the density of each species.

(*Turdus philomelos*), blackbirds (*Turdus merula*), dunnocks (*Prunella modularis*), greenfinches (*Chloris chloris*) and chaffinches (*Fringilla coelebs*). From James et al. (2011), it is assumed in the model is assumed that all other passerine birds have an insignificant effect on the models presented within this thesis. The study also gives the observed mean larval and nymphal burdens of these species, shown in table 3.4. Adult ticks were not found on passerine birds in Scotland by James et al. (2011), and so the adult burden for the passerine bird group is set to 0.

In order to have parameters for the passerine bird group as a whole, the tick burdens need to be weighted by the density of each bird species. Bird densities were found by taking the average densities from the Bird Breeding Survey (British Trust for Ornithology, 2016c), and are listed in table 3.4. The sum of these densities, 70 per km², is taken as the density of passerine birds in mixed woodland, with the density in conifer plantation taken as half of the mixed woodland density, at 35 per km². Passerine birds are assumed in the model not to be important tick hosts in non-wooded (open) habitats because both passerines and ticks tend to be less abundant in other habitats.

3.2.2 *Model equations*

$$
\begin{aligned}
\frac{dL_A}{dt} &= -S\left[F(t) \times P(t) \times L_A(t), L_{host}\right] - b_L L_A(t) \\
\frac{dL_D}{dt} &= S\left[F(t) \times P(t) \times L_A(t), L_{host}\right] - b_{WL} L_D(t) \\
\frac{dN_A}{dt} &= -S\left[F(t) \times P(t) \times N_A(t), N_{host}\right] - b_N N_A(t) \\
\frac{dN_D}{dt} &= S\left[F(t) \times P(t) \times N_A(t), N_{host}\right] - b_{WN} N_D(t) \\
\frac{dA_A}{dt} &= -S\left[F(t) \times P(t) \times A_A(t), A_{host}\right] - b_A A_A(t) \\
\frac{dA_D}{dt} &= S\left[F(t) \times P(t) \times A_A(t), A_{host}\right]
\end{aligned} \tag{3.7}
$$

Initial conditions at the start of each year:

$L_A(0) = a_T A_D(52)$; $L_D(0) = 0$; $N_A(0) = L_D(52)$; $N_D(0) = 0$; $A_A(0) = N_D(52)$; $A_D(0) = 0$.

Where:

$$
\begin{aligned}
T(t) &= \left(\frac{b-a}{2} \times \sin\left(\frac{t}{2.6\pi} - 0.5\pi\right)\right) + \frac{a+b}{2} \\
F(t) &= \begin{cases} 0 & T(t) \leqslant T_1, \\ \frac{T(t)-T_1}{T_2-T_1} & T_1 < T(t) \leqslant T_2, \\ 1 & T_2 < T(t) \end{cases} \\
P(t) &= \frac{1}{1 + exp\left[\frac{3}{4}(8 - T(t))\right]} \\
S(x, K) &= \frac{wK}{w + (K-w)exp\left(\frac{ln\left[\frac{w}{19(K-w)}\right]}{8K} x\right)} - w
\end{aligned} \tag{3.8}
$$

3.2.3 *Creating model predictions*

Using ArcGIS 10 (Environmental Systems Research Institute, 2014), all spatial environmental data used over Scotland were split into a 3km × 3km grid, with each cell containing the data for the maximum and minimum annual temperature, as well as the habitat type.

The cells were categorised by temperature and habitat types into groups, chosen so that each group covered approximately 100 cells. The full details of these 34 groups can be seen in appendix A.

For each of these groups a simulation was run on Mathematica Version 9 (Wolfram Research Inc., 2013) using appropriate host densities for that habitat (see table 3.2). Using these values of temperature, host densities and habitat categories, simulations were run for 70 years, while minimum and maximum temperatures were increased linearly over this time period in order to represent UK Climate Projections data (Jenkins et al., 2009). As the average annual temperature in Scotland is estimated to increase by 1-4°C by the 2080s, depending on emissions scenario, the models were run under three climate change scenarios: low, medium and high climate warming scenarios, with temperature rises of 1°C, 2.5°C and 4°C respectively. For comparison, simulations were also run with no change in temperature to represent the current climate. The full explanation for the choice in climate warming scenarios is provided in appendix A. It was assumed that each cell's habitat doesn't change over the time period, nor does host density. This is, of course, unlikely to occur in real life; this simplifying assumption is made in order for the effect of climate warming to be seen with full clarity, rather than being potentially blurred with the effects of habitat and host density change.

The model predicted an increase in tick abundance with climate warming (figure 3.5). Most areas which were predicted to not currently maintain ticks (white areas in figure 3.5 (a)), such as high altitude sites were predicted to be able to sustain ticks in 70 years' time under the medium and high climate warming scenarios. All but two of the habitat groups used (which are listed fully in appendix A) were predicted to have nymph densities of at least 1000 per km^2. The number of expected medium and high tick density sites was also predicted to increase with climate warming.

To quantify this more precisely, the mean nymph density across all cells and for the different habitat types run in the model can be considered (figure 3.6). Under all climate change scenarios the model predicted a marked increase in the mean nymph density overall by the 2080s, with a predicted tick density increase of 26.1% for the low temperature rise scenario and a predicted tick density increase of 98.7% for the high temperature rise scenario compared to current temperatures. Comparison of the predicted mean nymph density between the five types of habitat shows that semi-natural mixed woodland is predicted to contain considerably higher densities of ticks than the other habitat categories, with 2.4 times the number of nymphs than in the habitat with the second-highest predicted tick densities (conifer plantation).

For current temperatures, heather moorland areas were predicted to support considerably fewer nymphs than both mixed woodland and conifer plantation, but for the higher climate warming scenarios, this gap was predicted to be reduced (figure 3.6). This is likely to be because heather moorland tends to occur at higher elevations (and therefore cooler climates) than forested areas. This suggests that it is the cool climate which is currently limiting growth in

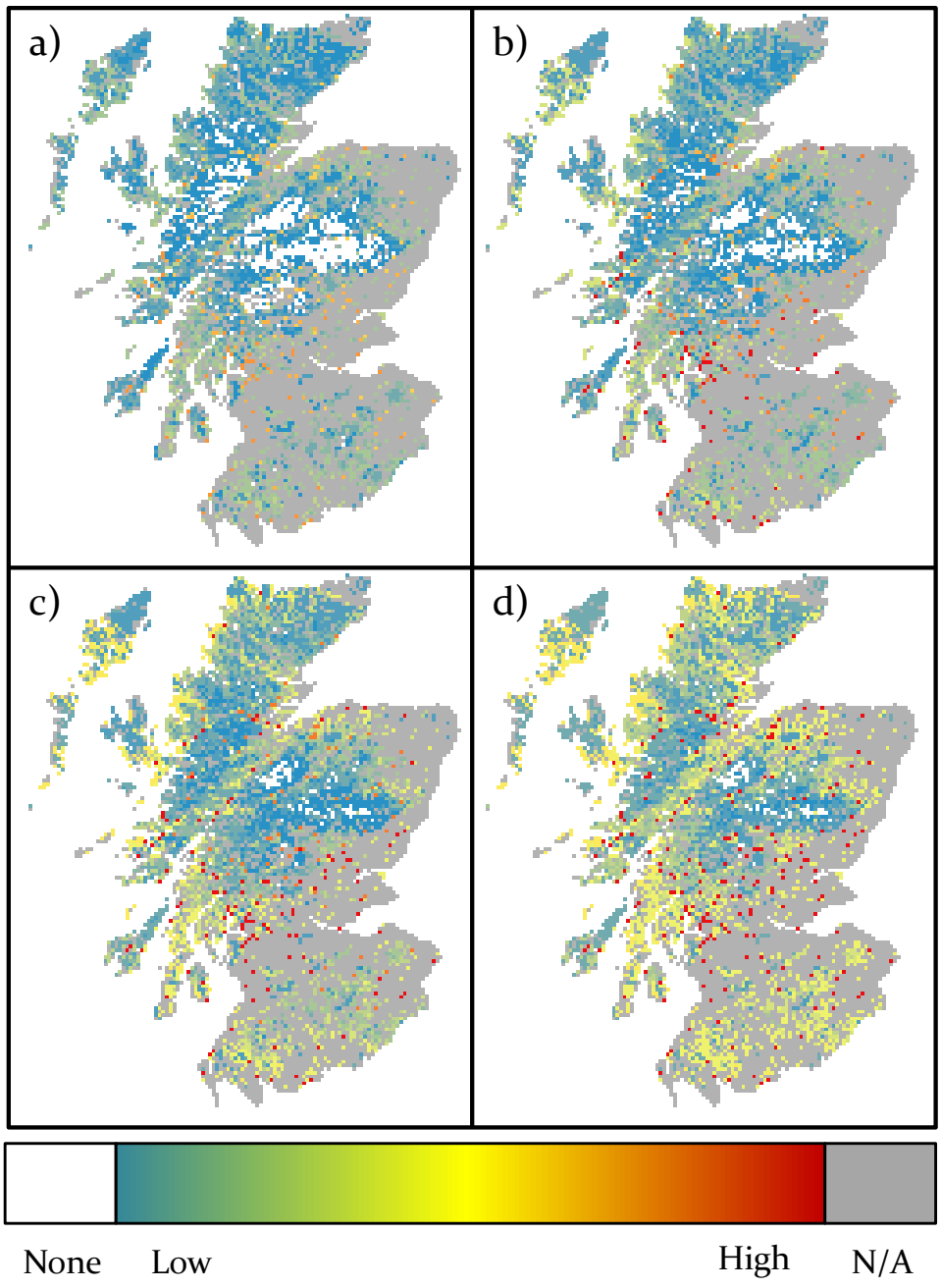

Figure 3.5: Maps of predicted tick densities after 70 years under the following climate warming scenarios: (a) no change in temperature (b) a final temperature increase of 1°C, (c) a final temperature increase of 2.5°C and (d) a final temperature increase of 4°C.

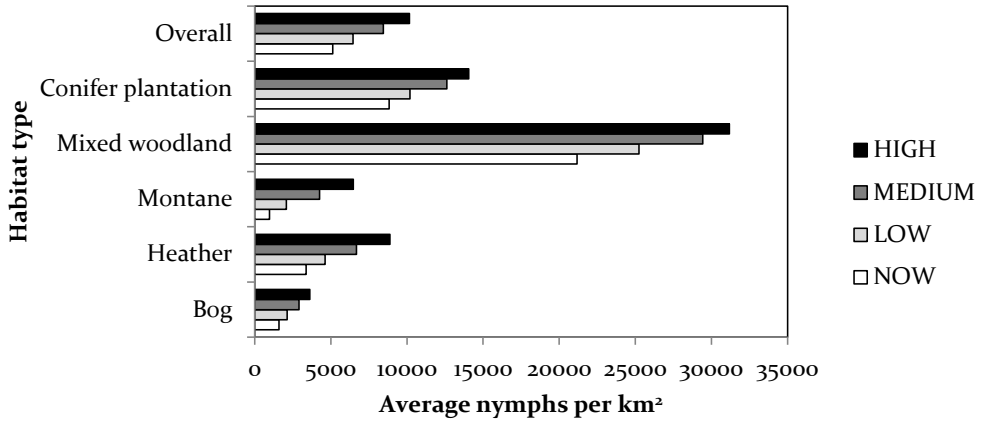

Figure 3.6: Predicted mean nymph density for each habitat modelled, plus the overall mean, under each climate change scenario (high, medium and low emissions, and no warming representing the current climate).

tick densities on many moorlands, and climate warming will allow future tick population growth in these areas, whereas in woodland areas temperature is less of a limiting factor for tick activity.

Montane areas were predicted to contain the lowest densities of ticks of all the habitat categories for current temperatures. This is to be expected as the climate is generally too cold for much tick activity at higher altitudes (see Gilbert 2010 for empirical data showing a dramatic climate-driven decrease in tick abundance with increasing altitude in Scotland). However, under climate warming scenarios, the model predicts that many montane areas will experience an increase in tick density, such that some montane areas are predicted to have higher tick densities than blanket bog habitats. This again suggests that montane tick densities are currently constrained by temperature whilst, in contrast, tick density in blanket bog habitats is constrained by other factors unrelated to climate, such as host densities. Indeed, that blanket bog contains low tick densities partly because

it lacks suitable hosts, especially deer, is supported by empirical data (Gilbert, 2013).

The dynamic GIS model developed in this chapter is the first step in integrating spatial and environmental information with models of population dynamics to allow predictions about how climate and land use changes might affect disease risk. Whilst this model makes a number of simplifying assumptions, as all models need to, it has allowed areas which are likely to see an increase in tick densities to be identified. Additionally, it has provided predictions that increases in temperature are likely to allow ticks to persist in some areas which cannot currently sustain them. It also allows the interactions between hosts and temperature to be teased apart and which areas have tick densities that are currently limited by temperature and which are currently limited by hosts to be identified. It is predicted by the model that, as temperatures rise, the warmest heather moorland areas and montane regions will increase their tick populations to a greater extent than will forested areas. This is because the model suggests that tick population growth on moorland and montane areas is limited by climate, whereas tick populations in lower elevation forested areas are limited more by other factors such as host abundance. The distinction between temperature- or host-limited tick population growth is an important one highlighted by the model and is crucial for making predictions of future tick and tick-borne disease prevalence under scenarios of different types of environmental change.

The model was run here for Scotland but is easily applicable to other areas and could be run on any map with data on minimum and maximum temperatures, habitat type and host communities. However, adjustments should also be made to the questing function ($P(t)$) to allow for the observed effect that a lower proportion of ticks from warmer climates are active at cooler temperatures than

are ticks from cooler climates (Gilbert et al., 2014). It may also be necessary to introduce a mechanism which allows ticks to feed twice within the same year for warmer climates where interstadial development times are faster (discussed in chapter 6).

The model presented here combined a dynamic tick population model with GIS information to visualise predicted tick densities at a national scale. However, tick densities may or may not relate to tick-borne disease risk, depending on the pathogen in question, the relative densities of competent and incompetent transmission hosts, as well as tick density. Therefore, the next two chapters will introduce mechanisms that describe the transmission of pathogens between vector and host, which will allow predictions to be made for disease risk across Scotland.

3.4 SENSITIVITY ANALYSIS

To gauge the sensitivity of the tick lifecycle model to its parameters, the two methods outlined in Watts et al. (2009) were used (described below). For each method, the output chosen was the final density of each tick instar after running the model over a 70 year time period.

3.4.1 *Method 1*

For this method, the model was run with each parameter varied in turn by ±10% in order to see whether they had a disproportionate effect on the model output. Those which had an effect of at least 1% are shown on table 3.5.

The only parameter/instar interaction which has a change of above 10% is that between larvae and L_{host}, the feeding limit for that stage. This, combined with the fact that only one other parameter has a noticeable effect on larvae

Decrease of 10%	**Larva**	**Nymph**	**Adult**	**Increase of 10%**	**Larva**	**Nymph**	**Adult**
T_1		1.0	2.0	T_1		-2.2	-3.2
T_2		2.0	3.3	T_2		-2.0	-3.3
b_L				b_L			
b_N		4.1	2.4	b_N		-3.9	-2.5
b_A			1.3	b_A			-1.3
b_{WL}	2.4	1.8	1.1	b_{WL}	-2.3	-1.8	-1.1
b_{WN}		1.0		b_{WN}		-1.0	
a_T				a_T			
w				w			
L_{host}	-10.4	-8.1	-5.4	L_{host}	10.4	7.4	4.1
N_{host}		-2.9	-1.7	N_{host}		2.1	1.2
A_{host}			-5.5	A_{host}			3.5

Table 3.5: The predicted percentage change in larva, nymph and adult density of altering the tick lifecycle model parameters by ±10%. Changes below 1% are not shown.

density, suggests that of the three instars, larvae are the most influenced by the potential meals available to them. Indeed, it appears that larva densities are largely unaffected by factors such as temperature or the number of eggs laid. Even for nymphs and adults, L_{host} continues to be one of the parameters with the most impact on density. This suggests that unlike larvae, these two stages are strongly influenced by the number of ticks reaching them from the previous stage. However, the effect is less pronounced, with temperature and mortality rates also having noticeable, if lower, effects.

With only one parameter/instar interaction having a disproportionate effect, and with the instar involved being separate to the one used in the model's predictions, it shows that the model output is relatively stable, providing reasonable faith in the predictions made. Indeed, the three parameters with the strongest effects, the weekly feeding limits for each stage (L_{host}, N_{host} and A_{host}), are

Parameter	Larva	Nymph	Adult
T_1		-0.16	-0.28
T_2		-0.21	-0.41
b_L			
b_N		-0.42	-0.31
b_A			-0.16
b_{WL}	-0.18	-0.15	
b_{WN}		-0.14	
a_T			
w			
L_{host}	0.97	0.80	0.56
N_{host}		0.23	0.14
A_{host}			0.54

Table 3.6: The Pearson's correlation coefficient of tick lifecycle model parameters with the densities of larvae, nymphs and adults from 1000 simulations where each parameter was randomly selected from within ±1% of the original value. Only correlations with an absolute value larger than 0.1 are shown.

composites of multiple values estimated from extensive research, so the fact that the model output relies so heavily on them is not a major issue.

3.4.2 *Method 2*

For this method, the model was run 1000 times, with the parameter values randomly selected from a range of ±1% within the values listed in table 3.1. These parameters were then correlated with the final levels of the three tick instars. Those correlations with an absolute value larger than 0.1 are presented in table 3.6.

The correlation between larva density and L_{host} is extremely high, at 0.97. For nymph density, L_{host} still have a high correlation, at 0.80, whilst the correlation

with nymph mortality is -0.42. For the density of adult ticks, L_{host} is still the parameter with the highest correlation, at 0.56, followed by A_{host} at 0.54.

3.4.3 *Sensitivity analysis summary*

Both methods of sensitivity analysis highlight the importance of the weekly feeding limit parameters on model output. In particular, the limit for larvae (L_{host}) was particularly influential, as it changed larval density by a disproportionate amount under Method 1, and under Method 2 explained 94.1% of variation in larval density, 64.0% of variation in nymphal density and 31.4% of variation in adult density. This parameter is composed of multiple values combined; therefore the scope for an erroneous value to skew the model output is reduced. Overall, the model appears relatively robust to changes in parameter values.

3.5 SUMMARY

This chapter aimed to introduce an original model for the *I. ricinus* lifecycle, dependent on environmental factors, which can be then used to predict the influence of climate change on tick density across Scotland.

The model was developed by focusing on the key mechanism of ticks feeding on blood hosts, and limiting the number which can feed in any given week based on the number of available hosts and therefore meals. By running the model for low, medium and high climate warming scenarios, the impact of temperature could be seen. Additionally, by splitting Scotland up into cells based on habitat type, the differences in habitat influence on predicted tick density could be determined.

For current temperatures, the highest tick densities were predicted to occur in mixed woodland habitats, followed by conifer plantation. The lowest tick density was predicted to occur in montane habitats. For all habitat types, tick density increased with higher climate warming, with an overall increase of between 26.1-98.7% in nymph density depending on the climate warming scenario. However, this increase was not equal across all habitat types. For areas such as mixed woodland, conifer plantation and blanket bog the rise in tick density was relatively slow, whilst for areas such as montane and heather moorland the rise in tick density was relatively fast. This suggests that whilst temperature will have an amplifying effect on tick density, this amplification will vary depending on further factors, such as host density. As temperature and habitat type have clear influences on the model output, this suggests that the model created is successful in meeting the aim of the chapter. The model created in this chapter will be a crucial building block for predicting the role of climate change on tick-borne disease risk first for Louping-ill (chapter 4) then for Lyme disease (chapter 5).

4

INTRODUCING PATHOGEN DYNAMICS TO THE TICK LIFECYCLE MODEL

4.1 INTRODUCTION

Red grouse (*Lagopus lagopus scoticus*), a gamebird, and sheep (*Ovis aries*) are livestock which are both of economic importance in Scotland. Grouse shooting was estimated to contribute £23.3 million to the GDP of Scotland in 2010 (Game and Wildlife Conservation Trust Scotland, 2010) whilst sheep were estimated to account for 6% of income from Scottish farming in 2014 (The Scottish Government, 2015). However, both red grouse and sheep can be infected with Louping-ill virus (LIV), a flavivirus spread by the sheep tick (*Ixodes ricinus*) which causes illness and death in both grouse and sheep. 78% of red grouse infected with LIV died in experimental conditions (Reid, 1975) whilst sheep mortality varies with farming practices (Hudson, 1992).

As explored in chapter 3, *I. ricinus* density and range are likely to increase with climate warming. As the climate across Scotland is projected to rise by several degrees before the end of this century (Jenkins et al., 2009), there are likely to be implications of climate warming on LIV risk. Therefore, the aim of this chapter is to predict the extent and patterns of climate warming on LIV risk, which can be

used to help inform policy on LIV risk mitigation strategies for grouse and sheep managers. To achieve this, the temperature-driven tick lifecycle model developed in chapter 3 was adapted to reflect LIV dynamics in typical moorland habitats, in order to create predictive maps for LIV risk across Scotland for various climate warming scenarios. The aim of this model is to predict potential LIV prevalence across Scotland and how this might change in response to climate change. The predictions made by the model are visualised spatially through the use of GIS mapping, to give an indication of which areas of Scotland are most suited for hosting LIV.

4.2 MODEL DEVELOPMENT

The host system used is akin to that used in Gilbert et al. (2001), where red grouse are the competent transmission hosts, and red deer (*Cervus elaphus*) and mountain hares (*Lepus timidus*) are solely tick-carrying hosts. In practice it is possible to remove sheep from the system through vaccination (Laurenson et al., 2007), and therefore sheep are not included in this model. However, they could be added as viraemic hosts to this model where necessary or, in contrast, the use of acaricide-treated sheep to reduce tick abundance in the environment could also be added to the model if needed (Porter et al., 2011). As this model is introducing LIV dynamics to the tick lifecycle model, only the most direct form of pathogen transmission is considered, namely from ticks biting grouse where either tick or grouse is infected. It is recognised that other forms of transmission may be important, such as non-viraemic transmission between ticks co-feeding on hares (Jones et al., 1997) and infection through grouse ingesting infected ticks (Gilbert et al., 2004), and the implementation of such infection and transmission mechanisms are discussed in chapter 5.

Parameter	Value	Definition and justification
T_1	8 (larvae); 5 (nymphs and adults)	Temperature at which ticks begin to emerge from overwintering. Randolph (2008).
T_2	12 (larvae); 9 (nymphs and adults)	Temperature at which all ticks have emerged from overwintering. Randolph (2008).
a_G	0.7175	Birth rate of grouse, for the weeks 19-22 within the model. Hudson (1992).
s_G	$\frac{0.522}{c}$	Density-dependent constraint on grouse. Chosen such that the grouse population would run to carrying capacity (c) in a disease-free system.
b_G	0.008	Mortality rate of grouse. Hudson (1992).
p	0.2	Aggregation parameter for nymphs on grouse. Chosen to allow the pathogen to persist.
α	0.8	Infected-induced mortality rate of grouse. Reid (1975).
σ	0.2	Recovery rate of grouse. Reid (1975).
g_L	15	Larval burden of grouse (Gilbert unpublished).
g_N	4	Nymphal burden of grouse (Gilbert unpublished).

Table 4.1: Table of parameters for the LIV model. All unmentioned parameters remain as in chapter 3.

The Louping-ill model is based on the tick lifecycle model presented in chapter 3. Therefore, within the model, each of the three tick instars (larvae, nymphs and adults) are split into two classes: active, describing those which are yet to feed in the current year, and developing, describing those which have fed and are either moulting into the next instar (larvae and nymphs) or are laying eggs (adults). As before in order to apply this model spatially, Scotland was split into 3km^2 cells, which were grouped by habitat type and temperature, the full details of which are presented in appendix A and are listed in table 4.2.

In order to expand the tick lifecycle model presented in chapter 3, it is necessary to consider the extra features and equations that need to be added to the model to allow for the existence of LIV in the system. As only larvae and nymphs feed on grouse, and transovarial transmission of LIV has been shown to be at best negligible in *I. ricinus* (Hudson, 1992), transmission can only occur to ticks when larvae or nymphs feed on infected grouse and from ticks to grouse when infected nymphs feed on them. Therefore, the developing larva class is split into susceptible ($L_{DS}(t)$) and infected ($L_{DI}(t)$) states.

Active nymphs are also split into susceptible ($N_{AS}(t)$) and infected ($N_{AI}(t)$) states. However, because the model assumes that grouse cannot feed adult ticks (see chapter 3), and because there is no transovarial LIV transmission to larval ticks, the model assumes that the infection status of ticks is irrelevant after they have fed at the nymphal stage. Therefore, the developing nymph state and both adult states (active and developing) are unchanged from the tick lifecycle model (chapter 3).

In the tick lifecycle model all hosts were assumed to be at constant density. In this model transmission host (grouse) dynamics and infection status need to be included. For equations representing the LIV infection status of grouse, susceptible ($G_S(t)$), infected ($G_I(t)$) and recovered ($G_R(t)$) states are used. Age-specific equations for grouse have been shown to have an effect on LIV dynamics by Porter et al. (2013b) with models used to predict the effect of treating grouse with acaricide. However, treating grouse with acaricide is not a routine practice for tick control and has been used only in scientific experiments. Therefore, this model uses non-age-structured SIR equations similar to those used in Gilbert et al. (2001). A schematic of the equations within this model can be seen in figure 4.1.

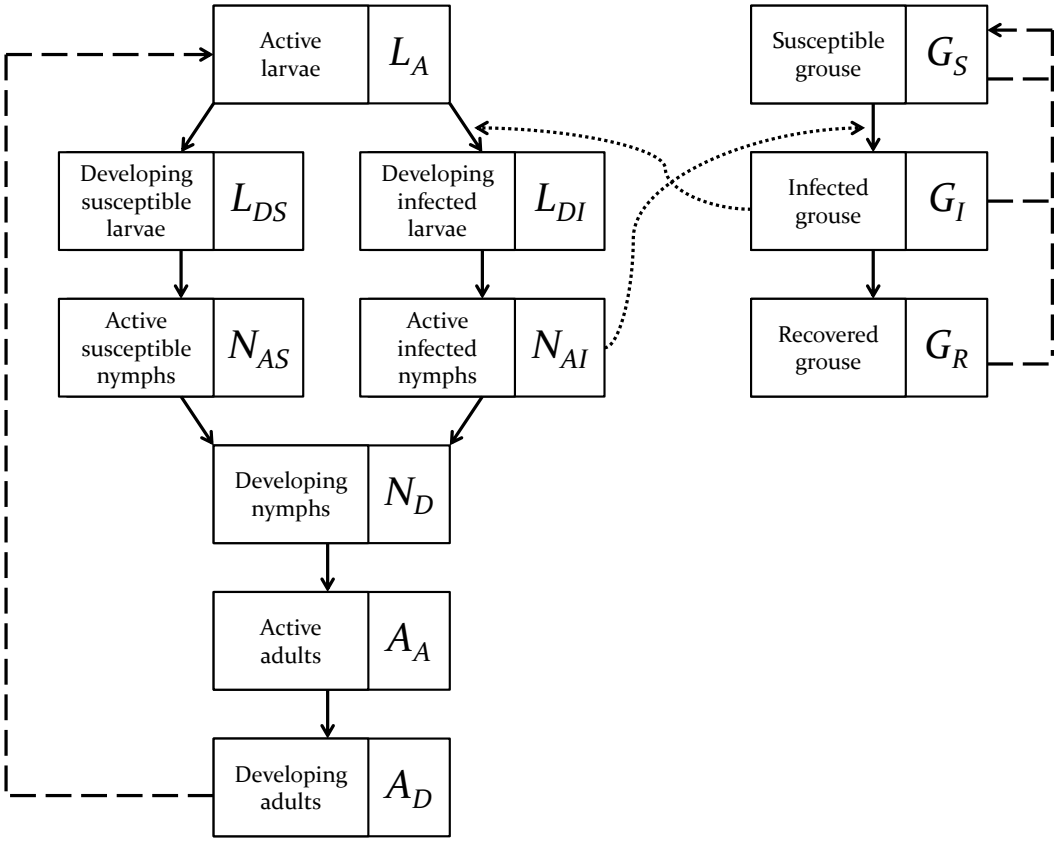

Figure 4.1: Schematic of the equations used within the LIV model, with routes of progression. Solid lines indicate routes of progression within the tick or grouse lifecycle, dashed lines represent adults giving birth, and dotted lines indicate routes of pathogen transmission between ticks and grouse.

In line with such models as those presented by Hudson et al. (1995), Norman et al. (1999) and Gilbert et al. (2001), and in the absence of evidence contrary, it is assumed that all tick-grouse interactions, where one of the two is infected with LIV, result in the pathogen being transmitted to the other.

In order to simplify the equations used, two ratios were introduced:

- ϕ: the proportion of blood meals available for larvae in a given week (L_{host}) that come from infected grouse. Calculated by equation 4.1, where g_L is the larval burden of grouse, as estimated by table 4.1.

$$\phi = \frac{G_I(t) \times g_L}{L_{host}} \tag{4.1}$$

- θ: the proportion of active nymphs which are infected. Calculated by equation 4.2, such that $N_{AS}(t) + N_{AI}(t) \neq 0$.

$$\theta = \frac{N_{AI}(t)}{N_{AS}(t) + N_{AI}(t)} \tag{4.2}$$

4.2.1 *Tick dynamics*

As grouse are only infective for a week (Reid, 1975), the only way in which larvae can receive the pathogen from grouse is if that grouse has been infected by a feeding nymph within the same week. Therefore, the timing of larval and nymphal feeding is crucial in modelling the pathogen transmission. Whilst the tick lifecycle model used the same threshold for tick emergence of 7°C for all instars, as suggested by Perret et al. (2000), Randolph (2004) observed that whilst nymph and adult ticks indeed emerge at the 7°C threshold previously used, larvae are estimated to emerge at the later threshold of 10°C. As the study by Randolph (2004) was undertaken in the UK, whilst that by Perret et al. (2000) was undertook in Switzerland, the former was deemed to be more relevant for modelling tick behaviour in Scotland. Therefore, for the LIV model the model assumes initial emergence from over-winter diapause at 7°C for nymphs and 10°C for larvae. Therefore, rather than using the same emergence-temperature function for all stages, two are needed; one for larvae ($F_L(t)$) and one for nymphs

and adults ($F_{NA}(t)$). They both take the same format as the emergence function used in the tick lifecycle model, reprinted in equation 4.3.

$$F(t) = \begin{cases} 0 & T(t) \leqslant T_1, \\ \frac{T(t)-T_1}{T_2-T_1} & T_1 < T(t) \leqslant T_2, \\ 1 & T_2 < T(t) \end{cases} \tag{4.3}$$

As explained in chapter 3 T_1 and T_2 are taken as 2°C below and above the estimated threshold, since it is unlikely that all ticks of a given instar will appear at exactly the same temperature. Therefore, for $F_L(t)$ T_1 and T_2 are taken as 8°C and 12°C respectively, whilst for $F_{NA}(t)$ 5°C and 9°C are used.

It is relatively straightforward to calculate how many larvae which move into the developmental state pick up the pathogen. From the tick lifecycle model (chapter 3) the total number of active larvae finding a blood meal in a given week is given by equation 4.4.

$$S\left[F_L(t) \times P(t) \times L_A(t), L_{host}\right] \tag{4.4}$$

Therefore, the number of larvae feeding on an infected grouse, and thus picking up the pathogen at each time point, is calculated by multiplying the above equation by the proportion of blood meals from infected hosts (ϕ). It follows that the number of larvae that feed without picking up the pathogen is calculated by multiplying the above equation by the proportion of blood meals from uninfected hosts ($1-\phi$). At the end of the year the developing larvae in

the susceptible ($L_{DS}(t)$) and infected ($L_{DI}(t)$) states move into the active nymph susceptible ($N_{AS}(t)$) and infected ($N_{AI}(t)$) states respectively.

As with the tick lifecycle model presented in chapter 3, the mechanism for ticks moving from the active to the developing stage is centred on the weekly feeding limit function. This function ($S(x, K)$) gives the number of ticks which successfully feed and move to the next stage, and requires an estimation of the weekly feeding limit for each instar, calculated by estimating the total hosts in the area and the number of ticks each host can carry (full details are included in chapter 3). As the active nymph state is now split into two groups (susceptible and infected), the weekly feeding limit function cannot simply be applied to each group separately, as this would clearly allow for twice the number of nymphs to move into the developing stage in a given week than should be allowed. The limit also cannot simply be halved and applied to each group separately. To see why, consider the scenario where there are only susceptible nymphs, which should clearly behave in the same manner as all nymphs do in the tick lifecycle model. However, in this LIV model, if it is assumed that the limit was halved for infected and susceptible nymphs then only half the amount of nymphs would be able to feed in a given week. Therefore, the combined total of active nymphs has to be fed into the weekly feeding limit function. Thus, the total number moving into the developing nymph state is given by equation 4.5.

$$S\left[F_{NA}(t) \times P(t) \times (N_{AS}(t) + N_{AI}(t)), N_{host}\right] \tag{4.5}$$

As there is no evidence that carrying the pathogen affects the ability of a nymph to find a meal, the total number of infected nymphs finding a meal can

be calculated as equation 4.5 multiplied by the proportion of infected nymphs (θ) and the total susceptible nymphs finding a meal as equation 4.5 multiplied by the proportion of susceptible nymphs ($1 - \theta$).

The equations for adult ticks remain unchanged from the tick lifecycle model.

4.2.2 *Grouse dynamics*

The grouse lifecycle mechanisms included within the model are birth, infection, recovery, natural mortality and infection-induced mortality.

Lab experiments conducted by Reid (1975) found that 29 of 37 (78.3%) of grouse died when infected with LIV, with the infective period lasting approximately one week. Since the model presented within this chapter has a time unit of one week, which coincides with the infectivity period for grouse, this means that by the next time step all grouse will have either died or recovered. Slightly rounding these percentages produces disease-induced mortality and recovery rates of 0.8 and 0.2 respectively. It is assumed that any grouse which died through natural causes during the experiments in Reid (1975) were counted as those claimed by the disease, therefore there is no natural mortality rate applied to grouse within the infected class.

The model created by Porter et al. (2011) use a natural grouse death rate of 0.087 per month, which suggests the natural grouse lifespan is approximately 11.5 months. However, Hudson (1992) states that the grouse lifespan is "less than three years", which for this model is taken to be around 130 weeks (approximately two and a half years). Inverting this gives a weekly mortality rate of 0.008.

Grouse clutch sizes and hatching successes were reported by Hudson (1992), and were averaged for this model to get an annual birth-per-hen value of 5.74. Hudson (1992) demonstrates that the grouse sex ratio appears to be equal; there-

fore here this value is halved to get a value of 2.87 for the number of grouse chicks born per grouse annually. The breeding season for grouse is between April-June (RSPB, a), which is taken to be across the whole of May, which corresponds to weeks 19-22 within the model. Therefore, the annual grouse birth rate in this model is divided by four to get a weekly birth value of 0.7175. The simple function shown in equation 4.6 is multiplied by grouse birth (a_G).

$$A_G(t) = \begin{cases} 0 & t \leqslant 19, \\ 1 & 19 < t \leqslant 22, \\ 0 & 22 < t \end{cases} \tag{4.6}$$

A density-dependence parameter (s_G) is used, given by equation 4.7, where c is the carrying capacity of grouse for the habitat, and the constant 0.522 is chosen to ensure that grouse numbers run to carrying capacity in a pathogen-free system.

$$s_G = \frac{0.522}{c} \tag{4.7}$$

Parasites are generally distributed amongst hosts with a negative binomial distribution, where many hosts will have none or few ticks, but a few will have many (Anderson and May, 1978; Woolhouse et al., 1997). The distribution of ticks on red grouse is no different (Elston et al., 2001). The negative binomial distribution gives the probability of how many failed trials are expected before reaching k successes, where p is the probability of a trial being a success and r

being the number of failed trials. The probability density function for the negative binomial distribution is shown in equation 4.8 (Wolfram Mathworld, 2016).

$$P_{k,p}(r) = \begin{pmatrix} r+k-1 \\ k-1 \end{pmatrix} p^k (1-p)^r \tag{4.8}$$

Due to the assumed 100% transmission rate it is irrelevant how many infected nymphs a susceptible host has feeding on it as long as it is above zero because, for example, 1 infected nymph or 20 infected nymphs will both result in one infected grouse. Therefore, calculating the proportion of hosts that would be bitten by zero infected ticks in a given week also gives the proportion of hosts which avoid picking up the pathogen that week and by logical extension the proportion which do become infected.

When applying the negative binomial distribution to tick distribution on hosts r represents the number of ticks each host carries, p is a parameter determining the shape of the distribution and k represents the average nymphs per host. The proportion of hosts that feed zero infected ticks in a week is required, and setting $r = 0$ simplifies equation 4.8 to p^k. The average nymphs per host (k) can be calculated using the formula presented in equation 4.9, where g_N is the maximum number of nymphs allowed to feed on grouse at any one time within the model.

$$k = \frac{\frac{g_N}{N_{host}} \times \theta \times S\left[F_{NA}(t) \times P(t) \times (N_{AS}(t) + N_{AI}(t)), N_{host}\right]}{G_S(t) + G_I(t) + G_R(t)} \tag{4.9}$$

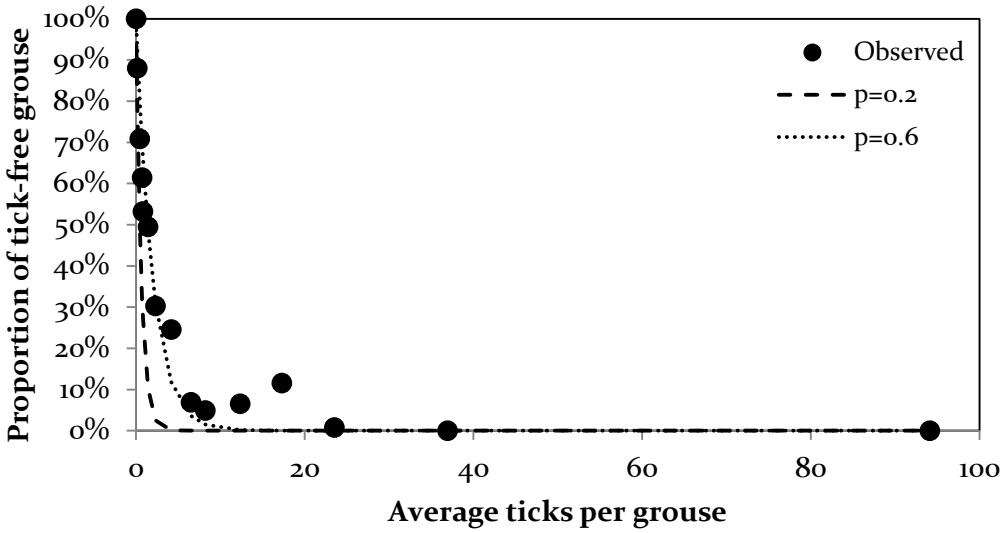

Figure 4.2: The proportion of grouse which carry no ticks compared to the average ticks per grouse. The dots represent different counts made from 1987-2000 (Gilbert unpublished), whilst the lines represent predictions made from the negative binomial distribution, where p is 0.2 (dashed) and 0.6 (dotted).

There is no obvious parallel showing how p relates to the distribution of nymphs biting grouse, so instead values were compared with empirical data collected at various locations and times (Gilbert unpublished data). For each study site within the empirical data, the average number of ticks per grouse and proportion of grouse not carrying any ticks were taken. These empirical values were then compared to the predictions the model made for various values of p. Treating p as 0.6 brought the distribution the closest to the data using the least squares method (figure 4.2). However, running the model using p as 0.6 caused the model to predict that LIV could not establish in any environment. Therefore, in order to understand the role of p in pathogen persistence, R_0 curves were estimated for various values of p through repeated simulations of the model. These can be seen in figure 4.3. The markers on figure 4.3 indicate grouse and

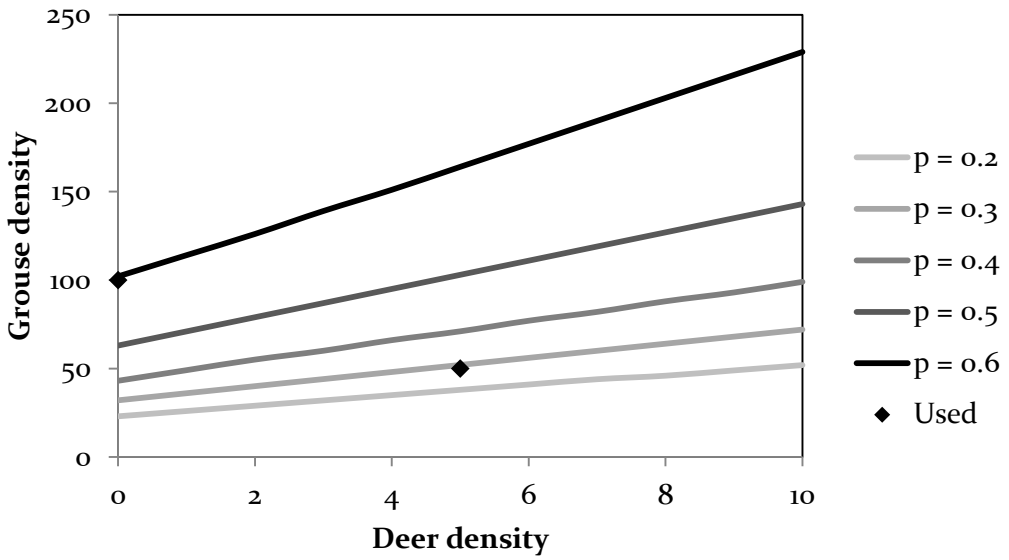

Figure 4.3: Predicted effect of grouse and deer density (per km²) on LIV persistence. Each line represents the basic reproduction number ($R_0 = 1$) of the pathogen (found through simulations) such that LIV survives above the line and dies out below. Each line represents the model outputs for various values of p, the parameter describing the negative binomial distribution of ticks among grouse. The markers represent the deer-grouse densities used heather habitats within the model.

deer density combinations which are selected as realistic scenarios, as explained in chapter 3. Therefore, p would need to be as low as 0.2 for LIV to persist in all heather moorland habitats. The aim of this model is not to provide estimations for the exact level of LIV persistence in Scotland, but rather to predict potential risk of LIV over Scotland depending on habitat and host distributions, and to predict any directional changes in LIV due to climate warming. Therefore 0.2 is used in order to allow the clearest comparison between habitats in the output. Susceptible grouse are multiplied by p^k to give the density (per km²) of grouse moving into the infected class each week.

A table of the parameters used within this model is presented in table 4.1.

4.2.3 *Model equations*

$$
\begin{aligned}
\frac{dL_A}{dt} &= -S\left[F_L(t) \times P(t) \times L_A(t), L_{host}\right] - b_L L_A(t) \\
\frac{dL_{DS}}{dt} &= (1-\phi) \times S\left[F_L(t) \times P(t) \times L_A(t), L_{host}\right] - b_{WL} L_{DS}(t) \\
\frac{dL_{DI}}{dt} &= \phi \times S\left[F_L(t) \times P(t) \times L_A(t), L_{host}\right] - b_{WL} L_{DI}(t) \\
\frac{dN_{AS}}{dt} &= -(1-\theta) \times S\left[F_{NA}(t) \times P(t) \times (N_{AS}(t) + N_{AI}(t)), N_{host}\right] \\
&\quad -b_N N_{AS}(t) \\
\frac{dN_{AI}}{dt} &= -\theta \times S\left[F_{NA}(t) \times P(t) \times (N_{AS}(t) + N_{AI}(t)), N_{host}\right] - b_N N_{AI}(t) \\
\frac{dN_D}{dt} &= S\left[F_{NA}(t) \times P(t) \times (N_{AS}(t) + N_{AI}(t)), N_{host}\right] - b_{WN} N_D(t) \\
\frac{dA_A}{dt} &= -S\left[F_{NA}(t) \times P(t) \times A_A(t), A_{host}\right] - b_A A_A(t) \\
\frac{dA_D}{dt} &= S\left[F_{NA}(t) \times P(t) \times A_A(t), A_{host}\right] \\
\frac{dG_S}{dt} &= -\left(1-p^k\right) G_S(t) - b_G G_S(t) \\
&\quad + \left[a_G \times A_G(t) - s_G \times A_G(t)\left(G_S(t) + G_I(t) + G_R(t)\right)\right] \\
&\quad \left(G_S(t) + G_I(t) + G_R(t)\right) \\
\frac{dG_I}{dt} &= \left(1-p^k\right) G_S(t) - (\alpha+\sigma) G_I(t) \\
\frac{dG_R}{dt} &= \sigma G_I(t) - b_G G_R(t)
\end{aligned}
\tag{4.10}
$$

Initial conditions at the start of each year:

$L_A(0) = a_T A_D(52)$; $L_{DS}(0) = 0$; $L_{DI}(0) = 0$; $N_{AS}(0) = L_{DS}(52)$; $N_{AI}(0) = L_{DI}(52)$; $N_D(0) = 0$; $A_A(0) = N_D(52)$; $A_D(0) = 0$; $G_S(0) = G_S(52)$; $G_I(0) = G_I(52)$; $G_R(0) = G_R(52)$.

Where:

$$
\begin{aligned}
T(t) &= \left(\frac{b-a}{2} \times \sin\left(\frac{t}{2.6\pi} - 0.5\pi\right)\right) + \frac{a+b}{2} \\
F(t) &= \begin{cases} 0 & T(t) \leqslant T_1, \\ \frac{T(t)-T_1}{T_2-T_1} & T_1 < T(t) \leqslant T_2, \\ 1 & T_2 < T(t) \end{cases} \\
P(t) &= \frac{1}{1+exp\left[\frac{3}{4}(8-T(t))\right]} \\
S(x,K) &= \frac{wK}{w+(K-w)exp\left(\frac{ln\left[\frac{w}{19(K-w)}\right]}{8K}x\right)} - w \\
A_G(t) &= \begin{cases} 0 & t \leqslant 19, \\ 1 & 19 < t \leqslant 22, \\ 0 & 22 < t \end{cases}
\end{aligned}
\tag{4.11}
$$

4.2.4 *Creating model predictions*

The same habitat categories are used as in chapter 3, however, only those with grouse present need to be considered; these comprise the 10 heather moorland habitats with grouse plus the 3 montane habitats (shown in table 4.2). As in chapter 3, it is assumed that there is no change in broad habitat type due to climate warming by the 2080s.

The Scottish climate is projected to warm by 1-4°C by the 2080s depending on whether a low, medium or high emissions scenario was projected (Jenkins et al., 2009). Therefore, the model was run for each habitat group for the following climate warming scenarios, as in chapter 3:

Code	Habitat type	Minimum temp (°C)	Maximum temp (°C)
HA1	Heather moorland (high grouse, no deer)	0.75	11.41
HA2	Heather moorland (high grouse, no deer)	1.53	12.28
HA3	Heather moorland (high grouse, no deer)	2.36	12.80
HA4	Heather moorland (high grouse, no deer)	3.48	13.19
HA5	Heather moorland (high grouse, no deer)	4.45	13.70
HB1	Heather moorland (low grouse, low deer)	0.28	11.00
HB2	Heather moorland (low grouse, low deer)	1.34	11.91
HB3	Heather moorland (low grouse, low deer)	1.97	12.48
HB4	Heather moorland (low grouse, low deer)	2.62	13.10
HB5	Heather moorland (low grouse, low deer)	3.93	13.78
M1	Montane	-1.03	8.91
M2	Montane	0.22	9.86
M3	Montane	1.85	10.96

Table 4.2: List of the 13 habitat groups in the LIV model. The code for each group refers to its habitat type and where it ranks on temperature, and is used for ease of reference. The full details of the creation of the groups is given in appendix A

- Current temperatures, for comparison
- Current temperatures + 1°C, as a low climate warming scenario
- Current temperatures + 2.5°C, as a medium climate warming scenario
- Current temperatures + 4°C, as a high climate warming scenario

Unlike the tick lifecycle model, which started at current temperatures and rose to the target temperature over 70 years, each trial of the LIV model began at the target temperature, and ran for 100 years on Mathematica Version 9 (Wolfram Research Inc., 2013). This is because there are potentially habitats where LIV would not persist in current temperatures due to reduced tick activity, but with climate warming these areas might become warm enough for tick activity and therefore for the pathogen to persist, if there are enough transmission hosts. There

is not currently a mechanism in the model for ticks to move into an area if it becomes suitable, taking this approach and initialising the model with ticks and pathogen in all areas provides a solution to this. The model was run for 100 years to allow the system to head towards a stable state. The model starts with 10% of nymphs carrying the infection, and all grouse susceptible.

The behaviour of the model was investigated under the conditions where temperatures increase beyond the 4°C used as the highest climate warming scenario. To achieve this, the coldest group for each habitat category (HA1, HB1 and M1; see table 4.2) were run for temperatures starting at their current level, and increasing in 1°C increments, until finally being run for a temperature increase of 10°C. This allows the behaviour of the model in relation to temperature to be clearly understood.

Additionally, in order to test whether the model exhibits a "dilution effect" (whereby the increased presence of deer can reduce LIV in the system, as infected ticks waste their bites on incompetent transmission hosts), such as that found by Norman et al. (1999) in a similar LIV system, the model was run for a variety of grouse and deer density combinations. The model was run for grouse densities starting at 10 per km², and increasing in 10 per km² increments until reaching 100 per km², and deer densities starting at 0 per km², and increasing in 1 per km² increments until reaching 10 per km². For this, the warmest heather group was used (HA5) under current climates.

4.3 Model predictions and discussion

4.3.1 *Louping-ill virus prevalence*

As the pathogen-induced mortality rate of grouse infected with LIV is high (up to 80%, Reid 1975), any attempt to measure the prevalence of the pathogen by using

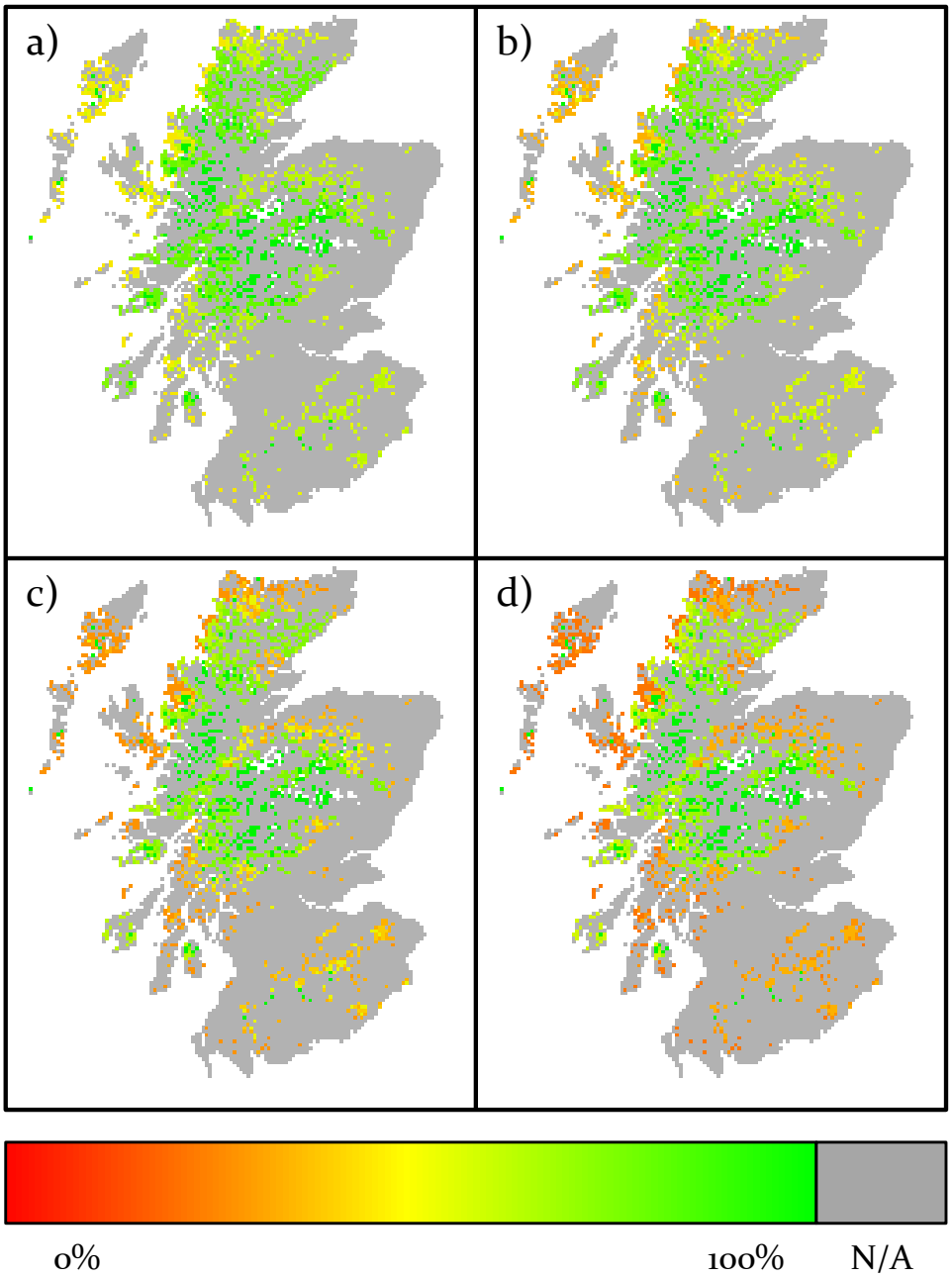

Figure 4.4: The predicted grouse survival across Scotland for the four temperature scenarios: (a) current temperatures, (b) low increase, (c) medium increase and (d) high increase. Grey cells indicate areas where the model is not run because red grouse do not exist due to inappropriate habitat. Maps created with ArcGIS 10 (Environmental Systems Research Institute, 2014).

the proportions of either infected ticks or infected grouse may be distorted by these grouse deaths. Consider a scenario where the pathogen persists; the grouse population will be rapidly reduced, with resistant grouse becoming dominant in the grouse population. This is a reduction in the total number of hosts who can transmit the pathogen, which will in turn sharply reduce the number of ticks which contract the pathogen from grouse. All of which will contribute to a low value of pathogen prevalence, therefore making it difficult to distinguish between areas where LIV persistence could sharply reduce the density of grouse and areas where LIV persistence has no major effect on grouse density. Instead, here, the suitability of an area for LIV to persist is measured by the percentage of the grouse population (carrying capacity) that survives the simulation after the model is run for 100 years. The model is set up so that the grouse population would stay at their carrying capacity without LIV present; and thus LIV is the only factor in the model preventing them reaching carrying capacity, so it can be assumed that there is an inverse relationship between the final number of surviving grouse and pathogen prevalence. Therefore, where low grouse survival occurs, it may be said that there is a higher LIV risk, and vice versa.

Figure 4.4 shows the predicted grouse survival across Scotland for the four climate warming scenarios (current climate, and climate projections under the low, medium and high emission scenarios). A clear trend that can be seen from these maps is that the pathogen appears to be most prevalent in coastal areas and least prevalent in the centre of the country. As temperatures increase this difference is exaggerated further, with parts of the north-west coast in particular predicted to have the highest LIV risk.

By breaking down the results by habitat group, the causes of these trends can be further understood. Figure 4.5 shows the grouse survival for the thirteen

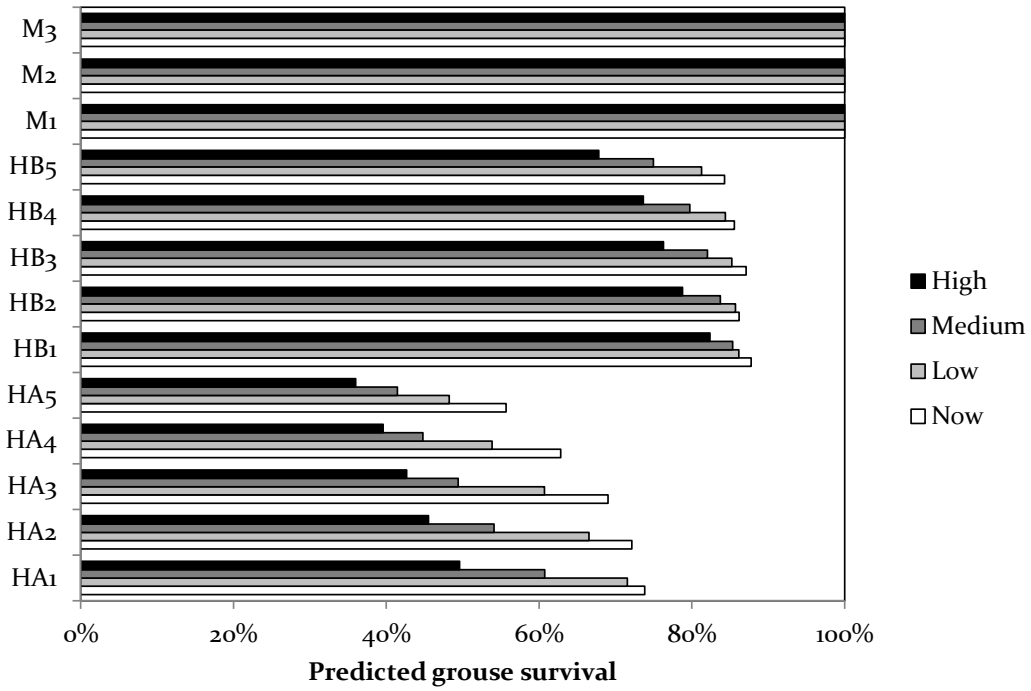

Figure 4.5: The predicted grouse survival for each temperature-habitat scenario. Survival is calculated as the density of grouse at the end of a 100-year simulation with LIV present, as a proportion of the grouse density in a disease-free state. The labels on the y-axis refer to the habitat groups used. The labels on the y-axis refer to the habitat groups used, listed in table 4.2

habitat groups, under each climate warming scenario. Firstly, LIV does not persist in montane habitats under any of the scenarios. This should not be surprising; these areas showed a lower average tick density (figure 4.6) due partly to the colder climate at high altitudes, and have the lowest grouse carrying capacity of the habitat types (Gilbert, 2010) where the model was run. However, the cold climate at high altitudes is not the only reason why montane habitats remain areas of low LIV risk; montane areas under the high climate warming scenario have a higher tick density than, for example, heather areas under the low climate warming scenario. As grouse density within the model is taken as 20 per km² in montane habitats, and 50 per km² in the low-grouse heather habitats, the low

Climate warming scenario	Now	Low	Medium	High
No risk	15.81%	15.81%	15.81%	15.81%
Low risk	36.38%	36.38%	28.98%	6.26%
Medium risk	37.08%	28.98%	16.05%	30.12%
High risk	10.74%	18.84%	39.17%	47.81%
Average grouse survival	**78.88%**	**75.13%**	**69.09%**	**63.62%**

Table 4.3: The percentage of cells where the model was run which fall into the four risk groups: no risk (where grouse survival is 100%), low risk (where grouse survival is between 80-100%), medium risk (where grouse survival is between 60-80%) and high risk (where grouse survival is below 60%). The average grouse survival across all cells is also shown.

density of grouse appears to be the dominant factor in explaining why LIV does not persist at high altitudes.

Grouse survival can be banded into four risk groups: no risk (where grouse survival is at 100%), low risk (where grouse survival is between 80-100%), medium risk (where grouse survival is between 60-80%) and high risk (where grouse survival is below 60%). Table 4.3 shows the proportion of cells where the model was run which fall into each risk group, as well as the average survival across the whole of Scotland for each climate warming scenario. In table 4.3, the 15.81% which always remain in the no risk group are the montane cells, meaning that all the heather moorland cells are in the low, medium and high risk groups. The proportion of cells in the high risk group increases by a factor of 1.8 from the current climate to the low climate warming scenario (from 10.74% of all cells where the model was run to 18.84%). This increase is even more dramatic for the medium and high climate warming scenarios, increasing by factors of 3.6 (up to 39.17%) and 4.5 (up to 47.81%) respectively. As only 84.19% of cells run in the model are heather moorland, it can be said that 57% of heather moorland habitats containing grouse are predicted to be of high risk under a temperature rise of 4°C.

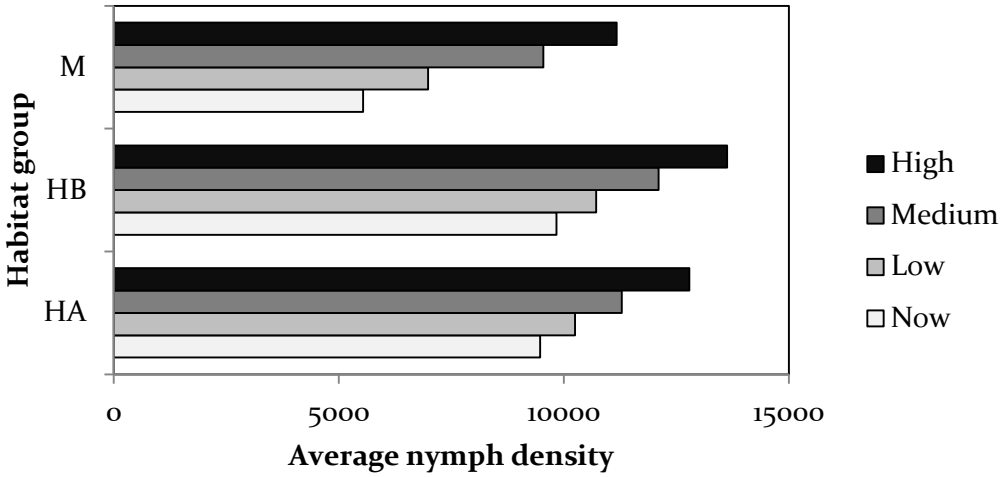

Figure 4.6: The predicted nymph density averaged across each habitat type for each climate warming scenario. The habitat group codes are explained in table 4.2

The average grouse survival across all cells (table 4.3) is predicted to decrease from 78.88% under current climates to 75.13% under the low climate warming scenario, 69.09% under the medium climate warming scenario and 63.62% under the high climate warming scenario. Measured in comparison to current climates, grouse survival is predicted to decrease by 4.76% for the low climate warming scenario, 12.41% for the medium climate warming scenario and 19.35% for the high climate warming scenario.

For all heather groups there is a clear decrease in grouse survival with climate warming. In order to fully explore this relationship the model was run for temperature increases from 0-10°C, starting at the coldest temperature for each habitat type (HA1, HB1 and M1, as per the groups listed in table 4.2) (figure 4.7). From this it is clear that montane habitats are predicted to continue having low risk of LIV under any temperature scenario. However, this is dependent on current host densities being maintained; in reality higher temperatures may see some hosts occupying higher-altitude areas in higher densities, which will change

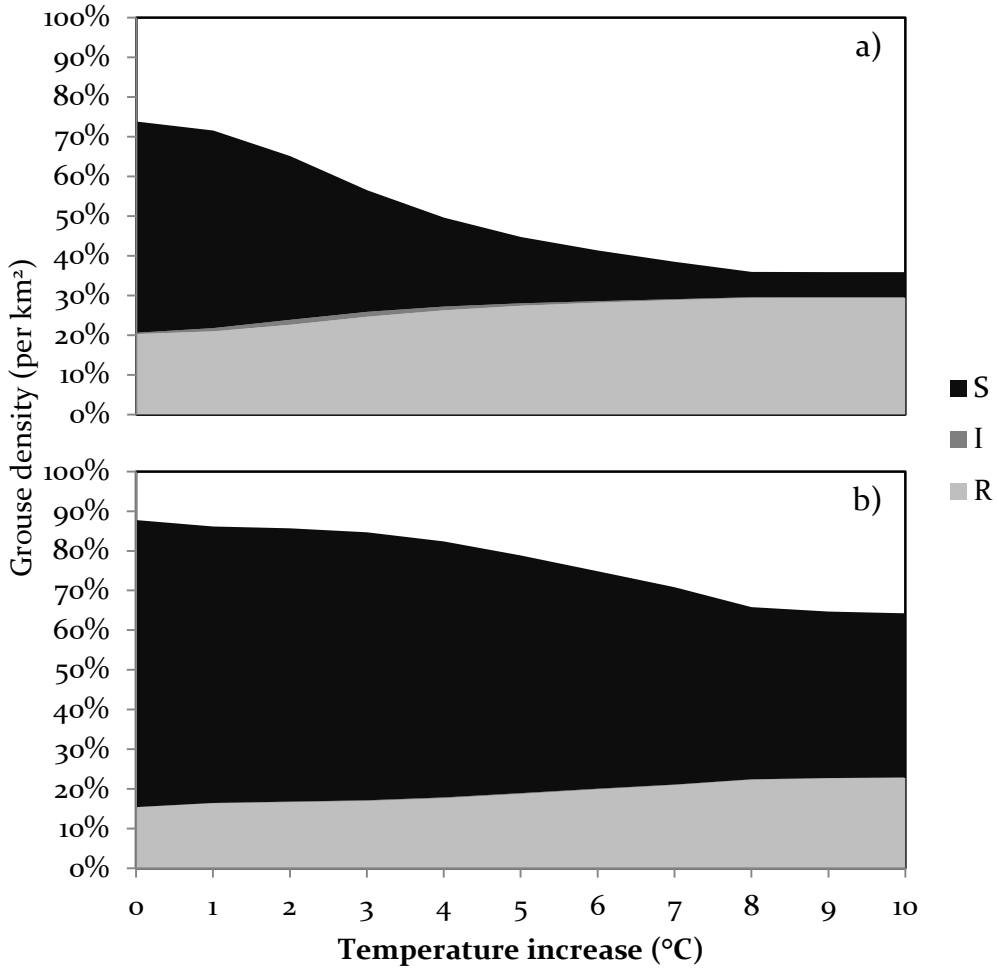

Figure 4.7: The number of susceptible (S), infected (I) and recovered (R) grouse (y-axis) for various temperature increases (x-axis), after the model was run for 100 years at each temperature, in order to demonstrate how the relationship between temperature and grouse survival for each habitat type. The y-axis height is the carrying capacity of the system. The habitats used are the coldest groups for (a) heather moorland with grouse and hares present (HA1) and (b) heather moorland with grouse, hares and deer present (HB1). For montane habitats the grouse population is made up of 100% susceptible grouse at all temperatures; i.e. the pathogen died out in each simulation.

the dynamics of the system. For the two heather types (HA, with high grouse density and no deer; HB, with low grouse and low deer density) it appears that

both reach an approximate equilibrium of grouse survival following an increase of 8°C. For all climate warming scenarios it appears that the presence of deer is predicted to result in a higher grouse survival rate than with deer absent. Furthermore it appears that heather areas with deer present are less affected by rising temperatures; the deer-free heather category (HA) is predicted to see a reduction in grouse survival from 74% for current temperatures to 36% with a rise of 10°C, whereas the heather category with deer present (HB) is predicted to see a change from 88% to 64% in grouse survival. Other than host densities, the only factor which distinguishes the HA groups from the HB groups is temperature. The average temperature of the HA groups ranges from 6.08 (HA1) to 9.08 (HA5), whilst the average temperature of the HB groups ranges from 5.64 (HB1) to 8.86 (HB5). So whilst the HA groups are generally warmer than the HB groups, this difference is slight and can't bias the results enough to explain the disparity in grouse survival between the two groups.

4.3.2 *Dilution effect*

As figure 4.3 showed, there appears to be a linear relationship between the density of deer present and the basic reproduction rate of the pathogen within the model. Since the heather areas with no deer present appear to have lower grouse survival, then it appears that higher deer density is correlated with lower LIV risk to grouse. To demonstrate this more fully, figure 4.8 (a) shows the prediction when the model is run for various deer/grouse densities under a consistent climate warming scenario. From this, it is clear to see that for any grouse carrying capacity the model predicts a positive relationship between the density of deer and the survival rate of grouse; therefore suggesting that deer

may have a diluting effect on LIV prevalence in ticks and thereby protect grouse with their presence.

The potential for an incompetent transmission host to have a diluting effect was first predicted by the model created by Norman et al. (1999), who modelled a tick and LIV system with grouse and mountain hares present, where mountain hares were assumed to be incompetent transmission hosts for LIV. This model predicted that for lower hare densities, increasing the hare densities was predicted to increased the pathogen persistence, before reaching a point where additional hares were predicted to reduce LIV persistence as infected tick bites were 'wasted' on incompetent hosts, as transmission through co-feeding was not included within the model. The dilution effect caused by increasing incompetent transmission host densities thereby reducing LIV persistence was again later predicted by Gilbert et al. (2001) in a three-host-tick-LIV model with grouse, mountain hares and deer, with deer acting as the incompetent transmission host (in this study mountain hares were modelled as competent hosts due to non-viraemic transmission between co-feeding ticks, as demonstrated in the lab by Jones et al. 1997).

The dilution effect has also been predicted by models of tick-borne encephalitis systems, such as in that created by Kiffner et al. (2011). The TBEV model created by Bolzoni et al. (2012) suggested that the dilution effect may operate even whilst the competent hosts, in this case rodents, are feeding increasing numbers of ticks, and that the rising proportion of incompetent meals, in this case from deer, drives the dilution effect. Hartfield et al. (2011) created a model of *B. burgdorferi* s.l. dynamics, which predicted that whilst the dilution effect is possible, it is unlikely to be strong.

However, in the aforementioned cases, the dilution effect is not predicted to begin immediately; rather, it takes effect only after an initial period where the presence of incompetent transmission hosts has aided pathogen persistence by increasing tick numbers. In the results presented here, the dilution effect is predicted to be immediate and almost linear. There are a few potential reasons why the dilution effect is predicted to be so powerful within the model presented here. The first of these is that the model may be parameterised such that it is too easy for ticks to survive; they potentially do not need deer present to survive (due to the presence of hares, which feed all stages of ticks) and so the effect of deer on diluting pathogen transmission outweighs the amplifying effect deer have on tick density. The prediction that ticks survive in all habitat-climate warming scenarios except the single coldest (M1 under current temperatures) could help explain this model prediction. In order to test whether harsher survival conditions for ticks results in the model predicting a less pronounced dilution effect, the simulations shown in figure 4.8 (a) were repeated, using a similar tick-LIV-grouse-deer system but with mountain hares absent. Such a system would see deer as the sole host of adult ticks, and therefore as a critical host to the system. However, as figure 4.8 (b) shows, other than the trivial case where grouse survival stays at 100% with no deer presence (since ticks die out with no host for adults), the predictions follow the same pattern as figure 4.8 (a). The only noticeable difference is the predicted lower rate of grouse survival compared to the equivalent grouse-deer system with hares present, suggesting that hares may also play a diluting role within the model. The predicted dilution effect of hares, however, may be mitigated by including transmission by co-feeding, discussed below.

The way in which deer are parameterised should also be scrutinised. Deer are estimated within the model to host an average of 15.8 larval ticks, 70.41 nymphs

and 81.25 adults at any one time, based on empirical data for peak tick questing months (Gilbert unpublished data). However, studies vary greatly in estimating the tick burdens found on deer. For instance, an empirical study by Mysterud et al. (2014) found averages of 7.76 larvae, 35.94 nymphs and 41.55 adults per red deer in Norway. Therefore, it is possible that by reducing the number of immature (larval and nymphal) stages hosted by deer within the model, the diluting effect of deer would be reduced, and therefore deer would have a detrimental effect on grouse by primarily feeding adult ticks and seeing a reduced number of 'wasted' bites by infected nymphs. The way the model is parameterised, the capacity of deer for hosting immature tick stages is 106% that of their capacity for hosting mature (adult) ticks. In order to see whether the dilution effect within the model is weakened when deer host fewer immature ticks, this percentage is reduced from 100% to 0% (figure 4.8, c). It can be seen that when deer host only 10% immature ticks compared to adults, increasing the deer density harms grouse survival initially, before the dilution effect outweighs the negative effect of additional deer. However, in this case, both the initial decrease and the later increase in grouse survival are of a very small magnitude. Unsurprisingly, when deer host no immature ticks, all increases in deer is predicted to reduce grouse survival. This demonstrates that by altering the ratio of immature to adult ticks on deer, it is possible to parameterise this model such that deer will initially harm grouse before the dilution effect begins to take hold, which is the behaviour shown by the models by Norman et al. (1999) and Gilbert et al. (2001). However, the negative effect of deer density on grouse survival is very weak, even when the model is parameterised to encourage it. Even if the model was parameterised so that deer hosted no immature ticks, the grouse survival decreased by less than 1% with the addition of 10 deer per km^2. The effect of reducing the capacity of

deer to host immature ticks is an interesting one. Whilst there is little evidence for the model to be parameterised in such a way that the dilution effect has a similar impact to that in other studies, the conflicting nature of the literature (as documented by Mysterud 2016) highlights a crucial gap in the current empirical knowledge.

Including transmission routes other than from ticks feeding on grouse may potentially change the diluting effect deer have on LIV within the model. For example, it has been documented that ticks feeding alongside each other on a host such as hares could transmit the pathogen to other ticks through saliva (Jones et al., 1997). Indeed, Norman et al. (2004) modelled this mechanism to predict that it could dramatically improve the ability of LIV to persist, with LIV even surviving in scenarios with no viraemic transmission host. Furthermore, by considering a general model Rosà et al. (2003) predicted that non-viraemic transmission reduces the role of the dilution effect. Another route of transmission not considered by this model is the ingestion of ticks by grouse chicks in the first three weeks of their lives, which Gilbert et al. (2004) estimate could be responsible for 73-98% of all infections of first-year grouse. Porter et al. (2011) investigated this route of transmission and found that ingestion generally led to an increase in virus persistence. A discussion of how these mechanisms might be incorporated is presented in chapter 5.

4.4 SENSITIVITY ANALYSIS

As in chapter 3, the two sensitivity analysis methods used by Watts et al. (2009) are undertaken here to see which parameters have the largest effect on the model.

For both methods, the output measured is the grouse survival after running the model for 100 years, to stay consistent with the measurement used when

a)	Grouse									
Deer	10	20	30	40	50	60	70	80	90	100
0	100	88	78	72	68	64	61	59	57	56
1	100	91	83	76	72	68	65	63	61	59
2	100	94	86	80	75	72	69	66	64	62
3	100	97	89	83	79	75	72	69	67	65
4	100	100	91	86	81	78	75	72	70	68
5	100	100	93	88	84	80	77	75	73	71
6	100	100	95	90	86	82	79	77	75	73
7	100	100	96	91	87	84	81	79	77	75
8	100	100	99	92	89	85	83	80	78	77
9	100	100	100	94	90	87	84	82	80	78
10	100	100	100	95	91	88	85	83	81	79

b)	Grouse									
Deer	10	20	30	40	50	60	70	80	90	100
0	100	100	100	100	100	100	100	100	100	100
1	81	62	53	48	45	43	42	41	40	40
2	90	75	67	61	56	53	50	48	46	45
3	95	81	74	69	65	61	58	55	53	52
4	100	85	78	74	70	67	64	62	59	57
5	100	89	82	77	74	71	69	66	64	62
6	100	91	84	80	76	74	72	70	68	66
7	100	94	87	82	79	76	74	72	70	69
8	100	97	89	84	80	78	76	74	72	71
9	100	100	91	86	82	79	77	76	74	73
10	100	100	92	88	84	81	79	77	75	74

(c)	Deer larvae + nymph capacity as a proportion of adult capacity										
Deer	100%	90%	80%	70%	60%	50%	40%	30%	20%	10%	0%
0	55.68	55.68	55.68	55.68	55.68	55.68	55.68	55.68	55.68	55.68	55.68
1	58.55	58.22	57.89	57.56	57.22	56.89	56.56	56.22	55.88	55.55	55.21
2	61.64	61.01	60.37	59.72	59.08	58.42	57.76	57.10	56.43	55.76	55.09
3	64.63	63.73	62.82	61.90	60.95	60.00	59.02	58.04	57.05	56.05	55.05
4	67.42	66.32	65.18	64.01	62.80	61.56	60.29	59.00	57.69	56.36	55.02
5	69.97	68.72	67.41	66.02	64.58	63.09	61.54	59.96	58.33	56.68	55.01
6	72.24	70.91	69.47	67.93	66.30	64.57	62.77	60.91	58.98	57.01	55.01
7	74.23	72.87	71.36	69.71	67.93	66.01	63.98	61.85	59.62	57.34	55.01
8	75.96	74.60	73.07	71.36	69.46	67.39	65.15	62.77	60.26	57.67	55.00
9	77.45	76.11	74.60	72.86	70.90	68.70	66.28	63.68	60.90	58.00	55.00
10	78.74	77.44	75.96	74.23	72.23	69.95	67.38	64.57	61.53	58.33	55.01

Figure 4.8: The grouse survival percentages predicted for various deer and grouse densities (per km^2), to show the role red deer play in diluting the effect of LIV within the model. The model is run for the warmest heather habitat under current temperatures. (a) uses the original model, (b) has hares absent, whilst (c) alters the capacity of immature ticks to feed on deer.

creating the model's prediction maps. In order to investigate the roles played by all hosts, the warmest habitat group with both grouse and deer present (HB5) was chosen with no temperature increase, which was used for both methods.

4.4.1 *Method 1*

Firstly, in order to predict whether any parameters had a disproportionate effect on predicted grouse survival, the model was run with each parameter altered by ±10% in turn. Table 4.4 shows the predicted percentage change in grouse survival for each run of the model.

As would be expected, the parameters directly relating to grouse population dynamics – grouse birth (a_G), grouse death (b_G) and the density dependence parameter of grouse (s_G) – cause the largest change in predicted grouse survival when altered. Of those, only grouse birth has a disproportionately large effect; a change of over 12% predicted from a change of 10% in either direction.

4.4.2 *Method 2*

To get a finer understanding of which parameters drive predicted grouse survival, the model was run 1000 times, with each parameter randomly varied by ±1%. The correlation between the parameter values used and the grouse survival is then measured to see how strong the relationship is. The predictions from this are shown on table 4.5.

As with Method 1, the grouse dynamic parameters are the ones which have the strongest effect on predicted grouse survival. Similarly, the parameters determining how many ticks can feed on a grouse in a given week (g_L and g_N) have

Parameter	Definition	Decrease of 10%	Increase of 10%
a	Minimum annual temperature		
b	Maximum annual temperature	+1.3%	-1.7%
T_{L1}	Threshold at which larvae begin to emerge		
T_{L2}	Threshold at which all larvae have emerged		
T_{NA1}	Threshold at which nymphs and adults begin to emerge		
T_{NA2}	Threshold at which all nymphs and adults have emerged		
b_L	Mortality rate for active larvae		
b_N	Mortality rate for active nymphs		
b_A	Mortality rate for active adults		
b_{WL}	Mortality rate for developing larvae	-1.0%	+1.0%
b_{WN}	Mortality rate for developing nymphs		
a_T	Larvae born per adult		
w	Parameter affecting the shape of the weekly feeding limit function		
b_G	Mortality rate for grouse	+4.4%	-4.1%
a_G	Birth rate for grouse	**-12.2%**	**+12.3%**
σ	Recovery rate for infected grouse	-1.7%	+1.5%
α	Infection-induced mortality for grouse		
s_G	Density-dependent constraint on grouse birth	+8.7%	-7.3%
Initial rate of infection for nymphs			
Deer density		-1.2%	+1.1%
Hare density		-1.1%	+1.0%
g_L	Larval capacity of grouse	+2.6%	-2.5%
g_N	Nymphal capacity of grouse	+2.1%	-1.8%
p	Aggregation parameter for nymphs on grouse	-1.5%	+1.5%

Table 4.4: Sensitivity analysis using Method 1, where the predicated percentage change in grouse survival from changing each parameter within the Louping-ill model by ±10% is found. In each case the model was run for the warmest heather habitat which contained grouse, hare and deer (HB5) with no temperature increase. Only the values which show a change of over ±1% are shown. Any changes above ±10% are highlighted in bold.

a higher predicted effect than those which solely deal with tick dynamics. None of the tick-specific parameters have a correlation larger than ±0.1.

As the values shown on table 4.5 are the Pearson's correlation coefficient (r) between the parameter values and grouse survival, the proportion of variation in grouse survival explained by the parameters (R^2) would be far lower, with only grouse death, grouse birth and the density dependence of grouse explaining over 10% of variation in model output, at 10%, 63% and 29% respectively.

4.4.3 *Sensitivity analysis summary*

It is clear from the two methods undertaken that the predictions from this model are primarily driven by the grouse dynamic parameters, in particular those relating to grouse birth (a_G and s_G) and death (b_G). These are based on empirical values (Hudson, 1992) and therefore should not be the cause of any unrealistic model outputs.

The parameter for the negative binomial aggregation of nymph bites on grouse (p) had been purposefully selected as lower than empirical evidence suggested in order to allow LIV to persist and to provide meaningful predictions, and is therefore the parameter based on the least sure footing. With this in mind, it is reassuring that this parameter does not have a disproportionate effect on the model predictions, only altering grouse survival by 1.5% for every 10% change in p (table 4.4).

Overall, the sensitivity analysis suggests that the model parameterisation is robust, such that even if some parameter values have been estimated inaccurately, it should not change the model output by very much.

Parameter	Definition	Pearson's correlation coefficient
a	Minimum annual temperature	-0.021
b	Maximum annual temperature	**-0.101**
T_{L1}	Threshold at which larvae begin to emerge	0.057
T_{L2}	Threshold at which all larvae have emerged	0.062
T_{NA1}	Threshold at which nymphs and adults begin to emerge	0.016
T_{NA2}	Threshold at which all nymphs and adults have emerged	0.063
b_L	Mortality rate for active larvae	-0.001
b_N	Mortality rate for active nymphs	0.029
b_A	Mortality rate for active adults	-0.007
b_{WL}	Mortality rate for developing larvae	0.059
b_{WN}	Mortality rate for developing nymphs	0.031
a_T	Larvae born per adult	-0.011
w	Parameter affecting the shape of the weekly feeding limit function	-0.030
b_G	Mortality rate for grouse	**-0.324**
a_G	Birth rate for grouse	**0.792**
σ	Recovery rate for infected grouse	0.096
α	Infection-induced mortality for grouse	0.022
s_G	Density-dependent constraint on grouse birth	**-0.541**
Initial rate of infection for nymphs		0.030
Deer density		0.062
Hare density		0.039
g_L	Larval capacity of grouse	**-0.196**
g_N	Nymphal capacity of grouse	**-0.158**
p	Aggregation parameter for nymphs on grouse	**0.135**

Table 4.5: Sensitivity analysis using Method 2, where the parameters within the LIV model are correlated with the predicted grouse survival rate, following 1000 model simulations where parameters were randomly altered by ±1% each time. Correlations with an absolute value larger than 0.1 are highlighted in bold.

4.5 SUMMARY

The model presented here demonstrates a novel approach for predicting the effect of climate change on tick-borne diseases over time and space. By adapting the

temperature-dependent tick lifecycle model presented in chapter 3, the changes in LIV risk to grouse under a variety of climate warming scenarios could be investigated.

For current temperatures, LIV is predicted to persist only on heather moorland, as montane habitats do not have sufficiently high temperatures. By using GIS software to map the model predictions across Scotland, the spatial distribution of areas which are suited to LIV could be predicted. Specifically, it appeared that coastal areas on the west of Scotland are the most suited to maintaining LIV due to warmer temperatures.

For all heather areas, grouse survival decreased with each rise in temperature, whilst for montane areas no climate warming scenario was enough for LIV to persist, due to inhibited tick densities. For the highest climate warming scenario studied, over half of heather moorland habitats containing grouse were predicted to fall into the high risk category (where grouse survival is below 60%). The overall grouse survival, measured against current climates, decreased by between 4.76% and 19.35% depending on the climate warming scenario. The reduction in grouse survival for higher climate warming scenarios was more dramatic in heather areas where deer were absent rather than present. This model prediction was not expected and highlights an important empirical gap in our knowledge concerning how the proportion of larvae feeding on deer rather than transmission hosts may be critical in determining whether deer have a dilution effect or an increasing effect on LIV.

By having a detailed model where temperature, host density and habitat all influence LIV dynamics, it is possible to predict the changes in LIV risk for future climate warming scenarios. Such predictions could be useful in informing policy on tick and tick-borne disease mitigation strategies, such as which areas, habitats

or host community scenarios may be increasingly at risk and therefore targeted for control methods.

5

ADAPTING THE NOVEL MODELLING APPROACH TO OTHER TICK-BORNE PATHOGEN SYSTEMS

5.1 INTRODUCTION

In chapter 4 a novel modelling approach was developed for predicting the influence climate change has on a tick-borne pathogen system, specifically that of Louping-ill virus (LIV). The model was used to predict the changes expected in disease risk under a variety of climate warming scenarios, and was useful in highlighting how different environmental factors can interact to drive tick-borne pathogen risk. This LIV model was an original approach, combining an environmentally-dependent mathematical model with GIS-based mapping. Therefore, it is important to demonstrate that this approach can be used for other systems, and that is the aim of this chapter.

There are a number of tick-borne infections which are of economic and public health interest across Britain. LIV, covered in chapter 4, kills sheep (*Ovis aries*) and red grouse (*Lagopus lagopus scoticus*) and is of particular importance in Scotland and northern England, where both sheep farming and red grouse hunting play a large role in the rural economy (Hudson, 1992). Closely related to LIV is the western variant of tick-borne encephalitis (TBE) virus, a pathogen of western

Europe which infects humans and can cause a variety of symptoms, ranging from muscle pain to paralysis and even death. Whilst TBE is not currently seen as a health risk within the UK, it is commonly found across much of Europe, and is therefore a risk for travellers (NHS Choices, 2015). Further tick-borne diseases such as Bartonellosis, Ehrlichiosis and Anaplasmosis can all cause serious health issues in humans, and have been recorded in many areas of Europe including the UK (BADA UK, 2016).

The most common tick-borne disease in humans in the northern hemisphere, including north America, Europe and the UK, is Lyme borreliosis, which is caused by the complex of spirochete bacteria *Borrelia burgdorferi* sensu lato. UK government figures show that recorded incidents of Lyme borreliosis has more than quadrupled in England since enhanced surveillance was introduced in 1996 (Public Health England, 2013) and increased almost 10-fold between 2000 and 2010 in Scotland (Health Protection Scotland, 2016). Infection with *B. burgdorferi* s.l. can cause various brain, skin and joint issues in humans. There are multiple strains, each with their own clinical symptoms and transmission host associations. Two particular strains of note are *Borrelia garinii*, which is transmitted by birds and is commonly associated with neuroborreliosis, a disorder of the nervous system, and *Borrelia afzelii*, which is transmitted by small mammals and is associated with acrodermatitis chronica atrophicans, a degenerative skin condition. Like LIV, the *B. burgdorferi* s.l. complex is transmitted by *Ixodes ricinus* ticks in Britain, where reservoir hosts such as small mammals and passerine birds maintain the pathogen, especially in woodland habitats (Gray, 1998).

The aim of this chapter is to extend the LIV model into a modelling framework which can be adapted for other tick-borne pathogen systems. Due to the importance of Lyme borreliosis, the modelling framework will be used to develop an

environment-dependent model of the two most prevalent strains of *B. burgdorferi* s.l.: *B. garinii* (bird-transmitted) and *B. afzelii* (rodent-transmitted). These are also useful systems for adapting the LIV model because they contrast greatly with the LIV system, being most prevalent in different habitats (woodland rather than heather moorland) and transmitted by different hosts (birds and rodents rather than red grouse). Therefore the aim of this chapter is to demonstrate how the novel modelling approach, originally built to represent LIV dynamics, can be adapted for different and ecologically contrasting pathogen systems.

To begin with, the LIV model is generalised in order to provide the basic models upon which the framework is built. From there, additional mechanisms are identified which can be added to the basic models if the a pathogen system requires them. The mechanisms concern alternative routes of pathogen transmission between tick and host, as well as tick- and disease-reduction treatment methods for tick hosts and systems with multiple transmission hosts. This framework is then adapted for *B. burgdorferi* s.l. (*B. afzelii* and *B. garinii*) dynamics. Using this model, predictions are made for the changes in disease risk for various climate warming scenarios. Using GIS mapping, these predictions are used to create predictive maps for the densities of infected ticks, as well as the prevalence of the pathogen across Scotland. As *B. burgdorferi* s.l. is more complex than LIV, there is less empirical information available to inform the model. Therefore, the model predictions will be primarily for demonstrative purposes. However, sensitivity analysis of the model will be used to highlight areas where empirical evidence is required in order for more robust predictions to be made.

Parameter	Definition and notes
a_T	Annual birth rate of ticks.
b_L	Mortality rate for active larvae.
b_N	Mortality rate for active nymphs.
b_A	Mortality rate for active adults.
b_{WL}	Mortality rate for developing larvae.
b_{WN}	Mortality rate for developing nymphs.
p	Aggregation parameter for nymphs feeding on hosts.
q	Aggregation parameter for adults feeding on hosts. *Only in the LNA model.*
a_H	Birth rate for hosts.
s_H	Density-dependence parameter for host birth.
b_H	Mortality rate for hosts.
α	Infected-induced mortality for hosts.
σ	Recovery rate for infected hosts.
δ	Waning immunity rate for recovered hosts.
h_L	Maximum larval capacity for the competent transmission host.
h_N	Maximum nymphal capacity for the competent transmission host.
h_A	Maximum adult capacity for the competent transmission host. *Only in the LNA model.*
a	Minimum local annual temperature.
b	Maximum local annual temperature.
T_1	Temperature at which ticks begin to emerge from overwintering.
T_2	Temperature at which all ticks have emerged from overwintering.

Table 5.1: The parameters used for the LN and LNA models and their definitions. All rates are per week unless otherwise stated.

5.2 EXTENDING THE LIV MODEL INTO A BROADER MODELLING FRAMEWORK

5.2.1 *Defining the basic models*

The first step in creating a modelling framework is to take the LIV model created in chapter 4 and generalise it to create basic models, which will be the basis for the framework. To begin with, adapting the LIV model from chapter 4

for a similar system where one competent transmission host (and multiple incompetent transmission hosts) is considered. To begin with, it is assumed that the transmission host only feeds larvae and nymphs (as red grouse do within the LIV model), and therefore the only way for the pathogen to be passed from tick to host is from an infected nymph biting a susceptible host, whilst the only way for the pathogen to be passed from host to tick is for a susceptible larva to bite an infected host. This system is hereafter referred to as the LN system to reflect the tick instars (larvae and nymphs) which are involved in pathogen transmission.

Waning host immunity is introduced to the system, denoted by δ, as this is assumed not to occur among recovered grouse, but may occur with other tick-borne infections and hosts. This mechanism aside, the transmission routes will remain the same as those within the LIV model, and therefore the mechanisms of the model will remain the same, with the only changes occurring in the parameter values used. The equations that make up the LN model are shown in section 5.2.2.1, whilst the definitions of each parameter are listed in table 5.1. The host equations in the system are denoted by H, rather than the G used in Chapter 4, as it reflects an unspecified host. Similarly, the parameters describing the larval and nymphal capacity of the host are given by h_L and h_N respectively.

When considering systems such as a LIV system with unvaccinated sheep, where the competent transmission host is regularly bitten by all three stages of tick life (hereafter referred to as the LNA system), any new equations which may need to be introduced should be considered. As with the previous models, it is assumed that transovarial transmission is not a factor (for a discussion on how this could be incorporated see section 5.2.4.1). Therefore, once adults have fed and are in the developing stage, their infection status does not need to be considered in the model. Thus, the only changes to the equations are splitting

the two previous stages, developing nymphs and active adults, into susceptible and infected classes.

The modelling approach assumes that the number of ticks of a given instar finding a meal is independent of the number of ticks of another instar finding a meal, which is a reasonable assumption, since ticks of different instars tend to find blood meals on different places on a hosts' body (e.g. Kiffner et al. 2010). Therefore, the addition of adults feeding on the competent transmission host has no effect on the equations used for larvae and active nymphs. However, as the infection status of developing nymphs now needs to be tracked, the proportion of feeding susceptible nymphs which feed on an infected host now need to be calculated. To this end, the ratio ϕ introduced in chapter 4, which represented the proportion of available blood meals for larvae which come from infected hosts, is used. This ratio is now split into two, listed in equations 5.1 and 5.2, where ϕ_L is identical to the ϕ previously used, whilst ϕ_N is identical except the parameters are altered for nymphs. Similarly, the ratio θ, which represents the proportion of active nymphs which are infected, is split into θ_N and θ_A, which represent nymphs and adults respectively (shown in equations 5.3 and 5.4), whilst k, the average number of nymphs on the transmission host, is split into k_N and k_A to represent the nymphs and adults separately (shown in equations 5.5 and 5.6).

$$\phi_L = \frac{H_I(t) \times h_L}{L_{host}} \tag{5.1}$$

$$\phi_N = \frac{H_I(t) \times h_N}{N_{host}} \tag{5.2}$$

$$\theta_N = \frac{N_{AI}(t)}{N_{AS}(t) + N_{AI}(t)} \tag{5.3}$$

$$\theta_A = \frac{A_{AI}(t)}{A_{AS}(t) + A_{AI}(t)} \tag{5.4}$$

$$k_N = \frac{\frac{h_N}{N_{host}} \times \theta \times S\left[F_{NA}(t) \times P(t) \times (N_{AS}(t) + N_{AI}(t)), N_{host}\right]}{H_S(t) + H_I(t) + H_R(t)} \tag{5.5}$$

$$k_A = \frac{\frac{h_A}{A_{host}} \times \theta \times S\left[F_{NA}(t) \times P(t) \times (A_{AS}(t) + A_{AI}(t)), A_{host}\right]}{H_S(t) + H_I(t) + H_R(t)} \tag{5.6}$$

When considering the number of uninfected nymphs receiving the pathogen by biting an infected host, the total number of susceptible nymphs finding a meal is given by equation 5.7, which is the same as with the LN model, and explained within chapter 4.

$$(1 - \theta_N) \times S\left[F_{NA}(t) \times P(t) \times (N_{AS}(t) + N_{AI}(t)), N_{host}\right] \tag{5.7}$$

Equation 5.7 is then multiplied by ϕ_N to represent the proportion of these susceptible nymphs which feed on an infected host.

The number of adults finding a meal in a given week is given by the same equation as equation 5.7, but with parameters representing adult rather than nymph behaviour, shown by equation 5.8.

$$(1 - \theta_A) \times S\left[F_{NA}(t) \times P(t) \times (A_{AS}(t) + A_{AI}(t)), A_{host}\right] \tag{5.8}$$

Of the dynamics within the model for hosts, the only one which is altered by the addition of adults feeding upon them is the risk of picking up the infection from a tick bite. In the previous model this was represented by equation 5.9.

$$\left(1 - p^{k_N}\right) H_S(t) \tag{5.9}$$

The rationale behind this is explained in chapter 4. This can be represented by equation 5.10, where $\mathrm{prob}(\bar{N})$ is the probability of a host not being bitten by an infected nymph.

$$[1 - \mathrm{prob}(\bar{N})] \times \textit{total susceptible hosts} \tag{5.10}$$

As explained above, it is assumed that the number of adult ticks biting a host is independent of the number of nymphs biting the same host. This is not an unreasonable assumption since adult and nymph ticks generally have mutually exclusive preferences for which part of an animal they prefer to feed, for example on roe deer (*Capreolus capreolus*) larvae are found on the head and ears, nymphs prefer the neck, while adults prefer inguinal areas (groin and armpit) (Kiffner et al., 2010). Therefore, by using $\mathrm{prob}(\bar{A})$ as the probability that a host isn't bitten by an infected adult, the number of hosts picking up the pathogen in a system where they can be fed upon by all stages of tick will be represented by equation 5.11.

$$[1 - (\mathrm{prob}(\bar{N}) \times \mathrm{prob}(\bar{A}))] \times \textit{total susceptible hosts} \tag{5.11}$$

The logic behind the likelihood that a host is not bitten by an infected adult ($prob(\bar{A})$) is no different to that for nymphs, except with potentially different parameter values. Therefore this is given by equation 5.12, where q is the aggregation parameter for adults.

$$prob(\bar{A}) = q^{k_A} \tag{5.12}$$

The full set of equations for the LNA model is listed in section 5.2.2.2, with parameters listed in table 5.2.

5.2.2 *Basic model equations*

For both the LN model and the LNA model, the following functions apply:

$$\begin{aligned}
T(t) &= \left(\frac{b-a}{2} \times \sin\left(\frac{t}{2.6\pi} - 0.5\pi\right)\right) + \frac{a+b}{2} \\
F(t) &= \begin{cases} 0 & T(t) \leqslant T_1, \\ \frac{T(t)-T_1}{T_2-T_1} & T_1 < T(t) \leqslant T_2, \\ 1 & T_2 < T(t) \end{cases} \\
P(t) &= \frac{1}{1+exp\left[\frac{3}{4}(8-T(t))\right]} \\
S(x,K) &= \frac{wK}{w+(K-w)exp\left(\frac{ln\left[\frac{w}{19(K-w)}\right]}{8K}x\right)} - w
\end{aligned} \tag{5.13}$$

5.2.2.1 *LN model*

$$
\begin{aligned}
\frac{dL_A}{dt} &= -S\left[F_L(t) \times P(t) \times L_A(t), L_{host}\right] - b_L L_A(t) \\
\frac{dL_{DS}}{dt} &= (1-\phi) \times S\left[F_L(t) \times P(t) \times L_A(t), L_{host}\right] - b_{WL} L_{DS}(t) \\
\frac{dL_{DI}}{dt} &= \phi \times S\left[F_L(t) \times P(t) \times L_A(t), L_{host}\right] - b_{WL} L_{DI}(t) \\
\frac{dN_{AS}}{dt} &= -(1-\theta) \times S\left[F_{NA}(t) \times P(t) \times (N_{AS}(t) + N_{AI}(t)), N_{host}\right] \\
&\quad -b_N N_{AS}(t) \\
\frac{dN_{AI}}{dt} &= -\theta \times S\left[F_{NA}(t) \times P(t) \times (N_{AS}(t) + N_{AI}(t)), N_{host}\right] - b_N N_{AI}(t) \\
\frac{dN_D}{dt} &= S\left[F_{NA}(t) \times P(t) \times (N_{AS}(t) + N_{AI}(t)), N_{host}\right] - b_{WN} N_D(t) \\
\frac{dA_A}{dt} &= -S\left[F_{NA}(t) \times P(t) \times A_A(t), A_{host}\right] - b_A A_A(t) \\
\frac{dA_D}{dt} &= S\left[F_{NA}(t) \times P(t) \times A_A(t), A_{host}\right] \\
\frac{dH_S}{dt} &= -\left(1-p^k\right) H_S(t) - b_H H_S(t) \\
&\quad + \left[\alpha_H - s_G\left(H_S(t) + H_I(t) + H_R(t)\right)\right] \\
&\quad \left(H_S(t) + H_I(t) + H_R(t)\right) + \delta H_R(t) \\
\frac{dH_I}{dt} &= \left(1-p^k\right) H_S(t) - (b_H + \alpha + \sigma) H_I(t) \\
\frac{dH_R}{dt} &= \sigma H_I(t) - (b_H + \delta) H_R(t)
\end{aligned}
\tag{5.14}
$$

Initial conditions at the start of each year:

$L_A(0) = \alpha_T A_D(52)$; $L_{DS}(0) = 0$; $L_{DI}(0) = 0$; $N_{AS}(0) = L_{DS}(52)$; $N_{AI}(0) = L_{DI}(52)$; $N_D(0) = 0$; $A_A(0) = N_D(52)$; $A_D(0) = 0$; $H_S(0) = H_S(52)$; $H_I(0) = H_I(52)$; $H_R(0) = H_R(52)$.

5.2.2.2 *LNA model*

$$
\begin{aligned}
\frac{dL_A}{dt} &= -S\left[F_L(t) \times P(t) \times L_A(t), L_{host}\right] - b_L L_A(t) \\
\frac{dL_{DS}}{dt} &= (1-\phi_L) \times S\left[F_L(t) \times P(t) \times L_A(t), L_{host}\right] - b_{WL} L_{DS}(t) \\
\frac{dL_{DI}}{dt} &= \phi_L \times S\left[F_L(t) \times P(t) \times L_A(t), L_{host}\right] - b_{WL} L_{DI}(t) \\
\frac{dN_{AS}}{dt} &= -(1-\theta_N) \times S\left[F_{NA}(t) \times P(t) \times (N_{AS}(t) + N_{AI}(t)), N_{host}\right] \\
&\quad -b_N N_{AS}(t) \\
\frac{dN_{AI}}{dt} &= -\theta_N \times S\left[F_{NA}(t) \times P(t) \times (N_{AS}(t) + N_{AI}(t)), N_{host}\right] - b_N N_{AI}(t) \\
\frac{dN_{DS}}{dt} &= (1-\theta_N) \times (1-\phi_N) \times S\left[F_{NA}(t) \times P(t) \times (N_{AS}(t) + N_{AI}(t)), N_{host}\right] \\
&\quad -b_{WN} N_{DS}(t) \\
\frac{dN_{DI}}{dt} &= (\theta_N + (1-\theta_N) \times \phi_N) \times S\left[F_{NA}(t) \times P(t) \times (N_{AS}(t) + N_{AI}(t)), N_{host}\right] \\
&\quad -b_{WN} N_{DI}(t) \\
\frac{dA_{AS}}{dt} &= -(1-\theta_A) \times S\left[F_{NA}(t) \times P(t) \times (A_{AS}(t) + AAI(t)), A_{host}\right] - b_A A_{AS}(t) \\
\frac{dA_{AI}}{dt} &= -\theta_A \times S\left[F_{NA}(t) \times P(t) \times (A_{AS}(t) + AAI(t)), A_{host}\right] - b_A A_{AI}(t) \\
\frac{dA_D}{dt} &= S\left[F_{NA}(t) \times P(t) \times (A_{AS}(t) + AAI(t)), A_{host}\right] \\
\frac{dH_S}{dt} &= -\left(1 - \left[p^{k_N} \times q^{k_A}\right]\right) H_S(t) - b_H H_S(t) \\
&\quad + \left[a_H - s_G\left(H_S(t) + H_I(t) + H_R(t)\right)\right]\left(H_S(t) + H_I(t) + H_R(t)\right) + \delta H_R(t) \\
\frac{dH_I}{dt} &= \left(1 - \left[p^{k_N} \times q^{k_A}\right]\right) H_S(t) - (b_H + \alpha + \sigma) H_I(t) \\
\frac{dH_R}{dt} &= \sigma H_I(t) - (b_H + \delta) H_R(t)
\end{aligned}
\tag{5.15}
$$

Initial conditions at the start of each year:

$L_A(0) = \alpha_T A_D(52)$; $L_{DS}(0) = 0$; $L_{DI}(0) = 0$; $N_{AS}(0) = L_{DS}(52)$; $N_{AI}(0) = L_{DI}(52)$; $N_{DS}(0) = 0$; $N_{DI}(0) = 0$; $A_{AS}(0) = N_{DS}(52)$; $A_{AI}(0) = N_{DI}(52)$; $A_D(0) = 0$; $H_S(0) = H_S(52)$; $H_I(0) = H_I(52)$; $H_R(0) = H_R(52)$.

5.2.3 *Expanding the models to represent systems with multiple viraemic transmission host types*

The modelling approach created so far is capable of dealing with systems with multiple tick hosts, however; so far only systems with one competent transmission host type have been considered. However, there are plenty of systems with multiple competent transmission hosts. For instance, whilst grouse were the only competent transmission hosts of LIV in the model presented in chapter 4, sheep are another potential competent transmission host of LIV, whilst hares can act as non-viraemic transmission hosts as ticks can transmit LIV through co-feeding. Therefore systems with multiple competent transmission hosts are highly plausible. This section concerns the modelling of systems with more than one viraemic transmission host, for non-viraemic transmission, see section 5.2.4.3.

5.2.3.1 *Modelling systems with two competent transmission hosts of the same pathogen*

The first system considered is one where both transmission hosts can carry the same strain of the pathogen; i.e. a tick which picks up the infection from one host would be able to transmit it to the second host. The addition of a second competent transmission host does not require a huge change from the LN or LNA models; rather, there would just need to be introduced three new classes to represent the additional host's susceptible, infected and recovered classes.

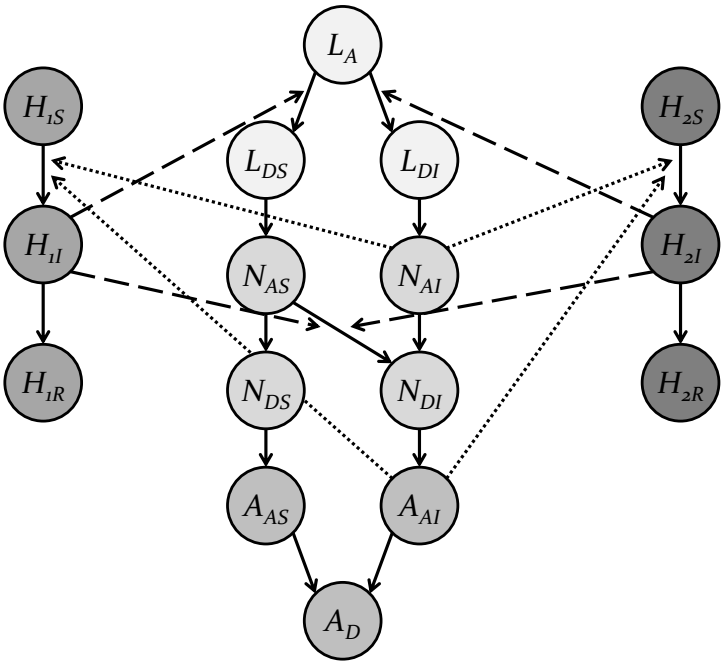

Figure 5.1: Schematic diagram displaying the progression routes for the model with two transmission hosts for the same pathogen. L, N and A refer to the three tick instars (larva, nymph and adult), H_1 and H_2 represent the two separate transmission host types, and S, I and R represent different infection statuses (susceptible, infected and recovered). Solid lines represent a progression to the next class, whilst dashed lines represent infected hosts transmitting the pathogen to ticks, and dotted lines represent infected ticks transmitting to hosts.

A schematic diagram demonstrating this system and the transmission routes involved is presented in figure 5.1.

When considering the interactions which result in the pathogen being transmitted, care will be needed to ensure that infected ticks are not counted twice when calculating how many of the two host groups pick up the pathogen.

5.2.3.2 *Modelling systems with two competent transmission hosts of separate strains*

The system becomes more complex when modelling a system where there are two competent transmission hosts, each of which can carry a different strain

of a pathogen. An example of this is modelled as a case study in section 5.3, where the two transmission host types are small mammals and passerine birds, each of which carry different strains of *B. burgdorferi* s.l. (*B. afzelii* and *B. garinii* respectively).

Firstly, a system where the two hosts only feed larval and nymphal ticks is considered. As ticks will not be able to transmit the pathogen when feeding as adults, their infection status after feeding as nymphs is not considered (as explained in chapter 4). This means that ticks only have one opportunity to become infected within the model, when feeding as larvae (whilst uninfected nymphs could feed on an infected host, the model does not consider their infection status at this stage). Similarly, ticks will only have one opportunity to infect a host, when feeding as infected nymphs. Therefore, this means that no tick can carry both strains of the pathogen at the same time within the model.

The simplest way to model such a system is to model each strain separately, using the LN model. As the groups of ticks with each strain are mutually exclusive, the total number of infected ticks can be found by simply adding the total ticks infected with each strain. This logic applies to systems with more than two transmission hosts as well, as long as each host only feeds larval and nymphal ticks.

However, when one or both transmission hosts can feed all three tick stages, the modelling required becomes more complex, as ticks will have two chances to pick up (at the larval and nymphal stage) and pass on (at the nymphal and adult stages) the pathogen. This means that ticks carrying both strains of the pathogen are a possibility, and therefore both strains have to be contained within the same model. To model this system, all infected tick classes will require splitting into infection classes for each strain. The logic which dictates that larvae can only pick

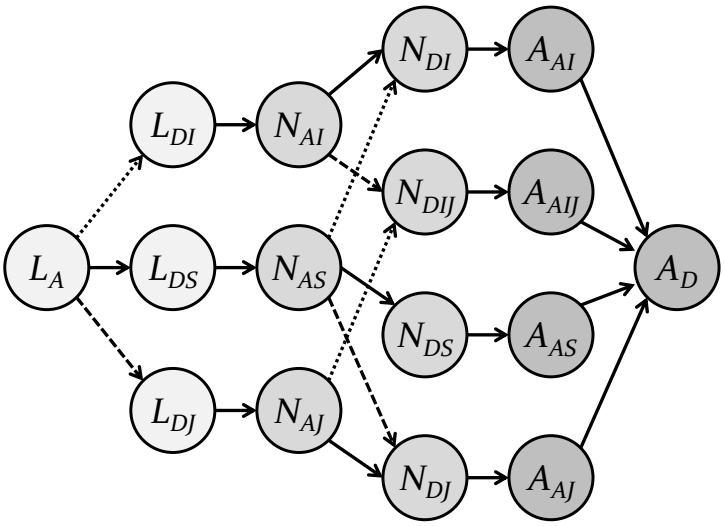

Figure 5.2: Schematic diagram displaying the progression routes for the model with two transmission hosts for two separate strains of the same pathogen. For tick dynamics only, where the subscript I denotes those which have one strain of the pathogen, and those with the subscript J have the other. Hosts are influenced in the same way as in figure 5.1, except that H_1 can only be infected by I or IJ ticks, and H_2 can only be infected by J or IJ ticks. Dashed lines represent tick progression routes which are influenced by H_1, and dotted lines represent routes influenced by H_2.

up one strain, as they only feed once, remains the same within the two strain model. Therefore the only tick states which will require the addition of a double-infected class will be developing nymphs and questing adults. A schematic of this system is presented in figure 5.2. As before, the main consideration required in expanding the model in such a way is avoiding over- or under-counting the influence of transmission routes.

This model can be used for systems where both transmission hosts only feed larval and nymphal ticks. This would be necessary if alternate transmission routes such as transovarial transmission (see section 5.2.4.1), non-viraemic transmission (see section 5.2.4.3) or ingestion of infected ticks (see section 5.2.4.4) are included, as the infection status of adult ticks will then become relevant.

5.2.4 *Incorporating alternate routes of transmission*

There are multiple mechanisms for pathogen transmission which have not yet been included in the modelling systems presented in this thesis. The inclusions of these are highly likely to change the behaviour of the model, and in particular could reduce the dilution effect caused by increasing deer densities predicted by the LIV model presented in chapter 4.

5.2.4.1 *Adapting the model for systems with transovarial transmission*

The mechanism which would be more straightforward to implement would be transovarial transmission, whereby the pathogen is passed from the adult female ticks to her larval tick offspring via eggs. Incorporating transovarial transmission into the model would be appropriate for tick-borne pathogen systems such TBE virus (Danielova and Holubova, 1991) and Babesiosis (Howell et al., 2007) where a small proportion of unfed larvae are infected because their mothers were infected and past on the pathogen via the eggs. In order to implement transovarial transmission within the model, the developing adult and questing larvae stages would have to be split into susceptible and infected classes. As density dependence is not considered for tick births, and assuming infection does not impair the breeding capabilities of ticks, the number of infected larvae at the start of a new year would simply be given by the tick birth parameter (a_T) multiplied by the number of infected developing adults and the transovarial transmission rate (represented by ζ), the latter of which would be the estimated proportion of larvae born from an infected adult which inherit the pathogen. The previous calculation, but with $(1-\zeta)$ replacing ζ, gives the number of uninfected

larvae born from infected adults, which is added to the births from uninfected adults to give the total number of uninfected larvae at the start of a new year.

5.2.4.2 *Adapting the model for reduced transmission rates*

A common assumption made across the models within this thesis is that all bites by a tick on a competent transmission host, where one is infected and the other susceptible, always results in transmission of the pathogen. In the absence of any empirical information on this infection coefficient, 100% is assumed for simplicity and is consistent with most other modelling of LIV and *B. burgdorferi* s.l. systems, such as Gilbert et al. (2001), Porter (2011) and Zhang and Zhao (2013). However, it is not difficult to adjust the model to take into account transmission rates below 100%. Let the host-to-tick transmission rate be represented by β and let the tick-to-host transmission rate be represented by λ. Firstly, when considering host-to-tick transmission, the number of uninfected ticks feeding on an infected host is simply multiplied by β to give the total number of ticks picking up the pathogen from feeding. Secondly, tick-to-host transmission was previously modelled by considering the negative binomial distribution of infected ticks on uninfected hosts. This can be updated to incorporate a lower transmission rate by multiplying the number of infected ticks within this calculation by λ. This essentially changes the calculation from estimating the distribution of infected ticks feeding on susceptible hosts to estimating the distribution of infected tick bites which would successfully transmit the pathogen on susceptible hosts. When β and λ are set to 1, these mechanisms behave equivalently to those in the previous models before these parameters were introduced.

5.2.4.3 *Adapting the model for non-viraemic transmission between co-feeding ticks*

Transmission of the pathogen between ticks co-feeding on the same host through saliva can be an important route of transmission (Jones et al., 1997), and has been observed in pathogen systems such as TBE virus in rodents (Labuda et al., 1993), LIV in mountain hares (Jones et al., 1997) and Thogoto virus in guinea pigs (Jones et al., 1990). A model created specifically to explore the dynamics of LIV transmission between ticks co-feeding on mountain hares was created by Norman et al. (2004), whereby a new parameter was introduced to the model used in Norman et al. (1999) for co-feeding, dependent on the presence of hares, susceptible ticks and infected ticks. Similar studies were also conducted by Gilbert et al. (2001) and Laurenson et al. (2003). In order to implement a co-feeding transmission mechanism to the modelling framework presented within this thesis, a similar mechanism can be adopted; the model already provides a way of calculating the numbers of uninfected and infected ticks feeding on a given host species, this would then need to be coupled to a parameter reflecting the co-feeding transmission rate for ticks.

5.2.4.4 *Adapting the model to incorporate host infection from the ingestion of ticks*

An additional transmission mechanism that could be included is the ingestion of infected ticks by newly-borne grouse chicks, which has been estimated to potentially account for 73-98% of LIV infections in first-year grouse (Gilbert et al., 2004). Porter (2011) developed a model with separate equations to represent feeding chicks. A similar structure can be incorporated into the model presented in chapter 4, where a new class is created to represent grouse chicks, which can be defined as grouse young enough to feed on invertebrates, which is approximately

3 weeks (Porter, 2011). A parameter can then be implemented to represent grouse chicks moving to the infected grouse state through ingesting infected ticks, whilst providing an estimation of ticks which are killed from being ingested. Such a system would also require a parameter to represent the proportion of grouse chicks maturing beyond a diet including invertebrates. As adult ticks are eaten by grouse chicks, their infection status is relevant for pathogen transmission. This means that the infection status of adult ticks has to be recorded within the model; therefore the LNA model would have to be used, rather than the LN model.

Porter (2011) found that including an ingestion mechanism of infection led to varying outcomes depending on parameter values; the model in Porter (2011) predicted that the ingestion route of infection could lead to increased pathogen persistence, or alternatively the increased tick mortality could reduce pathogen persistence. Therefore it is not certain what effect ingestion would have on the model presented in chapter 4. The ingestion model in Porter (2011) did predict that introducing ingestion resulted in the dilution effect (whereby very high deer densities cause a decline in LIV prevalence) being less apparent (i.e. very high deer densities no longer caused a decline in LIV prevalence). This effect of ingestion on the dilution effect of deer seems likely to be predicted within the modelling framework presented within this chapter also, since it would provide a secondary opportunity for infected ticks to transmit the pathogen to grouse, therefore reducing the likelihood of infected tick bites being 'wasted' on deer.

5.2.5 *Incorporating treatment of tick hosts*

The treatments that can be applied to tick hosts can be placed into two categories. The first are vaccines, which prevent a host from carrying the pathogen. The second are acaricides, which are poisonous to ticks and are used to reduce the tick

population. Both have been used to reduce tick-borne pathogen prevalence, and this section considers how they each would be represented within the modelling framework.

Mathematical models have been used to predict the impact of treatments on reducing disease risk (Porter, 2011), and the modelling framework presented in this chapter could be used in the same way by using the tools explained in this section.

5.2.5.1 *Treatment of hosts with vaccines*

Vaccinating hosts against pathogens is a commonly used method used to help control disease of livestock, companion animals and humans. For example, in areas with endemic LIV sheep are often vaccinated against LIV to increase survival in case of infection. In order to model vaccination the only change required would be a parameter introduced to represent hosts moving from the susceptible class to the recovered (which acts the same as an immune class).

If the application of vaccination varies throughout the year, this parameter can be replaced with a function, such as the piecewise function for grouse births used within chapter 4.

5.2.5.2 *Treatment of hosts with acaricide*

There are two ways in which acaricide can be used in a tick-borne pathogen system: either treating the competent transmission host or treating an incompetent transmission host. To take the example of LIV in the UK, these two approaches can be represented by the method of treating sheep (a competent transmission host) with acaricide (Laurenson et al., 2007) or by treating red deer (*Cervus elaphus*;

an incompetent transmission host), a method which is not legal within the UK, but has been modelled theoretically by Porter et al. (2013a).

For treating both competent and incompetent transmission hosts, the method of calculating the effect of acaricide treatment will fundamentally remain the same. In each case, the total ticks of a given stage feeding are multiplied by equation 5.16. Note that equation 5.16 is specific for larvae, for other stages the equation is updated for the relevant parameters.

$$\frac{\textit{treated host density} \times \textit{host larval capacity}}{L_{host}} \tag{5.16}$$

This is a similar method to that which was used to calculate the proportion of blood meals available to larvae that come from infected hosts (ϕ) in chapter 4. This calculation gives the number of ticks which will feed on a treated host in a given week, which can then be multiplied by the effectiveness of the acaricide (if below 100%) to provide the total ticks which will be killed by the treatment.

The only difference which will distinguish competent and incompetent transmission hosts is that in order to be effectively modelled, a fourth class for the competent transmission host will need to be required to represent those which have been treated, along with a parameter or function to represent the treatment being applied. For incompetent transmission hosts, the treated and non-treated host densities can be taken as constant.

A variety of direct and indirect treatment methods within a LIV system have been modelled including treating competent transmission hosts in red grouse (Porter et al., 2013b) and sheep (Porter et al., 2011), as well as incompetent transmission hosts red deer (Porter et al., 2013a). The outcome of these were

highly dependent on the densities of non-treated hosts, which is likely to be reflected if implemented in the model presented in chapter 4, given that the output of the LIV model was highly influenced by host densities.

5.2.6 *Summary*

The tools outlined above cover a wide variety of behaviour within tick-borne pathogen systems. By taking one of the two basic models outlined, it should be possible to develop an environmentally-dependent model for a tick-borne pathogen system by appending the appropriate mechanisms. If there are elements of the basic models which are not present within the pathogen system being modelled, then it should be possible to set their values to 0 in order to remove them from the system. The next stage for this framework is to use the case study of *B. burgdorferi* s.l. in Scotland in order to demonstrate how the framework can be applied.

5.3 BORRELIA BURGDORFERI S.L. CASE STUDY

To demonstrate how the modelling framework can be applied to a new tick-borne pathogen system, a case study of Lyme borreliosis, the causative agent of which is the *B. burgdorferi* s.l. complex, in Scotland is used.

5.3.1 *Model development*

There are multiple strains of *B. burgdorferi* s.l., which each have their own transmission hosts. The model created will focus on the dynamics of *B. afzelii* and *B. garinii* as these are the two strains most commonly found in Europe, including the UK, and have the broadest geographic range (e.g. Margos et al. 2011) and,

Parameter	Small mammal value	Passerine bird value	Red grouse value
a_H	0.4615 [A]	0.1538 [A]	0.7175 [B]
s_H	$\frac{0.4423}{c}$ [C]	$\frac{0.1474}{c}$ [C]	$\frac{0.522}{c}$ [C]
b_H	0.0192 [A]	0.0064 [A]	0.008 [B]
α	0 [D]	0 [D]	0 [D]
σ	0.01 [E]	0.01 [E]	0.01 [E]
Larva capacity	1.61 [A]	3.11 [A]	15
Nymph capacity	0.03 [A]	0.25 [A]	4
Adult capacity	0 [A]	0 [A]	0
Woodland density	11400 [A]	365 [A]	0
Plantation density	4250 [A]	35 [A]	0
Heather density	155 [A]	0 [A]	0, 50, 100
Montane density	0 [A]	0 [A]	20

Table 5.2: *B. burgdorferi* s.l. parameter table. The parameters used to adapt the LN model to *B. Burgdorferi* s.l. dynamics. All unexplained parameters remain the same as those used in chapter 4. Sources: [A] Weighted average values taken from all species within this host group. The methodologies behind these calculations are explained in the text; [B] Hudson (1992); [C] Chosen such that the host density runs to its carrying capacity; [D] Gray (1998); [E] Wright and Nielsen (1990).

for the purposes of this modelling exercise focusing on Scotland, are also the most prevalent strains in Scotland: James et al. (2013, 2014) found that in Scotland 48% of infected nymphs carried *B. afzelii* and 36% carried *B. garinii*, and Millins et al. similarly found 46% of infected nymphs carried *B. afzelii* and 29% carried *B. garinii* in Scotland. Furthermore, these two strains make an interesting contrast for modelling because they have different host systems: *B. afzelii* is maintained by small mammals such as wood mice and bank voles, which act as the competent transmission hosts (Hanincová et al., 2003a), whilst *B. garinii* is transmitted by birds (Hanincová et al., 2003b; James et al., 2011). Within this model it is assumed that these are the only two strains of *B. burgdorferi* s.l. and that the total *B. bur-*

gdorferi s.l. risk is the sum of these two strains. This is obviously a simplifying assumption and is made for ease of reference for the model predictions; empirical data show that 75-84% of nymphs infected with *B. burgdorferi* s.l. carried either *B. afzelii* or *B. garinii* (James et al., 2013, 2014; Millins et al.).

In both cases the hosts – small mammals and birds – are assumed to be not adversely affected by carrying the pathogen (Gray, 1998). Both sets of hosts are solely fed on by larval and nymphal ticks, with very few exceptions. As the system features two hosts which only feed larval and nymphal ticks, then each strain can be modelled separately using the LN model (as explained in section 5.2.3.2). Therefore, the infection status of ticks after the nymphal feeding stage – that is, developing nymphs, active adults and developing adults – are not tracked, as these are not involved in any transmission routes. In terms of human health concern, adult ticks are large enough to be usually detected and removed before the pathogen is passed on; therefore the main focus of these models is on the density of active nymphs. As it is easier to record tick densities at the end of a given year in the model, the measured tick density output used in these models is the density of developing larvae at the end of the year, which is equivalent in the model to the density of active nymphs at the start of the following year.

At this stage in the tick lifecycle, ticks will have only fed once, at the larval stage. It follows that as the hosts of *B. afzelii* and *B. garinii* are mutually exclusive, larvae are assumed in the model to carry at most only one strain of *B. burgdorferi* s.l. This means the total density of infected larvae is the sum of the densities of larvae infected with *B. afzelii* and those infected with *B. garinii*, and larvae carrying both strains do not need to be considered. As explained below (sections 5.3.1.2 and 5.3.1.3) squirrels are hosts of both strains. However their density relative to both small mammals and birds is far lower, so squirrels potentially

carrying both strains will be rare. Therefore infected larvae with both strains simultaneously are not considered. This means that for any model prediction of the density of infected ticks (which is a proxy for risk level), the model can be run twice, once parameterised for each strain, with the infected larvae summed to give the overall Lyme borreliosis risk. Such an approach also means that the strains can be analysed separately, with the predictions allowing the influence of hosts to be considered.

Whilst none of the competent transmission hosts within the system are adversely affected by carrying the pathogen (i.e. they do not get the clinical disease), for ease of use the terminology of the model is kept the same. Therefore, hosts carrying the pathogen in their bloodstream are still referred to as infected, and those which no longer pass on the pathogen to ticks are referred to as recovered. Recovery is still used to describe the transition between these two states for the host.

The densities of the incompetent transmission hosts are kept the same as in chapter 3. Therefore, within the model red deer have densities of 0.1 per km² in montane habitats, and 0, 5 and 15 per km² in heather moorland (as explained in chapter 3), mountain hares have densities of 8 per km² in heather moorland and 16 per km² in montane habitats, and roe deer have densities of 4 per km² in mixed woodland and 2 per km² in conifer plantation.

5.3.1.1 *Tick parameterisation*

The parameters governing tick behaviour are kept the same as in the LIV model presented in chapter 4, meaning that of the mechanisms in the LN model, waning immunity is absent. For most mechanisms, this is a fair assumption, since the presence of *B. burgdorferi* s.l. in the system should have no effect on ticks them-

Species	Woodland density (km²)	Non-woodland density (km²)	Larval burden (per host)	Nymphal burden per host)
Bank vole	5000	5	1.76	0.36
Common shrew	5000	100	0.39	0.08
Field vole	500	Negligible	1.37	0.28
Wood mouse	700	50	1.18	0.24
Grey squirrel	200	Negligible	13.20	7.75
Overall	**11400**	**155**	**1.31**	**0.36**

Table 5.3: The densities of the five species identified as important to *B. afzelii* persistence, and their larval and nymphal burdens (adults were not found on the species listed). The overall tick burdens are weighted by the woodland density of each species. Sources are given in section 5.3.1.2.

selves. The only parameter unlikely to be identical for a new pathogen system is the "aggregation parameter" (p) of nymphs upon a host (the nature of the negative binomial distribution of tick burdens among hosts), since this parameter could potentially differ between host species. Whilst research has shown that ticks appear to have a negative binomial distribution when feeding on rodents (James, 2010) and passerine birds (James et al., 2011), there isn't enough information to parameterise p, therefore this value is kept at 0.2. The reasoning behind selecting 0.2 as the value for p in the LIV model was that this low value allowed the pathogen to survive more freely, making it easier to compare different areas on their suitability for sustaining the infection. This reasoning still applies to the *B. burgdorferi* s.l. model.

5.3.1.2 *B. afzelii and small mammal dynamics*

The model assumes all small mammals have the same transmission competence and the same tick burdens, so that all small mammal species are merged together

into one host group in the model, termed "small mammal". The small mammals known to transmit *B. afzelii* comprise the bank vole (*Myodes glareolus*), common shrew (*Sorex araneus*), wood mouse (*Apodemus sylvaticus*) (Hanincová et al., 2003a) and grey squirrels (*Sciurus carolinensis*) (Millins et al., 2015). There is no information on the transmission competence of field voles (*Microtus agrestis*), but for the purposes of this model, here it is assumed that they can transmit *B. afzelii*. Small mammal densities were revised from those estimated in chapter 3. This revision also included finding values for small mammals in heather habitats, which previously had been treated as too low to be significant (after Gilbert et al. 2000), in order to understand the role they play in the prevalence of *B. afzelii* in heather moorland. The Joint Nature Conservation Committee review of British mammals (Harris et al., 1995) was used to find estimates of woodland and non-woodland densities of the aforementioned small mammals, which can be seen in table 5.3. The non-woodland densities are used as the estimates of small mammal density on heather moorland.

Pisanu et al. (2014) gave tick counts on road-killed squirrels across France to provide values for the average larval and nymphal burdens for squirrels, with no adult ticks found. Meanwhile, tick counts for the remaining small mammal species were taken from Gilbert et al. (2000), using the 98:2 split observed between larvae and nymphs. These tick counts were then averaged, weighted by the woodland densities of each species, to provide the larval and nymphal burden for the small mammal group as a whole (table 5.3).

A variety of sources were used to find the birth rate of the small mammal group. Bank voles were estimated to have 3-6 litters of 3-6 young per year, wood mice 4 litters of 4-7 young, grey squirrels 2 litters of 2-6 young (Nottinghamshire Wildlife Trust, 2016), common shrews were estimated to have 3-4 litters of 6

young (The Wildlife Trusts, 2016b), whilst field voles were estimated to have 5-6 litters of 4-5 young (The Mammal Society, 2016). From this information, an overall estimate of 4 litters of 6 young per year was taken, giving the total annual birth per individual as 24, and a weekly birth rate of 0.4615. As the different species had their litters at varying times across the year, birth was assumed to be constant throughout the year.

The lifespan of grey squirrels is estimated to be between 2-5 years; however, for the other species within the small mammal group, the lifespan is usually around 1 year (The Mammal Society, 2016). Since grey squirrels are the least abundant of the five species (making up under 2% of the total small mammal density), a lifespan of 1 year is taken for the small mammal group as a whole, which is inverted to give a weekly mortality rate of 0.0192.

Since the small mammal group is an amalgamation of several species, each with their own population cycles, the population is modelled to remain constant across the year, rather than the seasonal method used for grouse within the model presented in chapter 4. As small mammals are assumed to be not adversely affected by carrying the pathogen (Gray, 1998), the seasonality will likely not have as critical a role it had with grouse. This means infection-induced mortality is not included in the *B. afzelii* model for small mammals. Similarly, the mechanism for waning immunity is not included within the model, in the absence of evidence suggesting recovered small mammals eventually become susceptible.

In order to derive a value for the recovery rate of small mammals, the infectivity period is required. However, there is an overall dearth of research in this area for the species covered by the small mammal group. Therefore, experiments by Wright and Nielsen (1990) on white-footed mice (*Peromyscus leucopus*) in the USA are used to estimate a weekly recovery rate of 0.01.

Species	Woodland density (km²)	Non-woodland density (km²)	Larval burden (per host)	Nymphal burden (per host)
Blackbird	50	Negligible	11.62	1.83
Chaffinch	75	Negligible	7.50	0.50
Dunnock	20	Negligible	2.15	1.44
Greenfinch	10	Negligible	1.01	0.07
Song thrush	10	Negligible	0.32	0.14
Grey squirrel	200	Negligible	13.20	7.75
Overall	**11400**	**155**	**1.31**	**0.36**

Table 5.4: The densities of the six species identified as important to *B. garinii* persistence, and their larval and nymphal burdens (adults were not found on the species listed). The overall tick burdens are weighted by the woodland density of each species. Sources are given in section 5.3.1.3.

5.3.1.3 *B. garinii and Bird dynamics*

As with small mammals, the passerine bird host group is a combination of multiple species. This group is treated as one species, with identical values for parameters such as tick burdens, birth and mortality. In mixed woodland and coniferous plantation habitats, the bird species considered in the model are blackbirds (*Turdus merula*), chaffinches (*Fringilla coelebs*), dunnocks (*Prunella modularis*), greenfinches (*Chloris chloris*) and song thrushes (*Turdus philomelos*), identified as the key tick hosts by James et al. (2011) and can each carry *B. garinii*. Additionally, grey squirrels can also carry *B. garinii* (Millins et al., 2015); therefore despite not being a bird, grey squirrels are included in the passerine bird group. As with small mammals, the densities of these species were re-evaluated from those used in previous models within this thesis. The results of the Bird Breeding Survey (British Trust for Ornithology, 2016c) were used to find estimates of the density of each bird species within the passerine bird group. The maximum values for Scotland were used; since it is in woodland where passerine birds are

at their most dense. These are shown on table 5.4. These densities were used to weight the tick counts found by James et al. (2011) to derive larval and nymphal burdens for the passerine bird group (table 5.4).

The same method as with small mammals is used to find the birth rate for the passerine bird group. Blackbirds were estimated to have 2-3 broods of 3-5 young, song thrushes 2-3 broods of 3-5 young (RSPB, b), chaffinches 1 brood of 4-5 young (British Trust for Ornithology, 2016a), dunnocks 2-3 broods of 4-5 young (British Trust for Ornithology, 2016b) and greenfinches 2-3 broods of 3-8 young (British Garden Birds, 2015). From this, an estimate of two clutches a year of four young is used, giving an annual total birth per individual of 8 and a weekly birth rate of 0.1538.

The lifespan of blackbirds, chaffinches and song thrushes is taken as 3 years, whilst for dunnocks and greenfinches it is taken as 2 years (The Wildlife Trusts, 2016a). Factoring in the longer lifespan of grey squirrels, the lifespan used for the passerine bird group is 3 years, which is inverted to give a weekly mortality rate of 0.0064.

For heather moorland and montane habitats, the aforementioned passerine birds are assumed in the model to occur at insufficient densities to have a significant impact on *B. garinii* prevalence. However, pheasants can act as a competent transmission host for *B. burgdorferi* s.l. (Kurtenbach et al., 1998a,b). Unfortunately, there is not sufficient information on pheasant dynamics to include them within the model. Therefore, red grouse are used as the competent transmission host of *B. garinii* for heather moorland and montane habitats; as they are closely related game birds so seem likely to also be transmission hosts. The parameters and mechanics not related to infection remain the same as those used in chapter 4, including the use of a seasonal birth function.

The model assumes that neither passerine birds nor grouse suffer any increased mortality when infected (Gray, 1998), therefore infection-induced mortality is not included within the model. In the absence of any alternative evidence, the weekly recovery rate for both is set to 0.01, as is used with small mammals, whilst waning immunity is also absent from the model.

5.3.2 *Creating model predictions*

The models were run under the same conditions as the LIV model presented in chapter 4. Therefore, each model was run for 100 years on Mathematica Version 9 (Wolfram Research Inc., 2013) for each of the following climate warming scenarios, as per emissions scenarios predicted by UKCIP (Jenkins et al., 2009):

- Current temperatures (Now)
- Current temperatures + 1°C (Low)
- Current temperatures + 2.5°C (Medium)
- Current temperatures + 4°C (High)

For each simulation of the model, an initial infection rate among nymphs of 0.1 was used. The number and proportion of infected larvae at the end of the simulations is used as a measure of the pathogen spread, which is equivalent to the number and proportion of infected nymphs at the start of the following year. Nymphs are the instar most likely to infect humans (as unfed larvae will not have picked up the infection yet, and adults are easier for humans to find and remove), and therefore are the best proxy for disease risk within the model. Where small mammals were used as the competent transmission host, this reflects the prevalence of *B. afzelii*, and when birds (passerine or grouse) are used, *B.*

garinii is reflected. The overall abundance of *B. burgdorferi* s.l. is taken to be the sum of these. The density of infected ticks is the ubiquitously used indicator of tick-borne disease risk; therefore, as it is more useful for the outputs to be relevant to public health risk, the primary output from the model is the density of infected larvae (per km^2) at the end of running the model for 100 years, rather than the prevalence of the infection among larvae.

To get an overall impression of model predictions, the density of infected larvae (for *B. afzelii*, *B. garinii* and the two combined, which is taken as the density of larvae infected with *B. burgdorferi* s.l.) are mapped across Scotland for each of the four climate warming scenarios. The prevalence of *B. afzelii*, *B. garinii* and *B. burgdorferi* s.l. are also mapped across Scotland. Mapping was conducted using ArcGIS 10 (Environmental Systems Research Institute, 2014), the full details of which can be found in appendix A. In order to understand the influence of habitat types on model output, the density and prevalence of infected larvae in each habitat is found and plotted.

5.3.3 *Model predictions and discussion*

By considering the maps shown in figure 5.3, which demonstrate the total density of infected developing larvae at the end of the year, it is clear that with each climate warming scenario, the model predicts a small but perceptible rise in the number of developing larvae carrying *B. burgdorferi* s.l. (i.e. *B. garinii* plus *B. afzelii*). In particular, the central belt of Scotland sees a number of areas where climate warming is associated with a noticeable increase in the predicted density of infected developing larvae. By comparing the strain-specific maps (figure 5.3 middle and bottom rows), it can be seen that climate warming is predicted to cause virtually no change in the density of developing larvae infected with *B.*

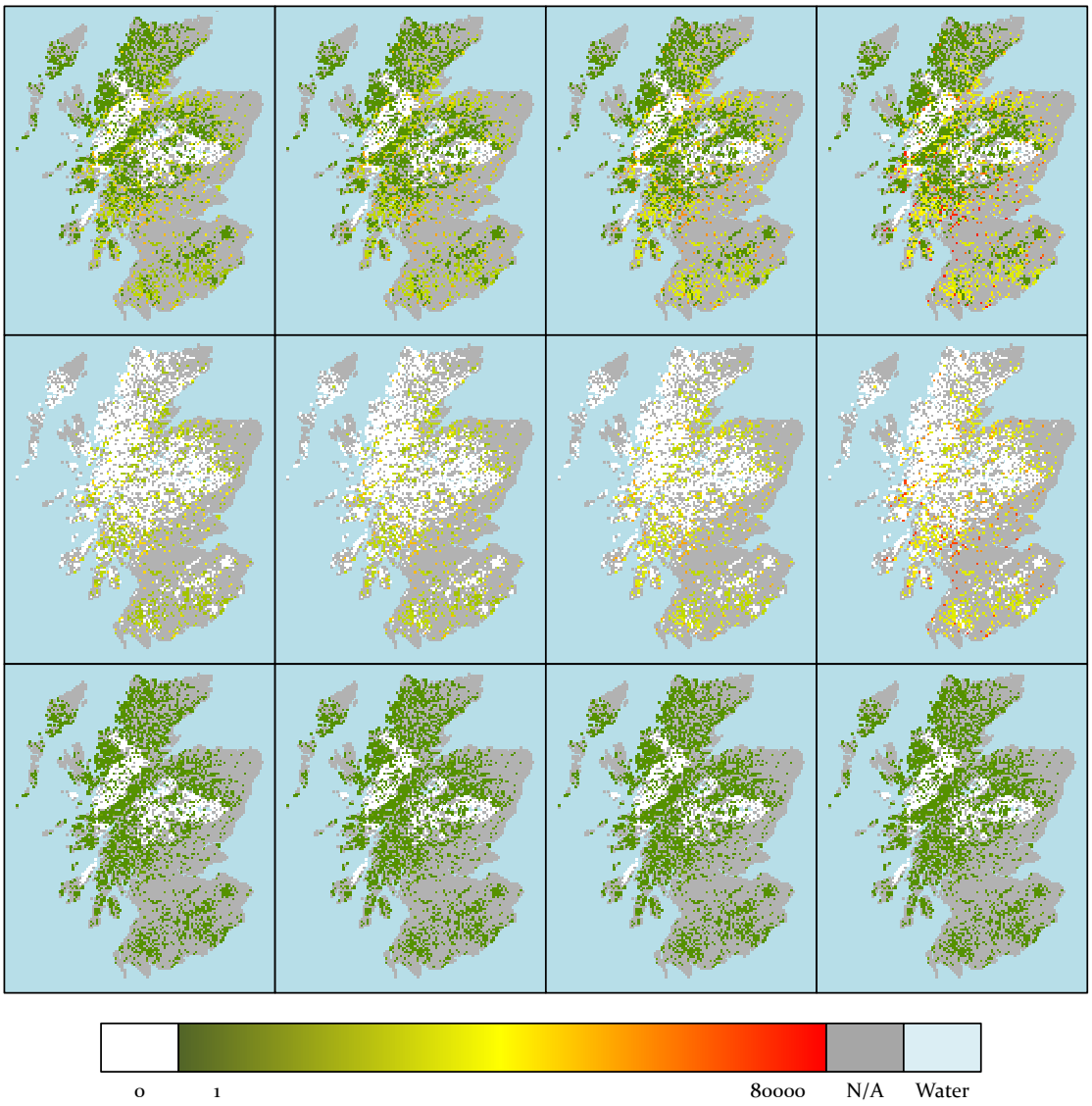

Figure 5.3: Maps displaying the predicted density (per km²) of larvae carrying *B. burgdorferi* s.l. (top) or its two strains *B. afzelii* (middle) or *B. garinii* (bottom). Dark grey cells indicate where the model was not run due to unsuitable habitats such as urban or arable land, and white cells indicate where the pathogen is predicted to die out. The maps display the predictions when the model is run for (from left to right) current temperatures, a 1°C increase, a 2.5°C increase and a 4°C increase.

garinii, suggesting that the model predictions that temperature-driven change in Lyme borreliosis risk is led by small mammal-mediated *B. afzelii* prevalence. This

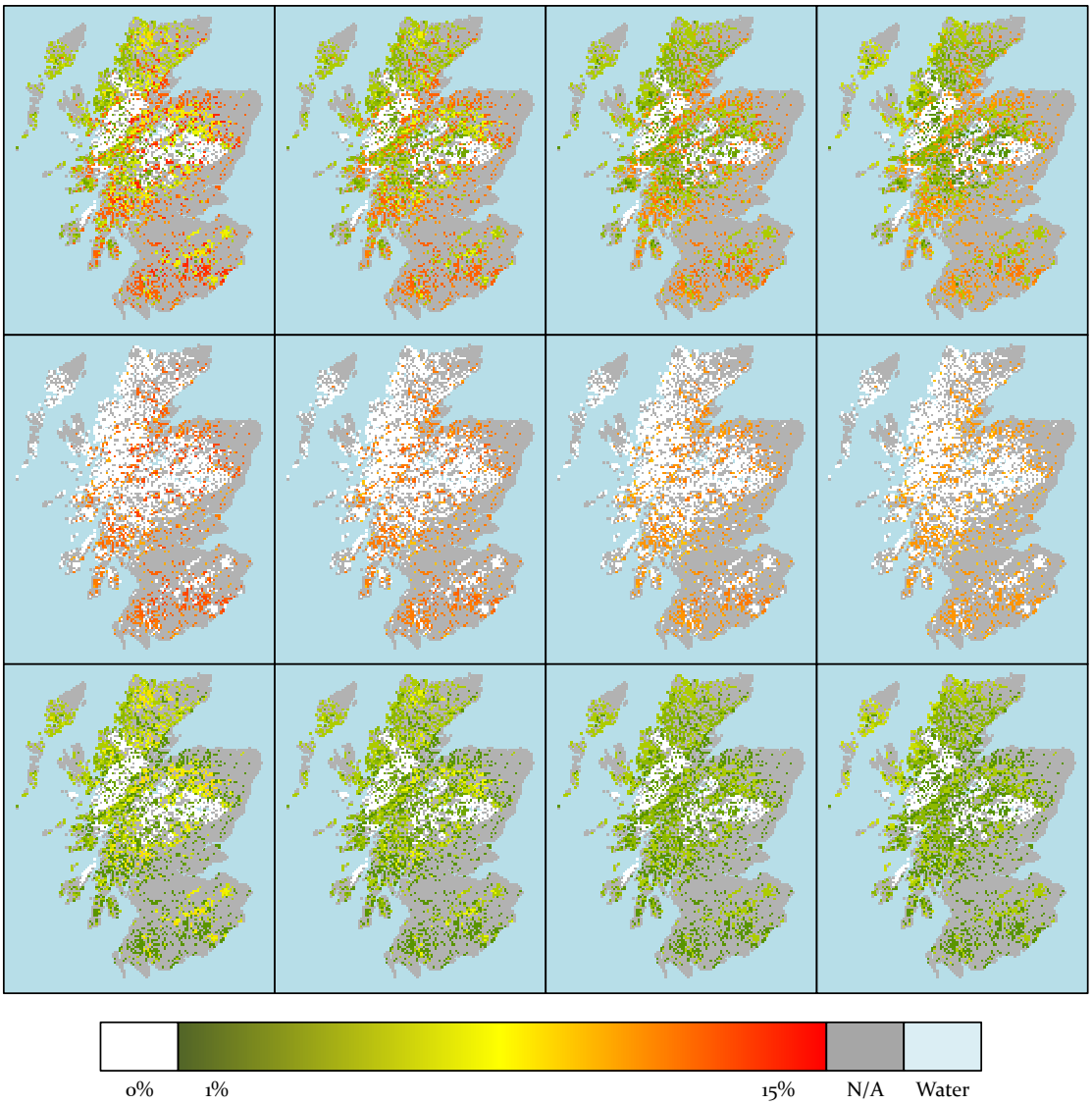

Figure 5.4: Maps displaying the predicted pathogen prevalence (proportion of infected developing larvae) for *B. burgdorferi* s.l. (top) or its two main strains *B. afzelii* (middle) or *B. garinii* (bottom). Dark grey cells indicate where the model wasn't run due to unsuitable habitats, and white cells indicate where the pathogen is predicted to die out.

may be due to the small mammal density being far higher than that of passerine birds (11400 per km² versus 365 per km² in mixed woodland, the densest habitat for both host groups), providing greater scope for an increase in disease risk with climate warming.

When examining the changes in the proportion of infected larvae (figure 5.4), it can be seen that *B. burgdorferi* s.l. prevalence in developing larvae will decrease with climate warming. This implies that whilst the density of infected larvae will increase, this will be outweighed by the increase in the density of uninfected larvae. In other words, with higher temperatures, the chances of an individual tick bite being from an infected tick will decrease, however the overall chance of being bitten by an infected tick will increase because there are more infected ticks. Therefore, the overall disease risk increases, as the density of infected larvae is taken as the primary measure of disease risk. This time, the strain-specific maps show that both *B. afzelii* and *B. garinii* both show a similar decrease in prevalence with rising temperatures (figure 5.4 middle and bottom).

These predictions can be broken down into habitats types in order to see which habitats are predicted to be most affected by rising temperatures (figure 5.5). It can be seen that for all habitat types, the predicted overall trend is for the density of infected developing larvae to go up as temperatures increase, despite *B. burgdorferi* s.l. prevalence among larvae to decrease. By considering the density of infected larvae within each habitat, it is clear that there is a significant difference in magnitude between the upland open habitats (heather and montane) habitats and the wooded habitats (plantation and woodland) habitats. Whilst the prevalence of *B. burgdorferi* s.l. in developing larvae is of a similar scale (between 3-6% for upland open habitats and between 10-14% for wooded habitats), the risk to public health is far greater in wooded habitats, where the density of infected developing larvae is more than a factor of 10 higher than in upland open habitats.

As the density of infected developing larvae (equivalent to the density of infected nymphs at the start of the following year) is used as the primary indicator of disease risk within the model, table 5.5 shows how this predicted disease risk

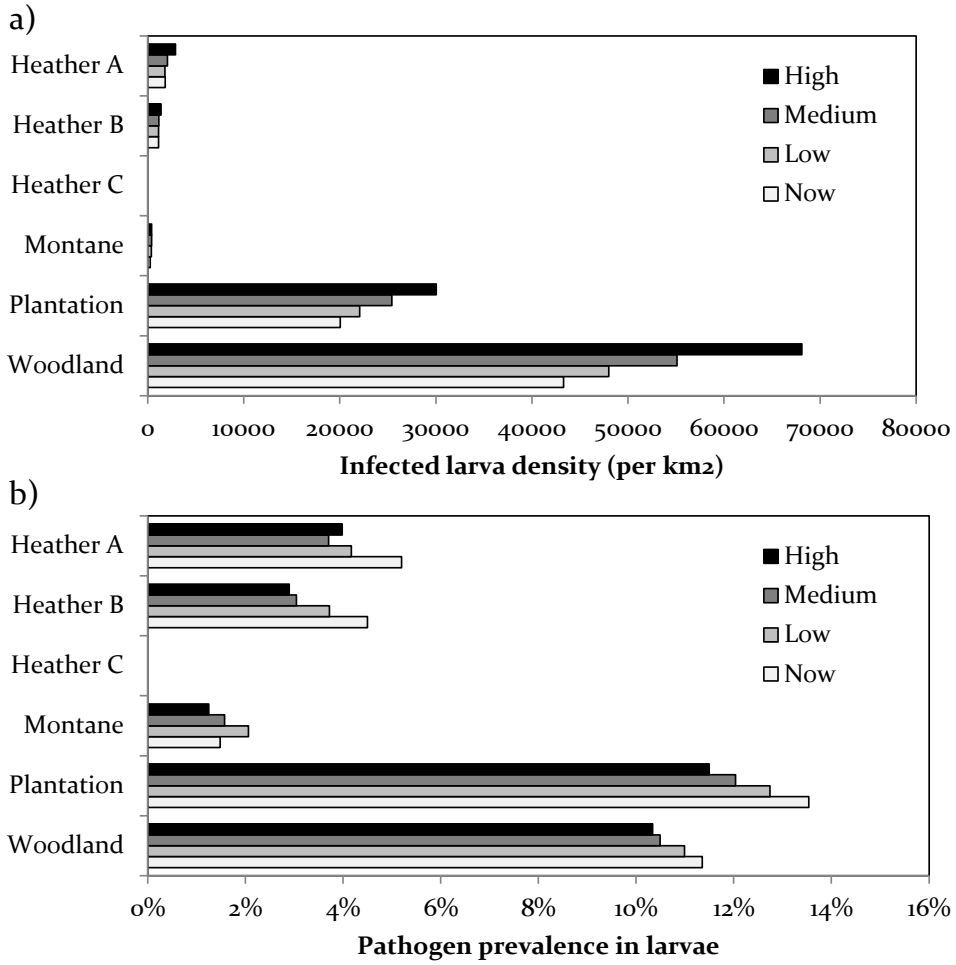

Figure 5.5: The predicted effect of habitat type and climate warming scenario on density of infected larvae (per km²) (a) and pathogen infection prevalence in larvae (b) for *B. afzelii* plus *B. garinii* combined, which is taken as a proxy for *B. burgdorferi* s.l. overall. Heather A areas are those with high grouse and no deer, Heather B areas are those with low grouse and low deer, whilst Heather C areas are those with no grouse and high deer. Plantation refers to cells which are classified as conifer plantation, whilst Woodland refers to cells which are classified as mixed woodland.

increases under each climate warming scenario for each habitat type, as well as the overall change. It can be seen that for the high climate warming scenario, disease risk is predicted to increase by over 50% for most habitat types. With the exception of a very small decrease in disease risk for heather moorland areas

Climate warming scenario	Low	Medium	High
Heather A	-2%	13%	58%
Heather B	-1%	2%	23%
Montane	52%	59%	64%
Woodland	11%	27%	57%
Plantation	10%	27%	50%
Overall	**9%**	**26%**	**52%**

Table 5.5: The change in predicted disease risk (measured as the density of infected developing larvae) for each habitat type under the climate warming scenarios, measured against the predicted disease risk for current climates. Heather A refers to heather moorland areas with high grouse and no deer and Heather B refers to heather moorland areas with low grouse and low deer. Heather C areas, which had no grouse and high deer, always displayed no disease risk.

under the low climate warming scenario, disease risk increases with climate warming.

These model predictions highlight the difference between prevalence and density of infected ticks. While prevalence should increase with the relative densities of transmission hosts, disease risk (the density of infected ticks) is a function of both prevalence and tick density. Therefore, conditions that promote tick survival and activity, such as increased temperature (Tomkins et al., 2014; Gilbert et al., 2014) and increased deer density (e.g. Gilbert et al. 2012) may increase disease risk even though these factors do not directly increase pathogen transmission. Outputs such as the model predictions provided here allow for both key parameters to be predicted (i.e. prevalence and risk).

A previous recent publication (Li et al., 2016) had similar aims to that of the case study in this chapter, namely to use an environmentally-dependent model to predict Lyme borreliosis risk across Scotland. Both studies looked at the density of infected nymphs as the main disease risk indicator across a variety of climate warming scenarios.

Li et al. (2016) took a very different modelling approach, using an agent-based model, in comparison to the coupled differential equations used within this chapter. However, there are similarities in how each model's predictions were influenced by environmental factors. Both models have questing dependent on temperature, and feeding success on host density. However, the model created by Li et al. (2016) also treats interstadial development as dependent on temperature, something which is not included explicitly within the models used in this thesis. However, the emergence function within the models in this thesis is temperature-dependent, and as this affects when ticks become available to quest in a new stage, this can be seen as a proxy for interstadial development. The model created by Li et al. (2016) includes seasonal variation in host densities, whilst in the model in this chapter these are kept constant. Seasonal variation can be seen as a more realistic assumption, although as highlighted earlier, care must be taken as different species have different breeding patterns. The study by Li et al. (2016) considers shorter-term predictions than those made in this thesis, and looks at the patterns of disease risk across the year. Therefore, including seasonal variation of hosts is more appropriate for this study than for the model presented in this chapter. The influence of hosts is very similar between the two modelling approaches; both model hosts as being able to feed the different tick instars in different rates (for example, adult ticks are more likely to feed on deer than larval ticks are), and the densities of hosts varies in the separate habitat types. Whilst migration of hosts and ticks is not explicitly considered in this thesis, this is included in the model by Li et al. (2016). Overall, the two models have similar approaches to modelling *B. burgdorferi* s.l. across Scotland. The significant mechanistic differences between the models are primarily a result of the slightly different aims of the two studies, specifically that the study by

Li et al. (2016) made shorter-term predictions of disease risk, compared to the longer-term predictions made in this chapter.

When considering the model predictions, Li et al. (2016) focused on the impact of elevation on disease risk, finding that higher altitudes reduced the disease risk. Whilst altitude is not explicitly measured in the model output in this chapter, the montane habitats by definition are at a high altitude, and display a negligible disease risk under any climate warming scenario. Additionally, Li et al. (2016) found that for each of their climate warming scenarios disease risk increases, a prediction shared in this chapter. When considering the spatial distribution of the predictions made by Li et al. (2016), no clear pattern (other than the aforementioned effect of altitude) can be observed; the four sites where the highest disease risk is predicted are at extremely different latitudinal and longitudinal locations in Scotland: Oban (midway up the western coast), Dumfries (close to the southern coast), Inverness (in the highlands, close to the northern coast) and Perth (central, close to the eastern coast). The only trend that be seen from these locations is that they are all reasonably close to the coastline. However, locations such as Thurso (on the northern coast), Golspie (on the eastern coast) and Thainstone (close to the eastern coast) are three of the four sites predicted to have the lowest disease risk. Therefore, as the predictions made in this thesis do not focus on individual locations, it is difficult to directly compare the results to those of Li et al. (2016).

5.3.4 *Sensitivity analysis*

In order to test the sensitivity of the *B. burgdorferi* s.l. model to its parameters, the two methods presented in Watts et al. (2009), described below, are used.

In both cases, the model is run for the warmest woodland habitat group (W_3, full explanation in appendix A) under the medium climate warming scenario (2.5°C). The output measured for both methods is the density of infected larvae after the model has been run for 100 years.

5.3.4.1 *Method 1*

In order to test which parameters had a disproportionate influence on the model predictions, each parameter within the model was altered by ±10% in turn, with the change in model output recorded (table 5.6).

The parameters with the most influence on model predictions are those affecting the density of infected hosts available for larvae to feed on. This includes parameters for the local minimum temperature (a) and the temperature threshold for larvae to begin questing (T_{L1}), both of which limit when larvae can begin questing for blood meals. Also important are the basic host dynamic parameters, such as birth (a_H) and natural mortality (b_H), which influence the number of available meals for larvae. Parameters pertaining to the infectivity of hosts, such as the recovery from infection (σ) and the parameter for the nature of tick aggregation on hosts (p) have a large effect, since they determine how many hosts become infected and for how long they can pass on the pathogen to larvae. Most important, however, is the number of nymphs hosts can feed (h_N), which decreases the number of infected larvae by 23.4% with just a 10% decrease in h_N. This parameter determines how effectively infected nymphs can pass the pathogen onto hosts and appears to be the most influential in the density of infected larvae.

Of the parameters listed above, the majority change the model output by a disproportionate amount (i.e. by more than the 10% that the parameters were

Parameter	Decrease of 10%	Increase of 10%
a	-5.2%	+6.8%
b	-2.6%	+2.0%
T_{L1}	**+10.9%**	-8.7%
T_{L2}	+1.0%	-1.0%
T_{NA1}		
T_{NA2}		
b_L		
b_N		
b_A		
b_{WL}	+2.6%	-2.5%
b_{WN}		
a_T		
w	+1.7%	-1.8%
b_H	+9.8%	**-11.1%**
a_H	**-11.3%**	**+11.3%**
σ	**+10.8%**	**-10.1%**
s_H	**+12.1%**	-9.9%
Initial infection of nymphs		
p	**+12.5%**	**-12.8%**
h_L	**-10.2%**	**+10.1%**
h_L	**-23.4%**	**+19.1%**

Table 5.6: The change in predicted infected larvae density when each parameter within the model is altered by ±10%. Only changes larger than ±1% are shown, and those with an absolute value greater than ±10% are highlighted in bold. The parameter definitions are given in table 5.1.

changed by), highlighting how sensitive the model is to parameters related to pathogen transmission.

5.3.4.2 *Method 2*

For an alternative view of the effect each parameter has on model output, the model was run 1000 times with each parameter randomly varied by up to ±1%.

Parameter	Correlation
a	**0.180**
b	0.062
T_{L1}	**-0.264**
T_{L2}	-0.020
T_{NA1}	-0.059
T_{NA2}	-0.046
b_L	-0.004
b_N	-0.037
b_A	-0.045
b_{WL}	-0.085
b_{WN}	0.014
a_T	-0.011
w	-0.049
b_H	**-0.294**
a_H	**0.293**
σ	**-0.284**
s_H	**-0.303**
Initial infection of nymphs	0.032
p	**-0.345**
h_L	**0.293**
h_L	**0.605**

Table 5.7: Pearson's correlation coefficient between the parameters in the model and the total number of infected larvae, after the model was run 1000 times, with each parameter altered by ±1%. Correlations with an absolute value larger than 0.1 are highlighted in bold. The parameter definitions are given in table 5.1.

The correlation between the parameter values used and the number of infected larvae was then used to test which parameters explained the most variation in the model output. These correlations are shown in table 5.7.

It is unsurprising that the same parameters highlighted by Method 1 had the highest correlation with infected larva density. Once again, the nymphal burden of hosts (h_N) is the parameter with the largest correlation with infected larva

density, at 0.605, followed by the tick aggregation parameter (p) with a negative correlation of 0.303. These are also the only two parameters which explain over 10% of the variance within the output, as h_N has an R^2 value of 0.366, whilst p has an R^2 value of 0.119.

5.3.4.3 *Sensitivity analysis summary*

It is clear that the model created for *B. burgdorferi* s.l. dynamics is most sensitive to parameters which dictate the number of available infected blood meals for larvae.

It should be noted that the values of some of these parameters, such as the recovery rate (σ) and the temperature at which larvae emerge (T_{L1}) are based on few empirical data, whilst parameters such as the nymphal capacity of hosts (h_N), host birth (a_H) and host mortality (b_H) are the result of multiple species having their demographies grouped together into a weighted average. Therefore the predictions from this *B. burgdorferi* s.l. model are likely to be not as robust as those from the LIV model (chapter 4). In order to develop a *B. burgdorferi* s.l. model with which more confidence can be placed, more work needs to be done to produce more concrete parameter values. Specifically, the sensitivity analysis indicates that the parameters which are based on little empirical evidence, yet are important in influencing the model output, are recovery from infection (σ) and the nature of the aggregation of ticks on hosts (p). The latter of these can be estimated from counts of ticks on hosts, specifically taking note of the number of hosts with no ticks present. The recovery rate is likely to require specific laboratory experiments (such as those conduced on white-footed mice by Wright and Nielsen (1990) in order to find an estimate for the value.

5.4 SUMMARY

The aim of this chapter was to extend the LIV model from chapter 4 into a modelling framework, which can be adapted for other tick-borne pathogen systems. By introducing new mechanisms to a generalised version of the LIV model, such a framework was created. This framework was then used to create a model reflecting the dynamics of *B. burgdorferi* s.l., the agent of Lyme borreliosis.

Adaptations to the LIV model were described to help provide the tools necessary to create models of other tick-borne pathogen systems as well as modifying the LIV model to incorporate further infection routes, additional hosts and control methods beyond those investigated thus far in this thesis. Specifically, this chapter described how the modelling framework could accommodate more than one transmission host type, alternative routes of transmission and the treatment of tick hosts.

As section 5.3 showed, re-parameterising the model to model *B. burgdorferi* s.l. dynamics is achievable. This exercise highlighted the need for more accurate and detailed empirical information on the length of time that transmission hosts can pass on the pathogen to ticks and the nature of the distribution of ticks on hosts for more accurate parameterisation and more robust model predictions. Whilst the uncertain nature of many of the parameter values used means that the quantitative accuracy of the predictions presented are uncertain, adapting the LIV model to *B. burgdorferi* s.l. is still informative for predicting general trends and invaluable in identifying gaps in empirical knowledge that are now needed for future model accuracy. For example, the model predicts that whilst the *B. burgdorferi* s.l. prevalence in ticks may decline with climate warming, a temperature-driven increase of tick populations means that the density of infected ticks (the key proxy for disease risk) is predicted to increase. Overall, the model

predicted that the Lyme borreliosis risk across Scotland would increase by over 50% under the highest climate warming scenario.

The creation of a *B. burgdorferi* s.l. model showed that it was possible to adapt the modelling framework to reflect the dynamics of a new tick-borne pathogen system, and the predictions matched those of a completely different modelling approach of the same Lyme borreliosis system in Scotland (Li et al., 2016). This model adaptation, while not validated with empirical data due to the temporal nature of climate change, is of use to policy on Lyme borreliosis awareness campaigns and mitigation strategies, and highlights gaps in our empirical knowledge to guide further research.

6

DISCUSSION

The aim of this thesis was to predict the impact climate change will have on tick-borne disease risk across Scotland, specifically Louping-ill and Lyme borreliosis. To this end, a novel modelling framework, which factored in a dependency on environmental factors, was developed. This framework utilised GIS tools and climate warming predictions to enable predictions of how disease risk will change across both space and time. This chapter summarises the modelling work done within this thesis, highlights the main findings, and discusses how they relate to the thesis aims and the global context. An analysis of the limitations of the modelling framework is provided, along with a discussion of the potential next steps to address these. The future research required to fill the gaps in knowledge highlighted by this thesis is also discussed.

6.1 DEVELOPING THE MODELLING FRAMEWORK

Previous modelling of tick and tick-borne pathogen systems were reviewed (chapter 2), identifying our current knowledge gaps in this area. It was found that one of the main areas where future modelling should focus was on the spatial patterns of disease risk, and the combination of environmental data with

mechanistic modelling. The modelling work in this thesis aimed to provide new insight by addressing these gaps.

6.1.1 *Creating a novel environment-dependent tick lifecycle model*

The first step in the development of the framework was to introduce an original model for the lifecycle of the sheep tick (*Ixodes ricinus*), incorporating the key environmental factors of temperature, host density and habitat. The model introduced in chapter 3 particularly focused on the mechanism for ticks finding a blood meal, which was broken down into three parts: emerging from overwintering, questing for a meal, and successfully finding a host. The proportion of ticks to have emerged was represented by a linear function between two temperature thresholds, which were based on empirical observations. Laboratory experiments by Gilbert et al. (2014) were used in order to find a function representing the proportion of emerged ticks questing for a given temperature. These two functions were used to find proportion of ticks questing for a meal in a given week, which was fed into a sigmoid function to calculate proportion of ticks successfully feeding. The maximum value of this feeding function was dependent on the number of available blood meals for ticks in that habitat. Therefore, the model was dependent on the environmental factors of temperature, hosts and habitat, as emergence and questing behaviour were temperature-dependent, whilst the number of available blood meals for ticks depended on the host density, which in turn was determined by the habitat.

Running the model for current climates predicted that the highest tick densities are to be expected in mixed woodland, followed by conifer plantation, with fewer ticks in open habitats such as heather moorland and grassland habitats. Running the model for low, medium and high climate warming scenarios predicted that in

all studied habitat types, tick densities would increase as temperatures rise. The overall increase in nymph densities compared to current climates was between 26.1-98.7% depending on the climate warming scenario. However, this increase in tick density was not equal across all habitats; for example, whilst mixed woodland areas saw a predicted increase of 47% for the high climate warming scenario compared to current climates, the same comparison for montane regions saw a predicted increase of 572%. Meanwhile, for blanket bog the increase was 128%, meaning that whilst blanket bog areas were predicted to have higher tick densities than montane areas under the current climate, for future climate warming scenarios they would be overtaken. This suggests that it is not just temperature which drives tick density changes within the model, but also host density and habitat have an effect on how large this change will be. Therefore, this demonstrates that the model output is influenced by environmental factors, and can be used as the foundation of the modelling framework.

6.1.2 *Introducing pathogen dynamics to the tick lifecycle model*

Following the creation of the tick lifecycle model, the next step was to introduce host and pathogen dynamics. The aim of this was to demonstrate that the model could be used to predict the effect climate change would have on disease risk. The pathogen system looked at in chapter 4 was that of Louping-ill virus (LIV), as this is the tick-borne pathogen which has the largest body of previous modelling work and empirical studies provide relatively robust parameter values. The focus of the chapter was to model a LIV system with one competent transmission host, red grouse (*Lagopus lagopus scoticus*), with red deer (*Cervus elaphus*) and mountain hares (*Lepus timidus*) acting solely as tick hosts. The tick lifecycle model was extended by introducing equations to represent the infectivity status of hosts and

ticks. The most important aspect introduced within this chapter was the use of the negative binomial distribution of tick burdens on hosts to calculate how many grouse are predicted to be bitten by infected ticks in a given week. .

The primary output of the model was the grouse survival, measured as a percentage of the carrying capacity for that area. For all climate warming scenarios, LIV was only predicted to persist on heather moorland. For these areas, LIV risk was predicted to increase as the climate warms. The proportion of cells where the model was run which were predicted to have high LIV risk (defined as those where the predicted grouse survival was reduced to under 60%) increased from 10.74% under current climates to 47.81% under the high climate warming scenario; this comprised of more than half of the heather moorland across Scotland containing grouse. Grouse survival was predicted to decrease from current climates by between 4.76-19.35% depending on the climate warming scenario. The main impact of such changes in grouse survival would be felt by grouse moor managers, who may experience a loss in income. Grouse moor managers may choose to take proactive measures to mitigate such losses, in which case the impact of increased LIV risk may be passed to the wider environment, where many moor management strategies can have a negative effect (Wightman and Tingay, 2015).

There was a clear distinction between heather moorland areas with red deer present, and those without, with areas lacking deer predicted to have lower grouse survival. This indicates that within the model a dilution effect of deer on LIV is predicted, whereby the presence of red deer results in infected ticks wasting their bites on hosts that do not transmit the virus, and therefore reducing infection of grouse with the pathogen. This chapter also demonstrated that the presence or strength of the dilution effect depended on the proportions of larval and

nymphal burdens on deer compared to transmission hosts. This is an indication that parameterisation of tick stages on different host types play an important role in the model predictions and highlights an important gap in our knowledge for further empirical research. Three recent studies of Lyme borreliosis risk discuss how the relative proportions of immature ticks feeding on different host types may determine whether or not there is a dilution effect (Mysterud, 2016; Gilbert, 2016a; Millins et al.). Combined with the influences that temperature and habitat had on the model predictions, this demonstrates that the aim of creating a model which allows environmental factors to be used to predict LIV risk has been met.

This model demonstrated the novel combination of a mechanistic LIV model with GIS tools, allowing for detailed empirical data to be used, and for the model predictions to be displayed spatially. Whilst previous studies had used such an approach for other tick-borne pathogen systems, none had been done for LIV. Even compared to other studies using GIS tools with tick-borne pathogen modelling, this thesis used an original method to represent the different natures of the various habitat types across Scotland (see appendix A).

6.1.3 *Adapting the novel modelling approach to other tick-borne pathogen systems*

In order to broaden the models created thus far into a modelling framework which can be applied to many tick-borne pathogen systems, the LIV model was generalised in chapter 5. This general model was adapted to reflect the dynamics of *Borrelia burgdorferi* sensu lato, the agent of Lyme borreliosis. The aim of this was to demonstrate that the LIV model could be used to model a different real-life tick-borne pathogen system, as well as to provide predictions of the impact climate change will have on Lyme borreliosis risk. The LIV model was generalised to create basic models which were the foundation of the framework. Following

this, techniques for modelling further tick-borne pathogen mechanisms were identified, which could be appended to the basic models if the pathogen system being modelled required. Specifically, within the chapter it was described how the modelling framework could be used to represent systems with more than one transmission host type, as well as including alternate routes of transmission and the treatment of tick hosts with either vaccines or acaricide.

Available empirical information was used to create a model that predicted the risk of *B. burgdorferi* s.l. across Scotland under current climate and with climate warming scenarios. Specifically, the model focused on two strains of the pathogen; *Borrelia afzelii*, where small mammals are the primary transmission host, and *Borrelia garinii*, where birds are the primary transmission host. The model was run for the same climate warming scenarios as previous models, this time focusing on two key model outputs: the total density of infected ticks and the prevalence of the pathogen in ticks. It was predicted that prevalence would decrease with climate warming, whilst the density of infected ticks increases. As the density of infected ticks is the more important factor when it comes to public health, it was concluded that climate warming will increase the risk of Lyme borreliosis for humans. Using the density of infected developing larvae as the primary indicator of disease risk, the model predicted that the disease risk would increase across Scotland by 52% with the highest climate warming scenario. This demonstrated that it was possible to adapt the modelling framework for a new tick-borne pathogen system, allowing the influence of climate change to be predicted.

The combination of a mechanistic model for *B. burgdorferi* s.l. dynamics with GIS mapping for Scotland was also done by Li et al. (2016). However, there are numerous differences between the methods used in chapter 5 and by Li et al. (2016). In particular, the type of mathematical models used, and the application

of GIS data to the model are distinct. Both studies predicted similar increases in Lyme borreliosis risk with climate warming.

6.2 LIMITATIONS AND FUTURE WORK

6.2.1 *Assumptions made when creating the models*

There are multiple assumptions made in the creation of the models presented which, whilst required for simplicity, will diminish the models' ability to reflect real life. This section will focus on two in particular: the assumption that ticks feed only once per year and the assumption that habitat type and host densities stay constant through each climate warming scenario.

6.2.1.1 *Feeding once per year*

The models within this thesis have assumed that ticks develop into the next stage each year, and each stage feeds only once, i.e. each tick feeds once per year. Whilst ticks feeding twice within a given year has been documented (e.g. Randolph et al. 2002), these observations were made south of Scotland, where such behaviour has not been demonstrated. As interstadial development is considered to be temperature-dependent (Randolph et al., 2002), it is likely that ticks based in Scotland are less likely to feed twice within the same year, if at all. However, under climate warming it is unclear how ticks based in Scotland will respond in terms of speed of interstadial development. Specifically it is unclear whether they begin to act like ticks from warmer climates (i.e. that all ticks are fundamentally the same and act differently due to climatic factors) or whether they maintain the same interstadial development times (i.e. that in identical situations ticks from different climates will act differently). Gilbert et al. (2014) found that ticks from Scotland,

Wales, England and France began questing at different temperatures in laboratory conditions, indicating that local adaptation had occurred to these populations at some point in time, although the mechanism and speed of this adaptation is not known. If the mechanism is genetic evolution rather than phenotypic plasticity, it is likely that ticks in Scotland will not immediately change their behaviour with climate warming. However, when ticks are exposed to new temperatures for far longer periods of time (such as the 70 years used to make model predictions) some changes in behaviour could potentially be observed depending on the mechanism of change. Given enough time, it is highly likely that with climate warming Scottish ticks will tend to feed more than once in a given year, as they now do in the south of England (Randolph et al., 2002).

In order to adapt the model in order to accommodate this change in interstadial development time, the emergence function outlined in chapter 3 would need to be replaced by a temperature-dependent function which allowed ticks in a developing class to move into the active class for the next instar. Inspiration could be drawn from the method used by Dobson and Randolph (2011) for this mechanism. However, this study uses a day-degree summation to predict when ticks would move into the next stage. This would be difficult to implement into the modelling framework presented in this thesis in its current form, and would likely necessitate a switch to a different type of modelling, such as the Leslie matrix method used by Dobson and Randolph (2011).

6.2.1.2 *Habitat type and host density change*

In order to make clear the effect of temperature on the model predictions, habitat type and host density were assumed not to change under the climate warming scenarios used within this thesis. In reality, climate warming is likely to change

both habitat cover and host densities across Scotland. For example, vegetation such as heather may be able to spread to colder areas, such as parts of the high-altitude montane regions, and with it the tick hosts assumed to be present in heather, such as red grouse and red deer. Therefore it is likely that the predictions made in this thesis regarding the density of ticks and the disease risk in high-altitude areas are in fact underestimating the effect climate warming will have.

If habitat types and host densities are to change with warmer climates then the relationships of these factors in relation to temperature would need to be modelled. For instance, roe deer are known to migrate to lower altitudes in winter, suggesting that their behaviour is driven by temperature (Mysterud, 1999), and such behaviour has been included in modelling tick-borne disease by Li et al. (2016). To be included in the modelling framework presented in this thesis, it would be likely that host movement between cells would also need to be included. This may also necessitate the inclusion of ticks being transported between cells by hosts. This would enable a more detailed analysis of how disease risk may spread spatially across Scotland. However, introducing numerous mechanisms into the modelling framework to represent changes in habitats and hosts may risk making the model too complicated to be of a functional use. If done carefully though, this would allow further impacts of climate change on tick-borne disease risk to be analysed.

6.2.2 *Parameterisation of the models*

As with all mathematical models of specific systems, the models presented are dependent on the values used for the parameters. Whilst many of these are based on thorough empirical studies, there are some with which far less faith can be placed, indeed in real life there is a lot of variability between sites and it is difficult

to determine the reason for those differences. Conducting sensitivity analysis on the models created gives an idea of the parameters which are of importance. A crucial set of parameter values which are based on little empirical data are the temperatures at which ticks emerge from overwintering. For example, it is recorded that nymphs emerge in spring from winter diapause when the average weekly maximum temperature reaches 7°C (Randolph, 2004), however due to natural variation among individuals it is unlikely that all nymphs emerge at exactly 7°C; therefore some estimation is needed for the temperature at which nymphs begin to emerge and the temperature at which all nymphs have emerged. Within the model these are taken to be 2°C either side of the 7°C suggested, however this is an arbitrary range. The other parameters which were important, yet based on little empirical evidence, were those relating to the infection status of hosts within the *B. burgdorferi* s.l. model, specifically the "recovery rate" of hosts, the rate at which hosts move from the infectious class (where they can pass the pathogen onto ticks) to the recovered class (where they no longer could). Estimations for this parameter did not exist for the hosts within the *B. burgdorferi* s.l. model; therefore this rate was based on experiments on white-footed mice (*Peromyscus leucopus*) in the USA (Wright and Nielsen, 1990).

For many of these less reliable parameter estimates, work could be done in order to find values which are more reliable. For the emergence of ticks from overwintering, a long-term study may be required, whereby a known number of ticks are placed within a patch of vegetation at the start of winter, and blanket drags are regularly carried out to determine how many questing ticks are present as the weather warms in the spring. As not all emerged ticks may necessary quest, the results of Gilbert et al. (2014) would have to be used to extrapolate the number of questing ticks into an estimate of emerged ticks. In order to find an

estimate of the recovery rate of *B. burgdorferi* s.l. reservoir hosts, the laboratory experiments conducted by Wright and Nielsen (1990) could be replicated with the tick hosts used within the *B. burgdorferi* s.l. model.

6.2.3 *Deterministic versus stochastic modelling*

The deterministic nature of the modelling undertook has its strengths, such as providing a clear demonstration of how factors affect the model output; however it also can fail to represent highly variable aspects within a model. For instance, the negative binomial distribution of ticks on hosts is used within the modelling framework to get an estimate of the proportion of hosts to be bitten by an infected host. However, this is the expected value which is used for every calculation. In reality, this proportion would just be the long-term average of this calculation, with the distribution of ticks on hosts varying each time. Therefore, creating a stochastic version of the modelling framework is a viable future option.

Whilst the parameters used within this thesis could be used as the average for the parameters within a stochastic model, estimations would be required for the variation in some cases. For example, within this thesis the density of mountain hares in heather woodland is taken as 8 per km^2. This is a parameter which will vary wildly across the country, but in order to represent this, the variation and distribution shape would be required. Therefore, the danger of creating a stochastic model is that these estimations make the model less robust, as more of it is reliant on weak data. Nonetheless, creating a stochastic version of the modelling framework is a valid future direction, and one which would be interesting for comparison with the current framework.

Climate warming scenario	Low	Medium	High
Tick density (chapter 3)	26.10%	65.25%	98.64%
LIV risk (chapter 4)	4.76%	12.41%	19.35%
B. burgdorferi s.l. risk (chapter 5)	9.43%	25.76%	51.59%

Table 6.1: Summary of the primary predictions made in each chapter. Each percentage is the increase from the predictions for current climates. The indicator of tick density was nymph density, the indicator of LIV risk was the decrease in grouse density compared to the carrying capacity, and the indicator of *B. burgdorferi* s.l. risk was the density of infected developing larvae. The climate warming scenarios were increases from current temperatures of 1°C (low), 2.5°C (medium) and 4°C (high), as explained in appendix A.

6.2.4 *Adapting the models for other vectors*

The models created were designed specifically for *I. ricinus* ticks, although they would be suitable for any *Ixodidae* tick, as they only feed once per stage (Randolph, 2008), with parameter adjustment where necessary. However, for *Argasidae* ticks, who feed multiple times per stage, the modelling within this thesis would not be appropriate. Similarly, adjusting the models for vectors other than ticks, such as mosquitoes, would be extremely difficult to adapt the modelling framework for, due to the differences in lifecycles. Many of these differences means that core assumptions made in chapter 3 would not apply. As the model presented in chapter 3 is the foundation of the modelling framework, it would be impractical to try and adapt the existing framework for a new vector.

Whilst the general method for using an environmentally-dependent model to create predictive maps (as laid out in appendix A) could easily be applied to other vector systems, the model itself would have to be recreated from scratch.

6.3 SUMMARY

Through the creation of a novel modelling approach, which focused on the environmental factors that influence tick behaviour, a modelling framework has been created to predict the influence climate change has on tick population dynamics, LIV risk, and other tick-borne disease risk. This framework allows the dynamics of many tick-borne pathogen systems to be modelled, however in this thesis two pathogens were focused on in particular: *B. burgdorferi* s.l. and LIV. Models created specifically to look at these two pathogens were used to predict the changes in disease risk under a variety of climate warming scenarios. It was predicted that in both cases disease risk will increase with climate warming. However, other factors also influenced the model output, namely the habitat type and host density. The main predictions made in each chapter are summarised in table 6.1.

Analysis of the model predictions allow for further insights. The LIV model created allowed greater understanding on how the mechanisms within the model influence the dilution effect. The most significant of these was the effect of the relative burden of immature tick stages on different host types. All the models created identified areas where future empirical data collection would improve the model predictions. The most pressing of these came from the *B. burgdorferi* s.l. model, which highlighted the need for improved data on the infectious behaviour of transmission hosts.

By considering previous mathematical modelling of tick and tick-borne pathogen dynamics, knowledge gaps were identified. This highlights the importance of the work within this thesis, as it addresses some of these gaps, furthering our understanding of tick-borne diseases. The combination of mechanistic modelling with GIS tools, and the focus on the impact of climate change, makes this a timely

contribution. The model predictions within this thesis give an indication of the effect of any changes to the Scottish environment (either natural or planned), and this means they have the potential to inform policy-making. The adaptable modelling framework presented in this thesis can be extended to further tick-borne pathogen systems. This may be particularly useful in cases where a new tick-borne pathogen has spread to a new region; the tools provided within this thesis would allow for a new mathematical model to be created quickly, allowing areas of potential risk to be predicted.

As the modelling approach taken in this thesis is a novel one, it was always likely that simplifying assumptions would have to be made, and that it would open up new avenues to be researched. However, by focusing on the influence environmental factors have on tick behaviour the aims of the thesis have been met, by providing an indication of how climate change will affect tick-borne disease risk across Scotland.

A

METHODOLOGY

This appendix details the methods used to set up the model predictions within the thesis. The first section concerns the transition of data to and from ArcGIS 10 (Environmental Systems Research Institute, 2014). This comprises the extraction of data from the database available at the James Hutton Institute in Aberdeen (section A.1.1), and the importing of model predictions into ArcGIS for the use of creating maps (section A.1.2). The aim of this is to provide a guide for replication. The second section give the full details and justifications for the creation of the conditions under which the models were run, specifically the creation of the habitat groups used (section A.2.1) and the rationale behind the choice of climate warming scenarios used (section A.2.2). The final section of this chapter gives the method of how the models were run (section A.3).

A.1 MANAGING GIS DATA

A.1.1 *Obtaining data from a GIS database*

In order to apply the models to Scotland, a 3km² fishnet grid (a net of rectangular cells) was applied to the country using ArcGIS. This cell size was chosen as the highest resolution which was still computationally manageable to manipulate,

based on the running speed of Microsoft Excel 2007 (Microsoft Corporation, 2007) with the cells uploaded. From the centre of each cell the following previously available data were appended: habitat type, deer density, maximum annual temperature, minimum annual temperature and average annual temperature. This data was then saved as a comma-separated value (CSV) file and opened in Microsoft Excel for easy use. The data was in the format where each row represents a cell, and each column represents a data type.

The habitat type data available for each cell was based on the UK Land Cover Map 2000 (Fuller et al., 2002), the deer density was taken from Deer Management Group counts up to 2006 (unpublished), whilst the annual temperatures were from Met Office long-term average data from 1971-2000 (Met Office, 2016).

A.1.2 *Creating predictive maps*

In order to display the spatial predictions from each model, Mathematica Version 9 (Wolfram Research Inc., 2013) was used to run the model for each relevant habitat group (explained further in section A.3). The output from these simulations was then added to the extracted GIS data in Microsoft Excel as a new column depending on their habitat group (see section A.2.1) and saved as a CSV file. The CSV file was then joined to the 3km² fishnet and saved as a separate layer, which was then coloured appropriately before being exported as an image file.

A.2 CREATING THE CONDITIONS FOR MODEL SIMULATIONS

A.2.1 *Habitat group creation*

Of the 12 habitat types listed within the GIS data, the following were identified as having the potential to support ticks: blanket bog, heather moorland, montane,

mixed woodland and conifer plantation. As grouse and deer are rarely kept together (Wightman and Tingay, 2015), heather moorland habitats were further split into three grouse-deer categories to more accurately reflect real-life moorland management:

- Heather A: high grouse, no deer
- Heather B: low grouse, low deer
- Heather C: no grouse, high deer

To separate the heather cells by host density, the Deer Management Group counts were used, as nationwide grouse density data was not available. By considering the distribution of deer densities (figure A.1), the heather cells were split according to their deer densities; those with under 5 per km² formed the Heather A group, those with under 10 per km² formed the Heather B group, whilst the rest formed the Heather C group.

The annual maximum, minimum and average temperature values for each cell were then considered. Within each habitat group the cells were ranked by their annual average temperature, and split into five groups (or three groups for montane and woodland areas, as these had far fewer cells) of approximately equal size (figure A.2). This method was chosen as it would allow for as much detail as possible within created maps. Had the cells been split into, for example, 2°C bands, the non-uniformly distributed nature of temperature across cells would have seen potentially hundreds of cells banded into a few groups, with only a few outwith. This would have led to predictive maps with huge areas of identical colouring, making it far harder to spot changes. Each of the habitat-temperature groups were assigned minimum and maximum temperature values based on the average of the cells within the group, which generally displayed similar

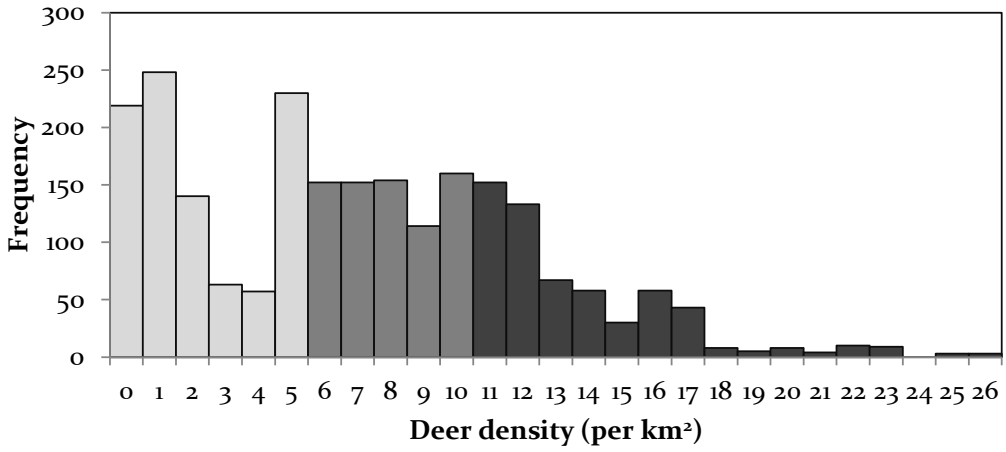

Figure A.1: Histogram showing the distribution of the deer densities within the GIS data. Values are taken from Deer Management Group counts from up to 2006. Light grey indicates the cells which were placed within the Heather A group (high grouse, no deer), medium grey indicates the cells which were placed within the Heather B group (low grouse, low deer), and dark grey indicates the cells which were placed within the Heather C group (no grouse, high deer).

temperature characteristics. These are the values used within the models, and are listed in table A.1.

A.2.2 *Climate warming scenario creation*

In order to predict the changes in tick and tick-borne disease that would be caused by climate warming, the UK Climate Impacts Programme (UKCIP) estimations were used (Jenkins et al. 2009). These suggested the average annual temperature in Scotland is expected to increase by between 1°C and 4°C by the 2080s. To represent this range, three temperature scenarios were used to run the model under: low (1°C rise over 70 years), medium (2.5°C rise over 70 years) and high temperature increase (4°C rise over 70 years). For comparison, simulations with no change in temperature to represent the current climate were also run.

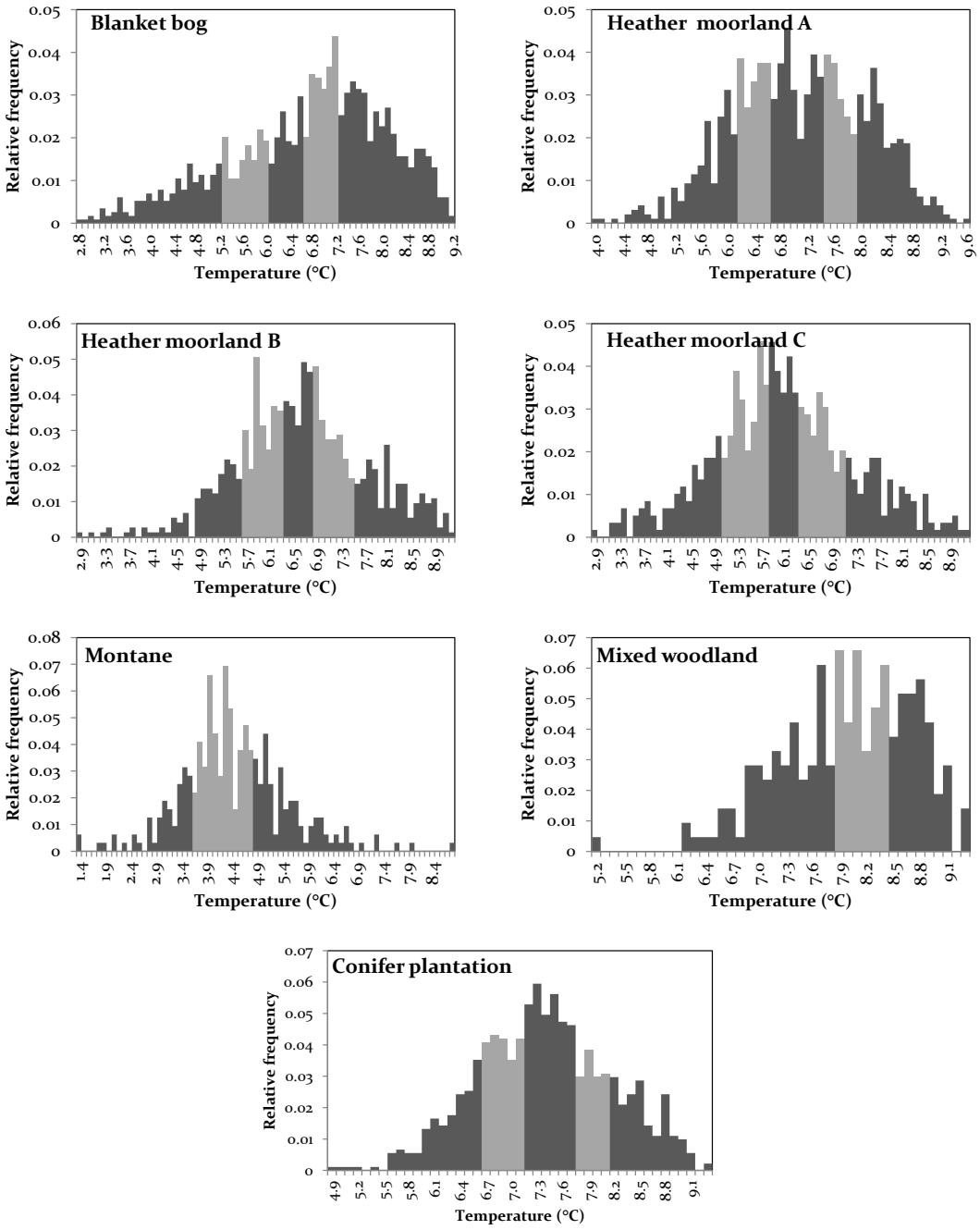

Figure A.2: Histograms displaying the average temperature of cells within each habitat category. The average temperatures are taken from Met Office long-term data from 1971-2000. The shading of each histogram represents the groups each habitat category were split into. The full list of groups is shown in table A.1.

The UKCIP estimations dealt with average annual temperatures. As the models within this thesis use minimum and maximum annual temperatures, how these will individually change over time has to be considered. For example, an average temperature increase of 1°C could have resulted from the maximum temperature increasing by 3°C and the minimum temperature decreasing by 1°C, or it could result from both increasing by 1°C. Therefore, historical temperature data recorded by NASA (NASA, 2012) was considered for the three Scottish sites with the most data: Aberdeen (1951-2011), Edinburgh (1953-1997) and Eskdalemuir (1933-2011) (figure A.3). By comparing the average temperatures for each quarter, it can be seen that the rate of increase is constant. Therefore, it can be assumed that the maximum and minimum annual temperature will increase at the same rate during the 70-year period covered by the UKCIP estimations.

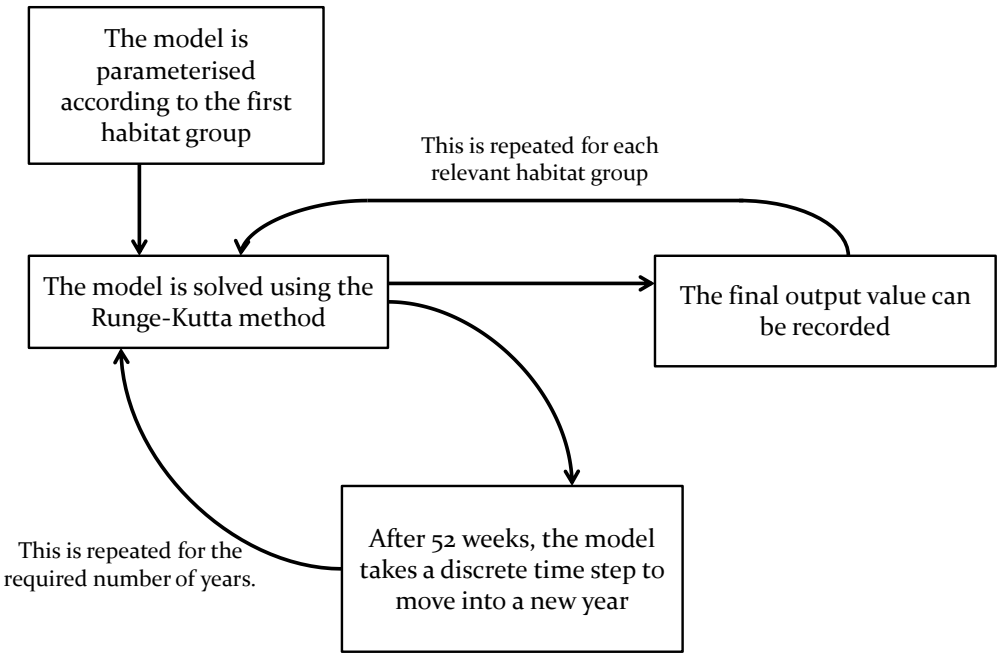

Figure A.4: Flowchart demonstrating the method used to apply the model across Scotland.

In order to map the predictions of the models within this thesis (given by equation 3.7 in chapter 3, equation 4.10 in chapter 4 and equation 5.14 in chapter 5) across Scotland, the models were run on Mathematica Version 9 (Wolfram Research Inc., 2013) for each habitat group separately.

To begin with, the parameters specific to each habitat (minimum temperature, maximum temperature and host densities) are entered into the model. The continuous time ODE model is run for $t = 0$ to $t = 52$ using the *NDSolve* function on Mathematica, which uses the Runge-Kutta method (where t denotes time, measured in weeks). A discrete time step is then taken, to denote the end of the year, where the densities in the ODE model at $t = 52$ are used to provide

new initial conditions for the following year. This process is then repeated for the required number of years, after which the final densities are taken. This is repeated for each relevant habitat group. A flowchart of this process is shown in figure A.4.

Code	Habitat type	Minimum temp (°C)	Maximum temp (°C)
B1	Blanket bog	-0.21	10.68
B2	Blanket bog	1.39	11.88
B3	Blanket bog	2.60	12.53
B4	Blanket bog	3.00	13.03
B5	Blanket bog	4.77	13.80
HA1	Heather moorland (high grouse, no deer)	0.75	11.41
HA2	Heather moorland (high grouse, no deer)	1.53	12.28
HA3	Heather moorland (high grouse, no deer)	2.36	12.80
HA4	Heather moorland (high grouse, no deer)	3.48	13.19
HA5	Heather moorland (high grouse, no deer)	4.45	13.70
HB1	Heather moorland (low grouse, low deer)	0.28	11.00
HB2	Heather moorland (low grouse, low deer)	1.34	11.91
HB3	Heather moorland (low grouse, low deer)	1.97	12.48
HB4	Heather moorland (low grouse, low deer)	2.62	13.10
HB5	Heather moorland (low grouse, low deer)	3.93	13.78
HC1	Heather moorland (no grouse, high deer)	-0.40	10.55
HC2	Heather moorland (no grouse, high deer)	0.61	11.52
HC3	Heather moorland (no grouse, high deer)	1.37	12.18
HC4	Heather moorland (no grouse, high deer)	1.91	12.69
HC5	Heather moorland (no grouse, high deer)	3.44	13.40
M1	Montane	-1.03	8.91
M2	Montane	0.22	9.86
M3	Montane	1.85	10.96
W1	Mixed woodland	2.60	13.67
W2	Mixed woodland	3.91	14.52
W3	Mixed woodland	4.64	15.09
P1	Conifer plantation	1.54	12.39
P2	Conifer plantation	2.41	12.99
P3	Conifer plantation	3.01	13.48
P4	Conifer plantation	3.64	13.96
P5	Conifer plantation	4.30	14.55

Table A.1: List of the 34 habitat groups used within each model. The code for each group refers to its habitat type and where it ranks on temperature, and is used for ease of reference.

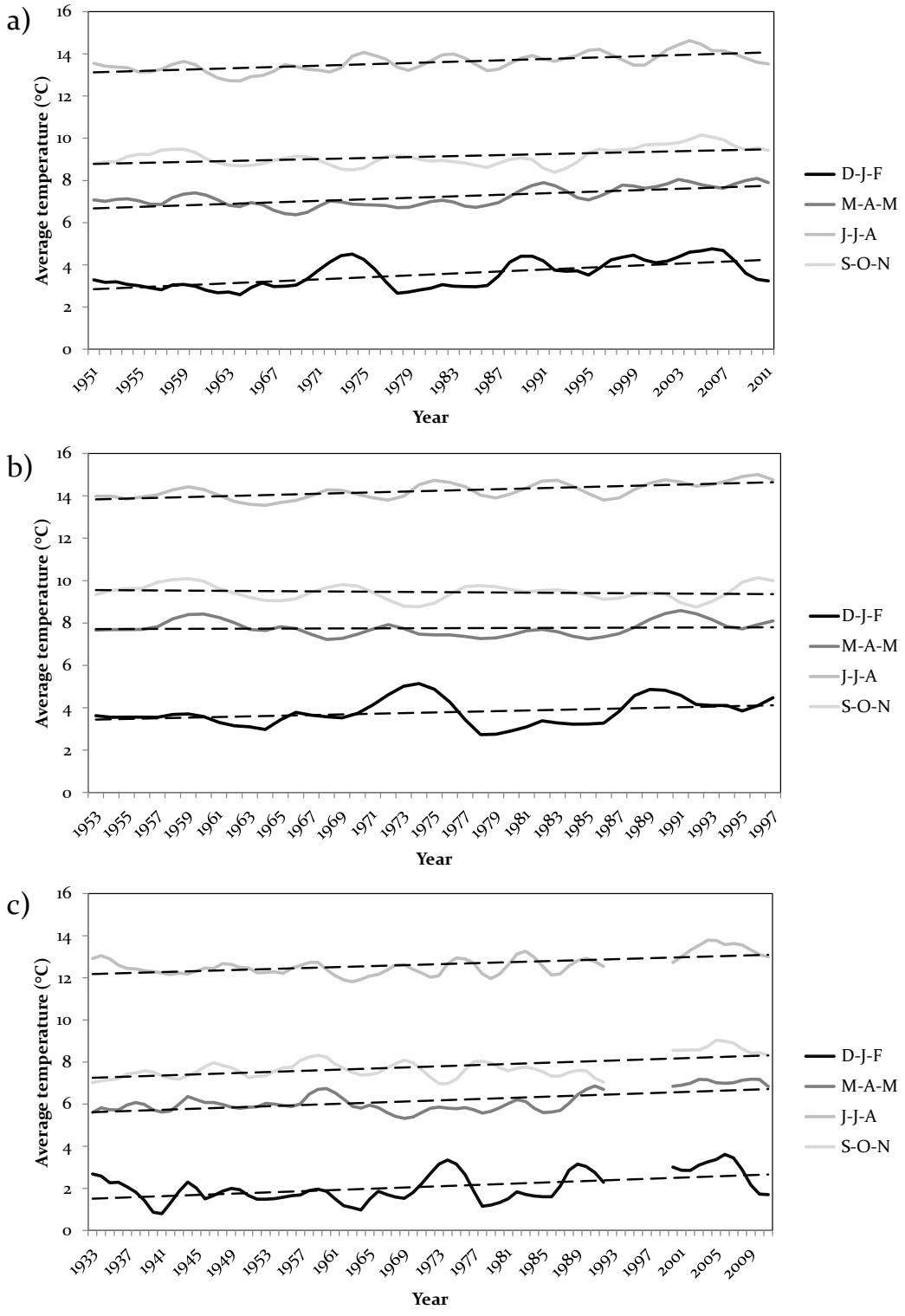

Figure A.3: The average temperature for each quarter (December-February, March-May, June-August and September-November) recorded by NASA for three sites: (a) Aberdeen (1951-2011), (b) Edinburgh (1953-1997) and (c) Eskdalemuir (1933-1992, 2000-2011). The dotted lines represent the linear regression line for each quarter.

B

MODEL CODES

This appendix presents the code used to run the models presented within this thesis, in order to facilitate replication. The names of parameters within the code may be slightly different to those within the text of this thesis. The models were run on Mathematica Version 9 (Wolfram Research Inc., 2013).

B.1 TICK LIFECYCLE MODEL (CHAPTER 3)

```
Clear["Global‘*"]; ThingL1 = {}; ThingL2 = {}; ThingN1 = {}; ThingN2 \
= {}; ThingA1 = {}; ThingA2 = {};
groups = ({
    {Cat, B1, B2, B3, B4, B5, B6, B7, B8, HA1, HA2, HA3, HA4, HA5,
     HB1, HB2, HB3, HB4, HB5, HC1, HC2, HC3, HC4, HC5, M1, M2, M3, G1,
      G2, G3, G4, G5, G6, G7, G8, G9, G10, W1, W2, W3, P1, P2, P3, P4,
      P5},
    {RowNo, 2, 3, 4, 5, 6, 7, 8, 9, 10, 11, 12, 13, 14, 15, 16, 17,
     18, 19, 20, 21, 22, 23, 24, 25, 26, 27, 28, 29, 30, 31, 32, 33,
     34, 35, 36, 37, 38, 39, 40, 41, 42, 43, 44, 45},
    {a, -0.80, 0.49, 1.44, 2.26, 2.83, 3.27, 3.86, 4.62, 0.75, 1.53,
     2.36, 3.48, 4.45, 0.28, 1.34, 1.97, 2.62, 3.93, -0.40, 0.61,
```

```
      1.37, 1.91, 3.44, -1.03, 0.22, 1.85, 1.58, 2.47, 2.85, 3.17,
      3.40, 3.63, 3.94, 4.25, 4.56, 5.01, 2.60, 3.91, 4.64, 1.54, 2.41,
       3.01, 3.64, 4.30},
     {b, 10.10, 11.25, 12.08, 12.70, 13.15, 13.53, 14.00, 14.60, 11.41,
       12.28, 12.80, 13.19, 13.70, 11.00, 11.91, 12.48, 13.10, 13.78,
      10.55, 11.52, 12.18, 12.69, 13.40, 8.91, 9.86, 10.96, 11.71,
      12.57, 12.95, 13.22, 13.44, 13.67, 13.96, 14.26, 14.54, 14.93,
      13.67, 14.52, 15.09, 12.39, 12.99, 13.48, 13.96, 14.55},
     {RedD, 1, 1, 1, 1, 1, 1, 1, 1, 0, 0, 0, 0, 0, 5, 5, 5, 5, 5, 15,
      15, 15, 15, 15, 0.1, 0.1, 0.1, 0, 0, 0, 0, 0, 0, 0, 0, 0, 0, 4,
      4, 4, 2, 2, 2, 2, 2},
     {Gr, 0, 0, 0, 0, 0, 0, 0, 0, 100, 100, 100, 100, 100, 50, 50, 50,
      50, 50, 0, 0, 0, 0, 0, 20, 20, 20, 0, 0, 0, 0, 0, 0, 0, 0, 0, 0,
      0, 0, 0, 0, 0, 0, 0, 0},
     {Ha, 10, 10, 10, 10, 10, 10, 10, 10, 10, 10, 10, 10, 10, 10, 10,
      10, 10, 10, 10, 10, 10, 10, 10, 20, 20, 20, 0, 0, 0, 0, 0, 0, 0,
      0, 0, 0, 0, 0, 0, 0, 0, 0, 0, 0},
     {SM, 0, 0, 0, 0, 0, 0, 0, 0, 0, 0, 0, 0, 0, 0, 0, 0, 0, 0, 0, 0,
      0, 0, 0, 0, 0, 0, 0, 0, 0, 0, 0, 0, 0, 0, 0, 0, 0, 0, 0, 8500, 8500, 8500,
       4250, 4250, 4250, 4250, 4250},
     {Brd, 0, 0, 0, 0, 0, 0, 0, 0, 0, 0, 0, 0, 0, 0, 0, 0, 0, 0, 0, 0,
      0, 0, 0, 0, 0, 0, 0, 0, 0, 0, 0, 0, 0, 0, 0, 0, 0, 0, 0, 70, 70, 70, 35,
      35, 35, 35, 35},
     {RoeD, 0, 0, 0, 0, 0, 0, 0, 0, 0, 0, 0, 0, 0, 0, 0, 0, 0, 0, 0, 0,
       0, 0, 0, 0, 0, 0, 0, 0, 0, 0, 0, 0, 0, 0, 0, 0, 0, 0, 0, 4, 4, 4, 2, 2,
      2, 2, 2}
    });
habitat = 17;
```

```
a = Part[groups, 3, habitat]; b =
 Part[groups, 4,
  habitat]; T1 = 5; T2 = 9; bL = 0.047; bN = 0.024; bA = 0.009; bowL \
= 0.25; bowN = 0.25; egg = 627.5;
Fzero = 50;
L0 = 1000000; N0 = 100000; A0 = 10000;
Ymax = 70;
increase = 4;
hosts = ({
    {RedDeer, Part[groups, 5, habitat], 15.18, 70.41, 81.25},
    {Grouse, Part[groups, 6, habitat], 15, 4, 0},
    {Hare, Part[groups, 7, habitat], 63.7, 37.4, 11.4},
    {SmallMammal, Part[groups, 8, habitat], 1.61, 0.03, 0},
    {Bird, Part[groups, 9, habitat], 3.11, 0.25, 0},
    {RoeDeer, Part[groups, 10, habitat], 10.78, 23.9, 29.82}
   });
hvalues = Transpose[hosts].hosts;

Do[
  T[t_] = ((b - a)/2*Sin[t/(2.6 \[Pi]) - 0.5 \[Pi]]) + (b + a)/2;
  F[t_] := \[Piecewise] {
     {0, T[t] \[LessSlantEqual] T1},
     {((T[t] - T1)/(T2 - T1)), T1 < T[t] < T2},
     {1, T[t] \[GreaterSlantEqual] T2}
    };
  P[t_] = 1/(1 + Exp[0.75 (8 - T[t])]);
  S[x_, K_] := (K*Fzero)/(
    Fzero + (K - Fzero)*Exp[Log[Fzero/(19*(K - Fzero))]/(8*K)*x]) -
```

```
  Fzero;
soln = NDSolve[{
   LQ'[t] == -S[F[t]*P[t]*LQ[t], Part[hvalues, 2, 3]] - bL*LQ[t],
   LM'[t] == S[F[t]*P[t]*LQ[t], Part[hvalues, 2, 3]],
   NQ'[t] == -S[F[t]*P[t]*NQ[t], Part[hvalues, 2, 4]] - bN*NQ[t],
   NM'[t] == S[F[t]*P[t]*NQ[t], Part[hvalues, 2, 4]],
   AQ'[t] == -S[F[t]*P[t]*AQ[t], Part[hvalues, 2, 5]] - bA*AQ[t],
   AM'[t] == S[F[t]*P[t]*AQ[t], Part[hvalues, 2, 5]],
   LQ[(Y - 1)*52] == L0,
   LM[(Y - 1)*52] == 0,
   NQ[(Y - 1)*52] == N0,
   NM[(Y - 1)*52] == 0,
   AQ[(Y - 1)*52] == A0,
   AM[(Y - 1)*52] == 0},
  {LQ, LM, NQ, NM, AQ, AM},
  {t, (Y - 1)*52, Y*52}];

Do[AppendTo[ThingL1, {k, LQ[k] /. soln[[1]]}], {k, (Y - 1)*52 + 1,
  Y*52}];
Do[AppendTo[ThingL2, {k, LM[k] /. soln[[1]]}], {k, (Y - 1)*52 + 1,
  Y*52}];
Do[AppendTo[ThingN1, {k, NQ[k] /. soln[[1]]}], {k, (Y - 1)*52 + 1,
  Y*52}];
Do[AppendTo[ThingN2, {k, NM[k] /. soln[[1]]}], {k, (Y - 1)*52 + 1,
  Y*52}];
Do[AppendTo[ThingA1, {k, AQ[k] /. soln[[1]]}], {k, (Y - 1)*52 + 1,
  Y*52}];
Do[AppendTo[ThingA2, {k, AM[k] /. soln[[1]]}], {k, (Y - 1)*52 + 1,
```

```
    Y*52}];

  LMend = LM[Y*52] /. soln;
  LQend = LQ[Y*52] /. soln;
  NQend = NQ[Y*52] /. soln;
  NMend = NM[Y*52] /. soln;
  AQend = AQ[Y*52] /. soln;
  AMend = AM[Y*52] /. soln;

  L0 = egg*AMend[[1]];
  N0 = bowL*LMend[[1]];
  A0 = bowN*NMend[[1]];

  a = a + increase/70;
  b = b + increase/70;

  LQ =.; LM =.; NQ =.; NM =.; AQ =.; AM =.;
  , {Y, 1, Ymax}] ;
Print[LM[52*Ymax] /. soln  [[1]]];
Print[NM[52*Ymax] /. soln  [[1]]];
Print[AM[52*Ymax] /. soln [[1]]];

ListPlot[{ThingL1, ThingL2}, Joined -> True, PlotRange -> All]
ListPlot[{ThingN1, ThingN2}, Joined -> True, PlotRange -> All]
ListPlot[{ThingA1, ThingA2}, Joined -> True, PlotRange -> All]
```

```
Clear["Global‘*"]; ThingL1 = {}; ThingL2 = {}; ThingN1 = {}; ThingN2 \
= {}; ThingA1 = {}; ThingA2 = {}; ThingL3 = {}; ThingN3 = {}; ThingG1 \
= {}; ThingG2 = {};  ThingG3 = {}; AnotherThing = {};
groups = ({
    {Cat, B1, B2, B3, B4, B5, B6, B7, B8, HA1, HA2, HA3, HA4, HA5,
     HB1, HB2, HB3, HB4, HB5, HC1, HC2, HC3, HC4, HC5, M1, M2, M3, G1,
      G2, G3, G4, G5, G6, G7, G8, G9, G10, W1, W2, W3, P1, P2, P3, P4,
      P5},
    {RowNo, 2, 3, 4, 5, 6, 7, 8, 9, 10, 11, 12, 13, 14, 15, 16, 17,
     18, 19, 20, 21, 22, 23, 24, 25, 26, 27, 28, 29, 30, 31, 32, 33,
     34, 35, 36, 37, 38, 39, 40, 41, 42, 43, 44, 45},
    {a, -0.80, 0.49, 1.44, 2.26, 2.83, 3.27, 3.86, 4.62, 0.75, 1.53,
     2.36, 3.48, 4.45, 0.28, 1.34, 1.97, 2.62, 3.93, -0.40, 0.61,
     1.37, 1.91, 3.44, -1.03, 0.22, 1.85, 1.58, 2.47, 2.85, 3.17,
     3.40, 3.63, 3.94, 4.25, 4.56, 5.01, 2.60, 3.91, 4.64, 1.54, 2.41,
      3.01, 3.64, 4.30},
    {b, 10.10, 11.25, 12.08, 12.70, 13.15, 13.53, 14.00, 14.60, 11.41,
      12.28, 12.80, 13.19, 13.70, 11.00, 11.91, 12.48, 13.10, 13.78,
     10.55, 11.52, 12.18, 12.69, 13.40, 8.91, 9.86, 10.96, 11.71,
     12.57, 12.95, 13.22, 13.44, 13.67, 13.96, 14.26, 14.54, 14.93,
     13.67, 14.52, 15.09, 12.39, 12.99, 13.48, 13.96, 14.55},
    {RedD, 1, 1, 1, 1, 1, 1, 1, 1, 0, 0, 0, 0, 0, 5, 5, 5, 5, 5, 15,
     15, 15, 15, 15, 0.1, 0.1, 0.1, 0, 0, 0, 0, 0, 0, 0, 0, 0, 0, 4,
     4, 4, 2, 2, 2, 2, 2},
    {Gr, 0, 0, 0, 0, 0, 0, 0, 0, 100, 100, 100, 100, 100, 50, 50, 50,
     50, 50, 0, 0, 0, 0, 0, 20, 20, 20, 0, 0, 0, 0, 0, 0, 0, 0, 0, 0,
```

```
     0, 0, 0, 0, 0, 0, 0, 0},
    {Ha, 10, 10, 10, 10, 10, 10, 10, 10, 10, 10, 10, 10, 10, 10,
     10, 10, 10, 10, 10, 10, 10, 10, 20, 20, 20, 0, 0, 0, 0, 0, 0, 0,
     0, 0, 0, 0, 0, 0, 0, 0, 0, 0, 0},
    {SM, 0, 0, 0, 0, 0, 0, 0, 0, 0, 0, 0, 0, 0, 0, 0, 0, 0, 0, 0, 0,
     0, 0, 0, 0, 0, 0, 0, 0, 0, 0, 0, 0, 0, 0, 0, 0, 0, 0, 8500, 8500, 8500,
      4250, 4250, 4250, 4250, 4250},
    {Brd, 0, 0, 0, 0, 0, 0, 0, 0, 0, 0, 0, 0, 0, 0, 0, 0, 0, 0, 0, 0,
     0, 0, 0, 0, 0, 0, 0, 0, 0, 0, 0, 0, 0, 0, 0, 0, 0, 0, 70, 70, 70, 35,
     35, 35, 35, 35},
    {RoeD, 0, 0, 0, 0, 0, 0, 0, 0, 0, 0, 0, 0, 0, 0, 0, 0, 0, 0, 0, 0,
      0, 0, 0, 0, 0, 0, 0, 0, 0, 0, 0, 0, 0, 0, 0, 0, 0, 0, 4, 4, 4, 2, 2,
     2, 2, 2}
   });
habitat = 10;
increase = 4;

a = Part[groups, 3, habitat] + increase; b =
 Part[groups, 4, habitat] +
  increase;  TL1 = 8; TL2 = 12; TNA1 = 5; TNA2 = 9; bL = 0.047; bN = \
0.024; bA = 0.009; bowL = 0.00995; bowN = 0.00333; egg = 627.5; \
\[Epsilon] = 0.0000001;
Fzero = 50;
bG = 0.008; aG = 0.7175; \[Sigma] = 0.2; \[Alpha] = 0.8; sG =
 0.00522*100/Part[groups, 6, habitat]; InitialInf = 0.1;
L0 = 100000; NS0 = 10000*(1 - InitialInf); NI0 =
 10000*InitialInf; A0 = 1000; GS0 =
 Part[groups, 6, habitat]; GI0 = 0; GR0 = 0;
```

```
Ymax = 100;


hosts = ({
    {RedDeer, Part[groups, 5, habitat], 15.8, 70.41, 81.25},
    {Hare, Part[groups, 7, habitat], 63.7, 37.4, 11.4},
    {SmallMammal, Part[groups, 8, habitat], 1.61, 0.03, 0},
    {Bird, Part[groups, 9, habitat], 3.11, 0.25, 0},
    {RoeDeer, Part[groups, 10, habitat], 10.78, 23.9, 29.82}
   });
hvalues = Transpose[hosts].hosts;


GL = 15;
GN = 4;


Do[
  T[t_] = ((b - a)/2*Sin[t/(2.6 \[Pi]) - 0.5 \[Pi]]) + (b + a)/2;
  FL[t_] := \[Piecewise] {
     {0, T[t] \[LessSlantEqual] TL1},
     {((T[t] - TL1)/(TL2 - TL1)), TL1 < T[t] < TL2},
     {1, T[t] \[GreaterSlantEqual] TL2}
    };
  FNA[t_] := \[Piecewise] {
     {0, T[t] \[LessSlantEqual] TNA1},
     {((T[t] - TNA1)/(TNA2 - TNA1)), TNA1 < T[t] < TNA2},
     {1, T[t] \[GreaterSlantEqual] TNA2}
    };
  P[t_] = 1/(1 + Exp[0.75 (8 - T[t])]);
  S[x_, K_] := (K*Fzero)/(
```

```
  Fzero + (K - Fzero)*Exp[Log[Fzero/(19*(K - Fzero))]/(8*K)*x]) -
  Fzero;
GB[t_] := \[Piecewise] {
   {0, Mod[t, 52] \[LessSlantEqual] 19},
   {1, 19 < Mod[t, 52] \[LessSlantEqual] 22},
   {0, Mod[t, 52] \[GreaterSlantEqual] 23}
  };
soln = NDSolve[{
   LQ'[t] == -S[FL[t]*P[t]*LQ[t],
       Part[hvalues, 2, 3] + GL*(GS[t] + GI[t] + GR[t])] - bL*LQ[t],
   LMS'[
     t] == (1 - ( GI[t]*GL)/(
        Part[hvalues, 2, 3] + GL (GS[t] + GI[t] + GR[t])))*
      S[FL[t]*P[t]*LQ[t],
       Part[hvalues, 2, 3] + GL*(GS[t] + GI[t] + GR[t])] -
     bowL*LMS[t],
   LMI'[
     t] == ( GI[t]*GL)/(
      Part[hvalues, 2, 3] + GL (GS[t] + GI[t] + GR[t]))*
      S[FL[t]*P[t]*LQ[t],
       Part[hvalues, 2, 3] + GL*(GS[t] + GI[t] + GR[t])] -
     bowL*LMI[t],
   NQS'[
     t] == -(NQS[t]/(NQS[t] + NQI[t] + \[Epsilon]))*
      S[FNA[t]*P[t]*(NQS[t] + NQI[t]),
       Part[hvalues, 2, 4] + GN*(GS[t] + GI[t] + GR[t])] - bN*NQS[t],
   NQI'[
     t] == -(NQI[t]/(NQS[t] + NQI[t] + \[Epsilon]))*
```

```
   S[FNA[t]*P[t]*(NQS[t] + NQI[t]),
    Part[hvalues, 2, 4] + GN*(GS[t] + GI[t] + GR[t])] - bN*NQI[t],
NM'[t] ==
 S[FNA[t]*P[t]*(NQS[t] + NQI[t]),
   Part[hvalues, 2, 4] + GN*(GS[t] + GI[t] + GR[t])] - bowN*NM[t],
AQ'[t] == -S[FNA[t]*P[t]*AQ[t], Part[hvalues, 2, 5]] - bA*AQ[t],
AM'[t] == S[FNA[t]*P[t]*AQ[t], Part[hvalues, 2, 5]],

GS'[t] == -(1 -
      0.2^((((GS[t]*GN)/(
            Part[hvalues, 2, 4] +
             GN*(GS[t] + GI[t] + GR[t]) + \[Epsilon])) (NQI[t]/(
            NQS[t] + NQI[t] + \[Epsilon]))*
           S[FNA[t]*P[t]*(NQS[t] + NQI[t]),
            Part[hvalues, 2, 4] +
             GN*(GS[t] + GI[t] + GR[t])])/(GS[t] + \[Epsilon])))*
   GS[t] - bG*
   GS[t] + (aG*GB[t] - sG*GB[t]*(GS[t] + GI[t] + GR[t]))*(GS[t] +
      GI[t] + GR[t]),
GI'[t] == (1 -
     0.2^((((GS[t]*GN)/(
           Part[hvalues, 2, 4] +
            GN*(GS[t] + GI[t] + GR[t]) + \[Epsilon])) (NQI[t]/(
           NQS[t] + NQI[t] + \[Epsilon]))*
          S[FNA[t]*P[t]*(NQS[t] + NQI[t]),
           Part[hvalues, 2, 4] +
            GN*(GS[t] + GI[t] + GR[t])])/(GS[t] + \[Epsilon])))*
   GS[t] - \[Sigma]*GI[t] - \[Alpha]*GI[t],
```

```
   GR'[t] == \[Sigma]*GI[t] - bG*GR[t],

   LQ[(Y - 1)*52] == L0,
   LMS[(Y - 1)*52] == 0,
   LMI[(Y - 1)*52] == 0,
   NQS[(Y - 1)*52] == NS0,
   NQI[(Y - 1)*52] == NI0,
   NM[(Y - 1)*52] == 0,
   AQ[(Y - 1)*52] == A0,
   AM[(Y - 1)*52] == 0,
   GS[(Y - 1)*52] == GS0,
   GI[(Y - 1)*52] == GI0,
   GR[(Y - 1)*52] == GR0},
  {LQ, LMS, LMI, NQS, NQI, NM, AQ, AM, GS, GI, GR},
  {t, (Y - 1)*52, Y*52}];

Do[AppendTo[ThingL1, {k, LQ[k] /. soln[[1]]}], {k, (Y - 1)*52 + 1,
  Y*52}];
Do[AppendTo[ThingL2, {k, LMS[k] /. soln[[1]]}], {k, (Y - 1)*52 + 1,
  Y*52}];
Do[AppendTo[ThingL3, {k, LMI[k] /. soln[[1]]}], {k, (Y - 1)*52 + 1,
  Y*52}];
Do[AppendTo[ThingN1, {k, NQS[k] /. soln[[1]]}], {k, (Y - 1)*52 + 1,
  Y*52}];
Do[AppendTo[ThingN3, {k, NQI[k] /. soln[[1]]}], {k, (Y - 1)*52 + 1,
  Y*52}];
Do[AppendTo[ThingN2, {k, NM[k] /. soln[[1]]}], {k, (Y - 1)*52 + 1,
  Y*52}];
```

```
Do[AppendTo[ThingA1, {k, AQ[k] /. soln[[1]]}], {k, (Y - 1)*52 + 1,
  Y*52}];
Do[AppendTo[ThingA2, {k, AM[k] /. soln[[1]]}], {k, (Y - 1)*52 + 1,
  Y*52}];
Do[AppendTo[ThingG1, {k, GS[k] /. soln[[1]]}], {k, (Y - 1)*52 + 1,
  Y*52}];
Do[AppendTo[ThingG2, {k, GI[k] /. soln[[1]]}], {k, (Y - 1)*52 + 1,
  Y*52}];
Do[AppendTo[ThingG3, {k, GR[k] /. soln[[1]]}], {k, (Y - 1)*52 + 1,
  Y*52}];
Do[AppendTo[
  AnotherThing, {k, NM[k] /. soln[[1]], GS[k] /. soln[[1]],
   GI[k] /. soln[[1]], GR[k] /. soln[[1]], LMS[k] /. soln[[1]],
   LMI[k] /. soln[[1]]}], {k, (Y - 1)*52 + 1, Y*52}];

LQend = LQ[Y*52] /. soln;
LMSend = LMS[Y*52] /. soln;
LMIend = LMI[Y*52] /. soln;
NQSend = NQS[Y*52] /. soln;
NQIend = NQI[Y*52] /. soln;
NMend = NM[Y*52] /. soln;
AQend = AQ[Y*52] /. soln;
AMend = AM[Y*52] /. soln;
GSend = GS[Y*52] /. soln;
GIend = GI[Y*52] /. soln;
GRend = GR[Y*52] /. soln;

L0 = egg*AMend[[1]];
```

```
  NS0 = LMSend[[1]];
  NI0 = LMIend[[1]];
  A0 = NMend[[1]];
  GS0 = GSend[[1]];
  GI0 = GIend[[1]];
  GR0 = GRend[[1]];



  LQ =.; LMS =.; LMI =.; NQS =.; NQI =.; NM =.; AQ =.; AM =.; GS =.;
  GI =.; GR =.;
  , {Y, 1, Ymax}] ;
Print[LMS[52*Ymax] /. soln  [[1]], ", ", LMI[52*Ymax] /. soln  [[1]]];
Print[NM[52*Ymax] /. soln  [[1]]];
Print[AM[52*Ymax] /. soln [[1]]];
Print[GS[52*Ymax] /. soln [[1]], ", ", GI[52*Ymax] /. soln [[1]],
  ", ", GR[52*Ymax] /. soln [[1]]];

ListPlot[{ThingL1, ThingL2, ThingL3}, Joined -> True, PlotRange -> All]
ListPlot[{ThingN1, ThingN2, ThingN3}, Joined -> True, PlotRange -> All]
ListPlot[{ThingA1, ThingA2}, Joined -> True, PlotRange -> All]
ListPlot[{ThingG1, ThingG2, ThingG3}, Joined -> True,
 PlotRange -> All]
```

B.3 BORRELIA BURGDORFERI S.L. MODEL (CHAPTER 5)

```
Clear["Global‘*"]; ThingL1 = {}; ThingL2 = {}; ThingN1 = {}; ThingN2 \
= {}; ThingA1 = {}; ThingA2 = {}; ThingL3 = {}; ThingN3 = {}; ThingH1 \
= {}; ThingH2 = {};  ThingH3 = {}; AnotherThing = {};
```

```
groups = ({
    {Cat, B1, B2, B3, B4, B5, B6, B7, B8, HA1, HA2, HA3, HA4, HA5,
     HB1, HB2, HB3, HB4, HB5, HC1, HC2, HC3, HC4, HC5, M1, M2, M3, G1,
      G2, G3, G4, G5, G6, G7, G8, G9, G10, W1, W2, W3, P1, P2, P3, P4,
      P5},
    {RowNo, 2, 3, 4, 5, 6, 7, 8, 9, 10, 11, 12, 13, 14, 15, 16, 17,
     18, 19, 20, 21, 22, 23, 24, 25, 26, 27, 28, 29, 30, 31, 32, 33,
     34, 35, 36, 37, 38, 39, 40, 41, 42, 43, 44, 45},
    {a, -0.80, 0.49, 1.44, 2.26, 2.83, 3.27, 3.86, 4.62, 0.75, 1.53,
     2.36, 3.48, 4.45, 0.28, 1.34, 1.97, 2.62, 3.93, -0.40, 0.61,
     1.37, 1.91, 3.44, -1.03, 0.22, 1.85, 1.58, 2.47, 2.85, 3.17,
     3.40, 3.63, 3.94, 4.25, 4.56, 5.01, 2.60, 3.91, 4.64, 1.54, 2.41,
      3.01, 3.64, 4.30},
    {b, 10.10, 11.25, 12.08, 12.70, 13.15, 13.53, 14.00, 14.60, 11.41,
      12.28, 12.80, 13.19, 13.70, 11.00, 11.91, 12.48, 13.10, 13.78,
     10.55, 11.52, 12.18, 12.69, 13.40, 8.91, 9.86, 10.96, 11.71,
     12.57, 12.95, 13.22, 13.44, 13.67, 13.96, 14.26, 14.54, 14.93,
     13.67, 14.52, 15.09, 12.39, 12.99, 13.48, 13.96, 14.55},
    {RedD, 1, 1, 1, 1, 1, 1, 1, 1, 0, 0, 0, 0, 0, 5, 5, 5, 5, 5, 15,
     15, 15, 15, 15, 0.1, 0.1, 0.1, 0, 0, 0, 0, 0, 0, 0, 0, 0, 0, 4,
     4, 4, 2, 2, 2, 2, 2},
    {Gr, 0, 0, 0, 0, 0, 0, 0, 0, 100, 100, 100, 100, 100, 50, 50, 50,
     50, 50, 0, 0, 0, 0, 0, 20, 20, 20, 0, 0, 0, 0, 0, 0, 0, 0, 0, 0,
     0, 0, 0, 0, 0, 0, 0, 0},
    {Ha, 10, 10, 10, 10, 10, 10, 10, 10, 10, 10, 10, 10, 10, 10, 10,
     10, 10, 10, 10, 10, 10, 10, 10, 20, 20, 20, 0, 0, 0, 0, 0, 0, 0,
     0, 0, 0, 0, 0, 0, 0, 0, 0, 0, 0},
    {SM, 0, 0, 0, 0, 0, 0, 0, 0, 155, 155, 155, 155, 155, 155, 155,
```

```
     155, 155, 155, 155, 155, 155, 155, 155, 0, 0, 0, 0, 0, 0, 0, 0,
     0, 0, 0, 0, 0, 11400, 11400, 11400, 4250, 4250, 4250, 4250, 4250},
    {Brd, 0, 0, 0, 0, 0, 0, 0, 0, 0, 0, 0, 0, 0, 0, 0, 0, 0, 0, 0, 0,
     0, 0, 0, 0, 0, 0, 0, 0, 0, 0, 0, 0, 0, 0, 0, 0, 0, 365, 365, 365,
     35, 35, 35, 35, 35},
    {RoeD, 0, 0, 0, 0, 0, 0, 0, 0, 0, 0, 0, 0, 0, 0, 0, 0, 0, 0, 0, 0,
      0, 0, 0, 0, 0, 0, 0, 0, 0, 0, 0, 0, 0, 0, 0, 0, 0, 4, 4, 4, 2, 2,
     2, 2, 2}
   });
habitat = 40;
increase = 2.5;

host = 2;
a = Part[groups, 3, habitat] + increase; b =
 Part[groups, 4, habitat] +
  increase;  TL1 = 8; TL2 = 12; TNA1 = 5; TNA2 = 9; bL = 0.047; bN = \
0.024; bA = 0.009; bowL = 0.00995; bowN = 0.00333; egg = 627.5; \
\[Epsilon] = 0.0000001;
Fzero = 50;
bH = If[host == 1, 0.0192, 0.0064]; aH =
 If[host == 1, 0.4615, 0.1538]; \[Sigma] = 0.01675; sH =
 If[host == 1, 0.004423, 0.001474]*100/(
  HS0 = If[host == 1, Part[groups, 8, habitat],
    Part[groups, 9, habitat]]);
InitialInf = 0.1;
L0 = 100000; NS0 = 10000*(1 - InitialInf); NI0 =
 10000*InitialInf; A0 = 1000; HS0 =
 If[host == 1, Part[groups, 8, habitat],
```

```
  Part[groups, 9, habitat]]; HI0 = 0; HR0 = 0;
Ymax = 100;
hosts = ({
    {RedDeer, Part[groups, 5, habitat], 15.18, 70.41, 81.25},
    {Grouse, Part[groups, 6, habitat], 15, 4, 0},
    {Hare, Part[groups, 7, habitat], 63.7, 37.4, 11.4},
    {SmallMammal, If[host == 1, 0, Part[groups, 8, habitat]] , 1.61,
     0.03, 0},
    {Bird, If[host == 2, 0, Part[groups, 9, habitat]], 3.11, 0.25, 0},
    {RoeDeer, Part[groups, 10, habitat], 10.78, 23.9, 29.82}
   });
hvalues = Transpose[hosts].hosts;

HL = If[host == 1, 1.61, 3.11];
HN = If[host == 1, 0.03, 0.25];

Do[
  T[t_] = ((b - a)/2*Sin[t/(2.6 \[Pi]) - 0.5 \[Pi]]) + (b + a)/2;
  FL[t_] := \[Piecewise] {
     {0, T[t] \[LessSlantEqual] TL1},
     {((T[t] - TL1)/(TL2 - TL1)), TL1 < T[t] < TL2},
     {1, T[t] \[GreaterSlantEqual] TL2}
    };
  FNA[t_] := \[Piecewise] {
     {0, T[t] \[LessSlantEqual] TNA1},
     {((T[t] - TNA1)/(TNA2 - TNA1)), TNA1 < T[t] < TNA2},
     {1, T[t] \[GreaterSlantEqual] TNA2}
    };
```

```
P[t_] = 1/(1 + Exp[0.75 (8 - T[t])]);
S[x_, K_] := (K*Fzero)/(
  Fzero + (K - Fzero)*Exp[Log[Fzero/(19*(K - Fzero))]/(8*K)*x]) -
  Fzero;
HB[t_] := \[Piecewise] {
   {0, Mod[t, 52] \[LessSlantEqual] 19},
   {1, 19 < Mod[t, 52] \[LessSlantEqual] 22},
   {0, Mod[t, 52] \[GreaterSlantEqual] 23}
  };
soln = NDSolve[{
   LQ'[t] == -S[FL[t]*P[t]*LQ[t],
       Part[hvalues, 2, 3] + HL*(HS[t] + HI[t] + HR[t])] - bL*LQ[t],
   LMS'[
     t] == (1 - ( HI[t]*HL)/(
        Part[hvalues, 2, 3] + HL (HS[t] + HI[t] + HR[t])))*
      S[FL[t]*P[t]*LQ[t],
       Part[hvalues, 2, 3] + HL*(HS[t] + HI[t] + HR[t])] -
     bowL*LMS[t],
   LMI'[
     t] == ( HI[t]*HL)/(
      Part[hvalues, 2, 3] + HL (HS[t] + HI[t] + HR[t]))*
      S[FL[t]*P[t]*LQ[t],
       Part[hvalues, 2, 3] + HL*(HS[t] + HI[t] + HR[t])] -
     bowL*LMI[t],
   NQS'[
     t] == -(NQS[t]/(NQS[t] + NQI[t] + \[Epsilon]))*
      S[FNA[t]*P[t]*(NQS[t] + NQI[t]),
       Part[hvalues, 2, 4] + HN*(HS[t] + HI[t] + HR[t])] - bN*NQS[t],
```

```
NQI’[
  t] == -(NQI[t]/(NQS[t] + NQI[t] + \[Epsilon]))*
   S[FNA[t]*P[t]*(NQS[t] + NQI[t]),
    Part[hvalues, 2, 4] + HN*(HS[t] + HI[t] + HR[t])] - bN*NQI[t],
NM’[t] ==
 S[FNA[t]*P[t]*(NQS[t] + NQI[t]),
   Part[hvalues, 2, 4] + HN*(HS[t] + HI[t] + HR[t])] - bowN*NM[t],
AQ’[t] == -S[FNA[t]*P[t]*AQ[t], Part[hvalues, 2, 5]] - bA*AQ[t],
AM’[t] == S[FNA[t]*P[t]*AQ[t], Part[hvalues, 2, 5]],

HS’[t] == -(1 -
      0.2^((((HS[t]*HN)/(Part[hvalues, 2, 4] +
               HN*(HS[t] + HI[t] + HR[t]) + \[Epsilon])) (NQI[
             t]/(NQS[t] + NQI[t] + \[Epsilon]))*
           S[FNA[t]*P[t]*(NQS[t] + NQI[t]),
            Part[hvalues, 2, 4] +
             HN*(HS[t] + HI[t] + HR[t])])/(HS[t] + \[Epsilon])))*
   HS[t] - bH*
   HS[t] + (aH - sH*(HS[t] + HI[t] + HR[t]))*(HS[t] + HI[t] +
     HR[t]),
HI’[t] == (1 -
     0.2^((((HS[t]*HN)/(Part[hvalues, 2, 4] +
              HN*(HS[t] + HI[t] + HR[t]) + \[Epsilon])) (NQI[t]/(
           NQS[t] + NQI[t] + \[Epsilon]))*
          S[FNA[t]*P[t]*(NQS[t] + NQI[t]),
           Part[hvalues, 2, 4] +
            HN*(HS[t] + HI[t] + HR[t])])/(HS[t] + \[Epsilon])))*
   HS[t] - bH*HI[t] - \[Sigma]*HI[t],
```

```
   HR’[t] == \[Sigma]*HI[t] - bH*HR[t],

   LQ[(Y - 1)*52] == L0,
   LMS[(Y - 1)*52] == 0,
   LMI[(Y - 1)*52] == 0,
   NQS[(Y - 1)*52] == NS0,
   NQI[(Y - 1)*52] == NI0,
   NM[(Y - 1)*52] == 0,
   AQ[(Y - 1)*52] == A0,
   AM[(Y - 1)*52] == 0,
   HS[(Y - 1)*52] == HS0,
   HI[(Y - 1)*52] == HI0,
   HR[(Y - 1)*52] == HR0},
  {LQ, LMS, LMI, NQS, NQI, NM, AQ, AM, HS, HI, HR},
  {t, (Y - 1)*52, Y*52}];

Do[AppendTo[ThingL1, {k, LQ[k] /. soln[[1]]}], {k, (Y - 1)*52 + 1,
  Y*52}];
Do[AppendTo[ThingL2, {k, LMS[k] /. soln[[1]]}], {k, (Y - 1)*52 + 1,
  Y*52}];
Do[AppendTo[ThingL3, {k, LMI[k] /. soln[[1]]}], {k, (Y - 1)*52 + 1,
  Y*52}];
Do[AppendTo[ThingN1, {k, NQS[k] /. soln[[1]]}], {k, (Y - 1)*52 + 1,
  Y*52}];
Do[AppendTo[ThingN3, {k, NQI[k] /. soln[[1]]}], {k, (Y - 1)*52 + 1,
  Y*52}];
Do[AppendTo[ThingN2, {k, NM[k] /. soln[[1]]}], {k, (Y - 1)*52 + 1,
  Y*52}];
```

```
Do[AppendTo[ThingA1, {k, AQ[k] /. soln[[1]]}], {k, (Y - 1)*52 + 1,
  Y*52}];
Do[AppendTo[ThingA2, {k, AM[k] /. soln[[1]]}], {k, (Y - 1)*52 + 1,
  Y*52}];
Do[AppendTo[ThingH1, {k, HS[k] /. soln[[1]]}], {k, (Y - 1)*52 + 1,
  Y*52}];
Do[AppendTo[ThingH2, {k, HI[k] /. soln[[1]]}], {k, (Y - 1)*52 + 1,
  Y*52}];
Do[AppendTo[ThingH3, {k, HR[k] /. soln[[1]]}], {k, (Y - 1)*52 + 1,
  Y*52}];
Do[AppendTo[
  AnotherThing, {k, NM[k] /. soln[[1]], HS[k] /. soln[[1]],
   HI[k] /. soln[[1]], HR[k] /. soln[[1]], LMS[k] /. soln[[1]],
   LMI[k] /. soln[[1]]}], {k, (Y - 1)*52 + 1, Y*52}];

LQend = LQ[Y*52] /. soln;
LMSend = LMS[Y*52] /. soln;
LMIend = LMI[Y*52] /. soln;
NQSend = NQS[Y*52] /. soln;
NQIend = NQI[Y*52] /. soln;
NMend = NM[Y*52] /. soln;
AQend = AQ[Y*52] /. soln;
AMend = AM[Y*52] /. soln;
HSend = HS[Y*52] /. soln;
HIend = HI[Y*52] /. soln;
HRend = HR[Y*52] /. soln;

L0 = egg*AMend[[1]];
```

```
  NS0 = LMSend[[1]];
  NI0 = LMIend[[1]];
  A0 = NMend[[1]];
  HS0 = HSend[[1]];
  HI0 = HIend[[1]];
  HR0 = HRend[[1]];

  LQ =.; LMS =.; LMI =.; NQS =.; NQI =.; NM =.; AQ =.; AM =.; HS =.;
  HI =.; HR =.;
  , {Y, 1, Ymax}] ;
Print[LMS[52*Ymax] /. soln  [[1]], ", ", LMI[52*Ymax] /. soln  [[1]]];
Print[NM[52*Ymax] /. soln  [[1]]];
Print[AM[52*Ymax] /. soln [[1]]];
Print[HS[52*Ymax] /. soln [[1]], ", ", HI[52*Ymax] /. soln [[1]],
  ", ", HR[52*Ymax] /. soln [[1]]];

ListPlot[{ThingL1, ThingL2, ThingL3}, Joined -> True, PlotRange -> All]
ListPlot[{ThingN1, ThingN2, ThingN3}, Joined -> True, PlotRange -> All]
ListPlot[{ThingA1, ThingA2}, Joined -> True, PlotRange -> All]
ListPlot[{ThingH1, ThingH2, ThingH3}, Joined -> True,
 PlotRange -> All]
```

BIBLIOGRAPHY

G. Amori, R. Hutterer, B. Kryštufek, N. Yigit, G. Mitsain, L.J. Palomo, H. Henttonen, V. Vohralík, I. Zagorodnyuk, R. Juškaitis, H. Meinig, and S. Bertolino. Myodes glareolus (Bank Vole), 2008. URL http://www.iucnredlist.org/details/4973/0.

R. M. Anderson and R. M. May. Regulation and Stability of Host-Parasite Population Interactions : I . Regulatory Processes. *Journal of Animal Ecology*, 47 (1):219–247, 1978.

BADA UK. Diseases, 2016. URL http://www.bada-uk.org/diseases.

L. Bolzoni, R. Rosà, F. Cagnacci, and A. Rizzoli. Effect of deer density on tick infestation of rodents and the hazard of tick-borne encephalitis. II: Population and infection models. *International Journal for Parasitology*, 42(4):373–381, 2012. ISSN 00207519. doi: 10.1016/j.ijpara.2012.02.006.

J. F. Braga. *Mapping tick bite risk in Scotland: present and future*. Masters thesis, University of Aberdeen, 2012.

British Garden Birds. Greenfinch, 2015. URL http://www.garden-birds.co.uk/birds/greenfinch.htm.

British Trust for Ornithology. Chaffinch, 2016a. URL https://www.bto.org/volunteer-surveys/gbw/gardens-wildlife/garden-birds/a-z-garden-birds/chaffinch.

British Trust for Ornithology. Dunnock, 2016b. URL https://www.bto.org/volunteer-surveys/gbw/gardens-wildlife/garden-birds/a-z-garden-birds/dunnock.

British Trust for Ornithology. Maps of population density and trends, 2016c. URL https://www.bto.org/volunteer-surveys/bbs/latest-results/maps-population-density-and-trends.

A. Buczek, K. Bartosik, and P. Kuczyński. The toxic effect of permethrin and cypermethrin on engorged Ixodes ricinus females. *Annals of Agricultural and Environmental Medicine*, 21(2):259–262, 2014. ISSN 18982263. doi: 10.5604/1232-1966.1108587.

L. Burbaite and S. Csányi. Roe deer population and harvest changes in Europe. *Estonian Journal of Ecology*, 58(3):169–180, 2009. ISSN 1736602X. doi: 10.3176/eco.2009.3.02.

F. Cagnacci, L. Bolzoni, R. Rosa, G. Carpi, H.C. Hauffe, M. Valent, V. Tagliapietra, M. Kazimirova, J. Koci, M. Stanko, M. Lukan, H. Henttonen, and A. Rizzoli. Effects of deer density on tick infestation of rodents and the hazard of tick-borne encephalitis. I: Empirical assessment. *International Journal for Parasitology*, 42(4):365–372, 2012.

L. M. Cooksey, D. G. Haile, and G. A. Mount. Computer simulation of Rocky Mountain spotted fever transmission by the American dog tick (Acari: Ixodidae). *Journal of medical entomology*, 27(4):671–680, 1990. ISSN 0022-2585 (Print).

M. Daniel, J. Kolár, and P. Zeman. GIS tools for tick and tick-borne disease occurrence. *Parasitology*, 129 Suppl:S329–S352, 2004. ISSN 0031-1820. doi: 10.1017/S0031182004006080.

V. Danielova and J. Holubova. Transovarial transmission rate of tick-borne encephalitis-virus in Ixodes-ricinus ticks. *Modern Acarology*, 1 and 2:B7–B10, 1991.

M. M. Davidson, H. Williams, and J. A. J. Macleod. Louping ill in man: A forgotten disease. *Journal of Infection*, 23(3):241–249, 1991.

O. Diekmann, J. A. P. Heesterbeek, and M. G. Roberts. The construction of next-generation matrices for compartmental epidemic models. *Journal of the Royal Society, Interface / the Royal Society*, 7(47):873–885, 2010. ISSN 1742-5689. doi: 10.1098/rsif.2009.0386.

A. D. M. Dobson. History and complexity in tick-host dynamics: discrepancies between 'real' and 'visible' tick populations. *Parasites & vectors*, 7(1):231, 2014. ISSN 1756-3305. doi: 10.1186/1756-3305-7-231.

A. D. M. Dobson and S. E. Randolph. Modelling the effects of recent changes in climate, host density and acaricide treatments on population dynamics of Ixodes ricinus in the UK. *Journal of Applied Ecology*, 48(4):1029–1037, 2011. ISSN 00218901. doi: 10.1111/j.1365-2664.2011.02004.x.

A. D. M. Dobson, T. J. R. Finnie, and S. E. Randolph. A modified matrix model to describe the seasonal population ecology of the European tick Ixodes ricinus. *Journal of Applied Ecology*, 48(4):1017–1028, 2011. ISSN 00218901. doi: 10.1111/j.1365-2664.2011.02003.x.

J. M. Dunn, S. Davis, A. Stacey, and M. A. Diuk-Wasser. A simple model for the establishment of tick-borne pathogens of Ixodes scapularis: A global sensitivity analysis of Ro. *Journal of Theoretical Biology*, 335:213–221, 2013. ISSN 00225193. doi: 10.1016/j.jtbi.2013.06.035.

D. A. Elston, R. Moss, T. Boulinier, C. Arrowsmith, and X. Lambin. Analysis of aggregation, a worked example: numbers of ticks on red grouse chicks. *Parasitology*, 122(Pt 5):563–569, 2001.

Environmental Systems Research Institute. ArcGIS, 2014.

L. Ferreri, M. Giacobini, P. Bajardi, L. Bertolotti, L. Bolzoni, V. Tagliapietra, A. Rizzoli, and R. Rosà. Pattern of Tick Aggregation on Mice: Larger Than Expected Distribution Tail Enhances the Spread of Tick-Borne Pathogens. *PLoS Computational Biology*, 10(11), 2014. ISSN 15537358. doi: 10.1371/journal.pcbi.1003931.

R. M. Fuller, G. M. Smith, J. M. Sanderson, R. A. Hill, and A. G. Thomson. The UK Land Cover Map 2000: Construction of a Parcel-Based Vector Map from Satellite Images. *The Cartographic Journal*, 39(1):15–25, 2002. ISSN 0008-7041. doi: 10.1179/caj.2002.39.1.15.

Game and Wildlife Conservation Trust Scotland. An Economic Study of Grouse Moors, 2010.

W. P. Gardiner, G. Gettinby, and J. S. Gray. Models based on weather for the development phases of the sheep tick, ixodes ricinus L. *Veterinary Parasitology*, 9(1):75–86, 1981. ISSN 03044017. doi: 10.1016/0304-4017(81)90009-1.

L. Gilbert. Altitudinal patterns of tick and host abundance: A potential role for climate change in regulating tick-borne diseases? *Oecologia*, 162(1):217–225, 2010. ISSN 00298549. doi: 10.1007/s00442-009-1430-x.

L. Gilbert. Can restoration of afforested peatland regulate pests and disease? *Journal of Applied Ecology*, 50(5):1226–1233, 2013. ISSN 00218901. doi: 10.1111/1365-2664.12141.

L. Gilbert. How landscapes shape Lyme borreliosis risk. *Ecology and Control of Vector Borne Diseases*, 5, 2016a.

L. Gilbert. Louping ill virus in the UK: a review of the hosts, transmission and ecological consequences of control. *Experimental and Applied Acarology*, 68(3): 363–374, 2016b. ISSN 15729702. doi: 10.1007/s10493-015-9952-x.

L. Gilbert, L. D. Jones, P. J. Hudson, E. A. Gould, and H. W. Reid. Role of small mammals in the persistence of Louping-ill virus: Field survey and tick co-feeding studies. *Medical and Veterinary Entomology*, 14(3):277–282, 2000. ISSN 0269283X. doi: 10.1046/j.1365-2915.2000.00236.x.

L. Gilbert, R. Norman, K. M. Laurenson, H. W. Reid, and P. J. Hudson. Disease persistence and apparent competition in a three-host community: An empirical and analytical study of large-scale, wild populations. *Journal of Animal Ecology*, 70(6):1053–1061, 2001. ISSN 00218790. doi: 10.1046/j.0021-8790.2001.00558.x.

L. Gilbert, L. D. Jones, M. K. Laurenson, E. A. Gould, H. W. Reid, and P. J. Hudson. Ticks need not bite their red grouse hosts to infect them with louping ill virus. *Proceedings. Biological sciences / The Royal Society*, 271 Suppl(Liv):S202–S205, 2004. ISSN 0962-8452. doi: 10.1098/rsbl.2003.0147.

L. Gilbert, G. Maffey, S. L. Ramsay, and A. J. Hester. The effect of deer Management on the abundance of Ixodes ricinus in Scotland. *Ecological Applications*, 22 (2):658–667, 2012.

L. Gilbert, J. Aungier, and J. L. Tomkins. Climate of origin affects tick (Ixodes ricinus) host-seeking behavior in response to temperature: Implications for resilience to climate change? *Ecology and Evolution*, 4(7):1186–1198, 2014. ISSN 20457758. doi: 10.1002/ece3.1014.

J. S. Gray. The fecundity of Ixodes ricinus (L.) (Acarina: Ixodidae) and the mortality of its developmental stages under field conditions. *Bulletin of Entomological Research*, 71:533–542, 1981.

J. S. Gray. Mating and behavioural diapause in Ixodes ricinus L. *Experimental & Applied Acarology*, 3(1):61–71, 1987. ISSN 01688162. doi: 10.1007/BF01200414.

J. S. Gray. The ecology of ticks transmitting Lyme borreliosis. *Experimental and Applied Acarology*, 22(5):249–258, 1998. ISSN 01688162. doi: 10.1023/A:1006070416135.

P. A. Hancock, R. Brackley, and S. C. F. Palmer. Modelling the effect of temperature variation on the seasonal dynamics of Ixodes ricinus tick populations. *International Journal for Parasitology*, 41(5):513–522, 2011. ISSN 00207519. doi: 10.1016/j.ijpara.2010.12.012.

K. Hanincová, S. M. Schäfer, S. Etti, H. S. Sewell, V. Taragelová, D. Ziak, M. Labuda, and K. Kurtenbach. Association of Borrelia afzelii with rodents in Europe. *Parasitology*, 126:11–20, 2003a.

K. Hanincová, V. Taragelová, J. Koci, S. M. Schäfer, R. Hails, A. J. Ullmann, J. Piesman, M. Labuda, and K. Kurtenbach. Association of Borrelia garinii and B. valaisiana with songbirds in Slovakia. *Applied and Environmental Microbiology*, 69(5):2825–2830, 2003b.

J. Hansen, M. Sato, and R. Ruedy. Perception of climate change. *Proc Natl Acad Sci U S A*, 109(37):E2415–23, 2012. ISSN 0027-8424. doi: 10.1073/pnas.1205276109.

S. Harris, P. Morris, S. Wray, and D. Yalden. A review of British mammals: population estimates and conservation status of British mammals other than cetaceans, 1995.

A. Harrison, S. Newey, L. Gilbert, D. T. Haydon, and S. Thirgood. Culling wildlife hosts to control disease: Mountain hares, red grouse and louping ill virus. *Journal of Applied Ecology*, 47(4):926–930, 2010. ISSN 00218901. doi: 10.1111/j.1365-2664.2010.01834.x.

N. A. Hartemink, S. E. Randolph, S. A. Davis, and J. A. P. Heesterbeek. The Basic Reproduction Number for Complex Disease Systems: Defining R 0 for Tick-Borne Infections. *The American Naturalist*, 171(6):743–754, 2008. ISSN 0003-0147. doi: 10.1086/587530.

M. Hartfield, K. A. J. White, and K. Kurtenbach. The role of deer in facilitating the spatial spread of the pathogen Borrelia burgdorferi. *Theoretical Ecology*, 4(1): 27–36, 2011. ISSN 18741738. doi: 10.1007/s12080-010-0072-2.

Health Protection Scotland. Lyme Disease, 2016. URL http://www.hps.scot.nhs.uk/giz/lymedisease.aspx.

V. Hönig, P. Š. Vec, O. Masař, and L. Grubhoffer. Tick-borne diseases risk model for South Bohemia (Czech Republic). *GIS Ostrava 2011*, 2011.

J. M. Howell, M. W. Ueti, G. H. Palmer, G. A. Scoles, and D. P. Knowles. Transovarial transmission efficiency of Babesia bovis tick stages acquired by Rhipicephalus (Boophilus) microplus during acute infection. *Journal of Clinical Microbiology*, 45(2):426–431, 2007. ISSN 00951137. doi: 10.1128/JCM.01757-06.

P. Hudson. *Grouse in Space and Time*. Game Conservancy Limited, 1992. ISBN 0 9500130 1 3.

P. J. Hudson, R. Norman, M. K. Laurenson, D. Newborn, M. Gaunt, L. Jones, H. Reid, E. Gould, R. Bowers, and A. Dobson. Persistence and transmission

of tick-borne viruses: Ixodes ricinus and louping-ill virus in red grouse populations. *Parasitology*, 111 Suppl(1995):S49–S58, 1995. ISSN 0031-1820. doi: 10.1017/S0031182000075818.

IPCC. Climate change 2007 : impacts, adaptation and vulnerability : Working Group II contribution to the Fourth Assessment Report of the IPCC Intergovernmental Panel on Climate Change, 2007. ISSN 15372537.

M. C. James. *The ecology, genetic diversity and epidemiology of Lyme borreliosis in Scotland*. Phd thesis, University of Aberdeen, 2010.

M. C. James, R. W. Furness, A. S. Bowman, K. J. Forbes, and L. Gilbert. The importance of passerine birds as tick hosts and in the transmission of Borrelia burgdorferi, the agent of Lyme disease: A case study from Scotland. *Ibis*, 153 (2):293–302, 2011. ISSN 00191019. doi: 10.1111/j.1474-919X.2011.01111.x.

M. C. James, A. S. Bowman, K. J. Forbes, F. Lewis, J. E. McLeod, and L. Gilbert. Environmental determinants of Ixodes ricinus ticks and the incidence of Borrelia burgdorferi sensu lato, the agent of Lyme borreliosis, in Scotland. *Parasitology*, 140(2):237–46, 2013. ISSN 1469-8161. doi: 10.1017/S003118201200145X.

M. C. James, L. Gilbert, A. S. Bowman, and K. J. Forbes. The Heterogeneity, Distribution, and Environmental Associations of Borrelia burgdorferi Sensu Lato, the Agent of Lyme Borreliosis, in Scotland. *Frontiers in public health*, 2:129, 2014. ISSN 2296-2565. doi: 10.3389/fpubh.2014.00129.

G. Jenkins, J. Murphy, D. Sexton, and J. Lowe. UK Climate Projections: Briefing report, 2009.

E. O. Jones, S. D. Webb, F. J. Ruiz-Fons, S. Albon, and L. Gilbert. The effect of landscape heterogeneity and host movement on a tick-borne pathogen. *Theoretical Ecology*, 4(4):435–448, 2011. ISSN 18741738. doi: 10.1007/s12080-010-0087-8.

L. D. Jones, C. R. Davies, G. M. Steele, and P. A. Nuttall. A novel mode of arbovirus transmission involving a nonviremic host. *Science (New York, N.Y.)*, 237(4816):775–777, 1987.

L. D. Jones, C. R. Davies, T. Williams, J. Gory, and P. A. Nuttall. Non-viraemic transmission of Thogoto virus: vector efficiency of Rhipicephalus appendiculatus and Amblyomma variegatum. *Transactions of the Royal Society of Tropical Medicine and Hygiene*, 84(6):846–848, 1990.

L. D. Jones, M. Gaunt, R. S. Hails, K. Laurenson, P. J. Hudson, H. Reid, P. Henbest, and E. A. Gould. Transmission of louping ill virus between infected and uninfected ticks co-feeding on mountain hares. *Medical and veterinary entomology*, 11(2):172–176, 1997. ISSN 0269-283X. doi: 10.1111/j.1365-2915.1997.tb00309.x.

S. Jore, H. Viljugrein, M. Hofshagen, H. Brun-Hansen, A. B. Kristoffersen, K. Nygård, E. Brun, P. Ottesen, B. K. Sævik, and B. Ytrehus. Multi-source analysis reveals latitudinal and altitudinal shifts in range of Ixodes ricinus at its northern distribution limit. *Parasites & vectors*, 4:84, 2011. ISSN 1756-3305. doi: 10.1186/1756-3305-4-84.

C. Kiffner, C. Lödige, M. Alings, T. Vor, and F. Rühe. Abundance estimation of Ixodes ticks (Acari: Ixodidae) on roe deer (Capreolus capreolus). *Experimental & applied acarology*, 52(1):73–84, 2010. ISSN 1572-9702. doi: 10.1007/s10493-010-9341-4.

C. Kiffner, T. Vor, P. Hagedorn, M. Niedrig, and F. Rühe. Factors affecting patterns of tick parasitism on forest rodents in tick-borne encephalitis risk areas, Germany. *Parasitology Research*, 108(2):323–335, 2011. ISSN 09320113. doi: 10.1007/s00436-010-2065-x.

A. D. Kirby, A. A. Smith, T. G. Benton, and P. J. Hudson. Rising burden of immature sheep ticks (Ixodes ricinus) on red grouse (Lagopus lagopus scoticus) chicks in the Scottish uplands. *Medical and Veterinary Entomology*, 18(1):67–70, 2004. doi: 10.1111/j.0269-283X.2004.0479.x.

K. Kurtenbach, D. Carey, A. N. Hoodless, P. A. Nuttall, and S. E. Randolph. Competence of pheasants as reservoirs for Lyme disease spirochetes. *Journal of medical entomology*, 35(1):77–81, 1998a.

K. Kurtenbach, M. Peacey, S. G. T. Rijpkema, A. N. Hoodless, P. A. Nuttall, and S. E. Randolph. Differential transmission of the genospecies of Borrelia burgdorferi sensu lato by game birds and small rodents in England. *Applied and Environmental Microbiology*, 64(4):1169–1174, 1998b.

M. Labuda and P. A. Nuttall. Tick-borne viruses. *Parasitology*, 129 Suppl:S221–S245, 2004. ISSN 0031-1820. doi: 10.1017/S0031182004005220.

M. Labuda, P. A. Nuttall, O. Kožuch, E. Elečková, T. Williams, E. Zuffová, and A. Sabó. Non-viraemic transmission of tick-borne encephalitis virus: a mechanism for arbovirus survival in nature. *Experientia*, 49(9):802–805, 1993.

M. K. Laurenson, R. Norman, H. W. Reid, I. Pow, D. Newborn, and P. J. Hudson. The role of lambs in louping-ill virus amplification. *Parasitology*, 120 (Pt 2: 97–104, 2000. ISSN 00311820. doi: 10.1017/S0031182099005302.

M. K. Laurenson, R. A. Norman, L. Gilbert, H. W. Reid, and P. J. Hudson. Identifying disease reservoirs in complex systems: Mountain hares as reservoirs of ticks and louping-ill virus, pathogens of red grouse. *Journal of Animal Ecology*, 72(1):177–185, 2003. ISSN 00218790. doi: 10.1046/j.1365-2656.2003.00688.x.

M. K. Laurenson, I. J. McKendrick, H. W. Reid, R. Challenor, and G. K. Mathewson. Prevalence, spatial distribution and the effect of control measures on louping-ill virus in the Forest of Bowland, Lancashire. *Epidemiology and infection*, 135(6): 963–973, 2007.

S. Li, L. Gilbert, P. A. Harrison, and M. D. A. Rounsevell. Modelling the seasonality of Lyme disease risk and the potential impacts of a warming climate within the heterogeneous landscapes of Scotland. *J Royal Soc Interface*, 2016. ISSN 1742-5689. doi: 10.1098/rsif.2016.0140.

E. Lindgren, L. Tälleklint, and T. Polfeldt. Impact of climatic change on the northern latitude limit and population density of the disease-transmitting European tick Ixodes ricinus. *Environmental Health Perspectives*, 108(2):119–123, 2000. ISSN 00916765. doi: 10.1289/ehp.00108119.

A. Lorenz, R. Dhingra, H. H. Chang, D. Bisanzio, Y. Liu, and J. V. Remais. Inter-model comparison of the landscape determinants of vector-borne disease: Implications for epidemiological and entomological risk modeling. *PLoS ONE*, 9(7), 2014. ISSN 19326203. doi: 10.1371/journal.pone.0103163.

G. Margos, St. A. Vollmer, N. H. Ogden, and D. Fish. Population genetics, taxonomy, phylogeny and evolution of Borrelia burgdorferi sensu lato. *Infection, Genetics and Evolution*, 11(7):1545–1563, 2011.

J. M. Medlock, K. M. Hansford, A. Bormane, M. Derdakova, A. Estrada-Peña, J. George, I. Golovljova, T. G. T. Jaenson, J. Jensen, P. M. Jensen, M. Kazimirova, J. Oteo, A. Papa, K. Pfister, O. Plantard, S. E. Randolph, A. Rizzoli, M. M. Santos-Silva, H. Sprong, L. Vial, G. Hendrickx, H. Zeller, and W. Van Bortel. Driving forces for changes in geographical distribution of Ixodes ricinus ticks in Europe. *Parasites & vectors*, 6(November 2012):1, 2013. ISSN 1756-3305. doi: 10.1186/1756-3305-6-1.

Met Office. UK climate - Historic station data, 2016. URL http://www.metoffice.gov.uk/public/weather/climate-historic/#?tab=climateHistoric.

Microsoft Corporation. Microsoft Excel 2007, 2007.

C. Millins, A. Magierecka, L. Gilbert, A. Edoff, A. Brereton, E. Kilbride, M. Denwood, R. Birtles, and R. Biek. An invasive mammal (the gray squirrel, Sciurus carolinensis) commonly hosts diverse and atypical genotypes of the zoonotic pathogen Borrelia burgdorferi sensu lato. *Applied and Environmental Microbiology*, 81(13):4236–4245, 2015. ISSN 0099-2240. doi: 10.1128/AEM.00109-15.

C. L. Millins, L. Gilbert, P. Johnson, M. C. James, E. Kilbride, R. Birtles, and R. Biek. Spatial and temporal heterogeneity in the abundance and distribution of Ixodes ricinus and Borrelia burgdorferi sensu lato in Scotland: implications for risk prediction (in review). *Parasites and Vectors*.

G. A. Mount and D. G. Haile. Computer simulation of population dynamics of the American dog tick (Acari: Ixodidae). *Journal of medical entomology*, 26(1): 60–76, 1989. ISSN 00222585.

A. Mysterud. Seasonal migration pattern and home range of roe deer (Capreolus capreolus) in an altitudinal gradient in southern Norway. *Journal of Zoology*, 247:479–486, 1999.

A. Mysterud. Contrasting emergence of Lyme disease across ecosystems. *Nature Communications*, 7, 2016. doi: 10.1038/ncomms11882.

A. Mysterud, I. Hatlegjerde, and O. Sørensen. Attachment site selection of life stages of Ixodes ricinus ticks on a main large host in Europe, the red deer (Cervus elaphus). *Parasites & Vectors*, 7(1):510, 2014. ISSN 1756-3305. doi: 10.1186/s13071-014-0510-x.

NASA. GISTEMP, 2012. URL http://data.giss.nasa.gov/gistemp/.

NASA/GISS. Climate Change: Vital Signs of the Planet: Global Temperature, 2016. URL http://climate.nasa.gov/vital-signs/global-temperature/.

NHS Choices. Tick-borne encephalitis, 2015. URL http://www.nhs.uk/conditions/tick-borne-encephalitis/Pages/Introduction.aspx.

R. Norman, R. G. Bowers, M. Begon, and P. J. Hudson. Persistence of tick-borne virus in the presence of multiple host species: tick reservoirs and parasite mediated competition. *Journal of theoretical biology*, 200(1):111–118, 1999. ISSN 0022-5193. doi: 10.1006/jtbi.1999.0982.

R. Norman, D. Ross, M. K. Laurenson, and P. J. Hudson. The role of non-viraemic transmission on the persistence and dynamics of a tick borne virus - Louping ill in red grouse (Lagopus lagopus scoticus) and mountain hares (Lepus timidus). *Journal of Mathematical Biology*, 48(2):119–134, 2004. ISSN 03036812. doi: 10.1007/s00285-002-0183-5.

R. A. Norman, A. J. Worton, and L. Gilbert. Past and future perspectives on mathematical models of tick-borne pathogens. *Parasitology*, pages 1–10, 2015. ISSN 1469-8161. doi: 10.1017/S0031182015001523.

Nottinghamshire Wildlife Trust. Animal Facts, 2016. URL http://www.nottinghamshirewildlife.org/animal-facts/.

P. A. Nuttall and L. D. Jones. Non-viraemic tick-borne virus transmission: mechanism and significance. *Modern Acarology*, pages 3–6, 1991.

N. H. Ogden, L. R. Lindsay, G. Beauchamp, D. Charron, A. Maarouf, C. J. O 'callaghan, D. Waltner-Toews, and I. K. Barker. Investigation of Relationships Between Temperature and Developmental Rates of Tick Ixodes scapularis (Acari: Ixodidae) in the Laboratory and Field. *J. Med. Entomol*, 41(4):622–633, 2004. ISSN 0022-2585. doi: 10.1603/0022-2585-41.4.622.

N. H. Ogden, M. Bigras-Poulin, C. J. O'Callaghan, I. K. Barker, L. R. Lindsay, A. Maarouf, K. E. Smoyer-Tomic, D. Waltner-Toews, and D. Charron. A dynamic population model to investigate effects of climate on geographic range and seasonality of the tick Ixodes scapularis. *Int J Parasitol*, 35(4):375–389, 2005. doi: 10.1016/j.ijpara.2004.12.013.

N. H. Ogden, M. Bigras-Poulin, C. J. O'callaghan, I. K. Barker, K. Kurtenbach, L. R. Lindsay, and D. F. Charron. Vector seasonality, host infection dynamics and fitness of pathogens transmitted by the tick Ixodes scapularis. *Parasitology*, 134(Pt 2):209–227, 2007. ISSN 0031-1820. doi: 10.1017/S0031182006001417.

N. H. Ogden, L. R. Lindsay, and P. A. Leighton. Predicting the rate of invasion of the agent of Lyme disease Borrelia burgdorferi. *Journal of Applied Ecology*, 50(2): 510–518, 2013. ISSN 00218901. doi: 10.1111/1365-2664.12050.

K. J. Park, P. A. Robertson, S. T. Campbell, R. Foster, Z. M. Russell, D. Newborn, and P. J. Hudson. The role of invertebrates in the diet, growth and survival of red grouse (Lagopus lagopus scoticus) chicks. *Journal of Zoology*, 254(2):137–145, 2001.

F. J. Pérez-Barbería, R. J. Hooper, and I. J. Gordon. Long-term density-dependent changes in habitat selection in red deer (Cervus elaphus). *Oecologia*, 173(3): 837–847, 2013. ISSN 00298549. doi: 10.1007/s00442-013-2686-8.

S. Perkins. *Transmission dynamics of tick-borne diseases associated with small mammals*. Phd thesis, University of Stirling, 2003.

J. L. Perret, E. Guigoz, O. Rais, and L. Gern. Influence of saturation deficit and temperature on Ixodes ricinus tick questing activity in a Lyme borreliosis-endemic area (Switzerland). *Parasitology research*, 86(7):554–557, 2000.

B. Pisanu, J. L. Chapuis, A. Dozières, F. Basset, V. Poux, and G. Vourc'h. High prevalence of Borrelia burgdorferi s.l. in the European red squirrel Sciurus vulgaris in France. *Ticks and Tick-borne Diseases*, 5(1):1–6, 2014.

T C Porco. A mathematical model of the ecology of Lyme disease. *IMA journal of mathematics applied in medicine and biology*, 16(3):261–296, 1999. ISSN 0265-0746. doi: 10.1093/imammb/16.3.261.

R. Porter, R. Norman, and L. Gilbert. Controlling tick-borne diseases through domestic animal management: A theoretical approach. *Theoretical Ecology*, 4(3): 321–339, 2011. ISSN 18741738. doi: 10.1007/s12080-010-0080-2.

R. Porter, R. A. Norman, and L. Gilbert. An alternative to killing? Treatment of reservoir hosts to control a vector and pathogen in a susceptible species. *Parasitology*, 140(2):247–257, 2013a. doi: http://dx.doi.org/10.1017/S0031182012001400.

R. Porter, R. A. Norman, and L. Gilbert. A model to test how ticks and louping ill virus can be controlled by treating red grouse with acaricide. *Medical and Veterinary Entomology*, 27(3):237–246, 2013b. ISSN 0269283X. doi: 10.1111/j.1365-2915.2012.01047.x.

R. B. Porter. *Mathematical models of a tick borne disease in a British game bird with potential management strategies*. PhD thesis, University of Stirling, 2011.

Public Health England. Lyme borreliosis epidemiology and surveillance: data analysis for laboratory-confirmed cases, 2013. URL https://www.gov.uk/government/publications/lyme-borreliosis-epidemiology/lyme-borreliosis-epidemiology-and-surveillance.

S. E. Randolph. Tick ecology: processes and patterns behind the epidemiological risk posed by ixodid ticks as vectors. *Parasitology*, 129(Supplement S1):S37–S65, 2004. ISSN 1469-8161. doi: 10.1017/S0031182004004925.

S. E. Randolph. Dynamics of tick-borne disease systems: minor role of recent climate change. *Revue scientifique et technique (International Office of Epizootics)*, 27(2):367–381, 2008. ISSN 0253-1933.

S. E. Randolph and D. J. Rogers. A generic population model for the African tick Rhipicephalus appendiculatus. *Parasitology*, 115(03):265–279, 1997. ISSN 1469-8161. doi: 10.1017/S0031182097001315.

S. E. Randolph, R. M. Green, A. N. Hoodless, and M. F. Peacey. An empirical quantitative framework for the seasonal population dynamics of the tick Ixodes ricinus. *International Journal for Parasitology*, 32(8):979–989, 2002. ISSN 00207519. doi: 10.1016/S0020-7519(02)00030-9.

H. W. Reid. Experimental infection of red grouse with louping-ill virus (Flavivirus group). I. The viraemia and antibody response. *Journal of Comparative Pathology*, 85(2):223–229, 1975.

A. Rizzoli, R. Rosa, B. Mantelli, E. Pecchioli, H. Hauffe, V. Tagliapietra, T. Beninati, M. Neteler, and C. Genchi. Ixodes ricinus, transmitted diseases and reservoirs. *Parassitologia*, 46(1-2):119–122, 2004. ISSN 0048-2951.

R. Rosà and A. Pugliese. Effects of tick population dynamics and host densities on the persistence of tick-borne infections. *Mathematical Biosciences*, 208(1): 216–240, 2007. ISSN 00255564. doi: 10.1016/j.mbs.2006.10.002.

R. Rosà, A. Pugliese, R. Norman, and P. J. Hudson. Thresholds for disease persistence in models for tick-borne infections including non-viraemic transmission, extended feeding and tick aggregation. *Journal of Theoretical Biology*, 224(3): 359–376, 2003. ISSN 00225193. doi: 10.1016/S0022-5193(03)00173-5.

RSPB. Red grouse, a. URL https://www.rspb.org.uk/discoverandenjoynature/discoverandlearn/birdguide/name/r/redgrouse/.

RSPB. Birds by name, b. URL http://www.rspb.org.uk/discoverandenjoynature/discoverandlearn/birdguide/name/.

F. Ruiz-Fons and L. Gilbert. The role of deer as vehicles to move ticks, Ixodes ricinus, between contrasting habitats. *International Journal for Parasitology*, 40(9): 1013–1020, 2010. ISSN 00207519. doi: 10.1016/j.ijpara.2010.02.006.

A. Schwarz, W. A. Maier, T. Kistemann, and H. Kampen. Analysis of the distribution of the tick Ixodes ricinus L. (Acari: Ixodidae) in a nature reserve of western Germany using Geographic Information Systems. *International Journal*

of Hygiene and Environmental Health, 212(1):87–96, 2009. ISSN 14384639. doi: 10.1016/j.ijheh.2007.12.001.

J. A. Sherratt. Multiannual Cycles in Field Vole Populations: Spatial Data and Spatiotemporal Models, 2008. URL http://www.macs.hw.ac.uk/{~}jas/talks/maryland{_}oct08{_}biology.pdf.

V. Tagliapietra, R. Rosà, D. Arnoldi, F. Cagnacci, G. Capelli, F. Montarsi, H. C. Hauffe, and A. Rizzoli. Saturation deficit and deer density affect questing activity and local abundance of Ixodes ricinus (Acari, Ixodidae) in Italy. *Veterinary Parasitology*, 183(1-2):114–124, 2011. ISSN 03044017. doi: 10.1016/j.vetpar.2011.07.022.

The Mammal Society. Full Species Hub, 2016. URL http://www.mammal.org.uk/species-hub/full-species-hub/full-species-hub-list/.

The Scottish Government. Economic Report on Scottish Agriculture, 2015.

The Wildlife Trusts. Birds, 2016a. URL http://www.wildlifetrusts.org/wildlife/species-explorer/birds.

The Wildlife Trusts. Common Shrew, 2016b. URL http://www.wildlifetrusts.org/species/common-shrew.

K. Tilly, P. A. Rosa, and P. E. Stewart. Biology of Infection with Borrelia burgdorferi. *Infectious Disease Clinics of North America*, 22(2):217–234, 2008. ISSN 08915520. doi: 10.1016/j.idc.2007.12.013.

J. L. Tomkins, J. Aungier, W. Hazel, and L. Gilbert. Towards an Evolutionary Understanding of Questing Behaviour in the Tick Ixodes ricinus. *PLoS ONE*, 9(10), 2014. doi: 10.1371/journal.pone.0110028.

E. J. Watts, S. C. F. Palmer, A. S. Bowman, R. J. Irvine, A. Smith, and J. M. J. Travis. The effect of host movement on viral transmission dynamics in a vector-borne disease system. *Parasitology*, 136(10):1221–1234, 2009. ISSN 0031-1820. doi: 10.1017/S0031182009990424.

A. Wightman and R. Tingay. The Intensification of Grouse Moor Management in Scotland, 2015.

M. L. Wilson and A. Spielman. Seasonal activity of immature Ixodes dammini (Acari: Ixodidae). *Journal of Medical Entomology*, 26:408–414, 1985.

Wolfram Mathworld. Negative Binomial Distribution, 2016. URL http://mathworld.wolfram.com/NegativeBinomialDistribution.html.

Wolfram Research Inc. Mathematica, 2013.

M. E. Woolhouse, C. Dye, J. F. Etard, T. Smith, J. D. Charlwood, G. P. Garnett, P. Hagan, J. L. Hii, P. D. Ndhlovu, R. J. Quinnell, C. H. Watts, S. K. Chandiwana, and R. M. Anderson. Heterogeneities in the transmission of infectious agents: implications for the design of control programs. *Proc Natl Acad Sci U S A*, 94(1): 338–342, 1997. ISSN 0027-8424 (Print); 0027-8424 (Linking). doi: 10.1073/pnas.94.1.338.

S. D. Wright and S. W. Nielsen. Experimental infection of the white-footed mouse with Borrelia burgdorferi. *American Journal of Veterinary Research*, 51(12): 1980–1987, 1990. ISSN 00029645.

X. Wu, V. R. Duvvuri, Y. Lou, N. H. Ogden, Y. Pelcat, and J. Wu. Developing a temperature-driven map of the basic reproductive number of the emerging tick vector of Lyme disease Ixodes scapularis in Canada. *Journal of Theoretical Biology*, 319:50–61, 2013. ISSN 00225193. doi: 10.1016/j.jtbi.2012.11.014.

P. Zeman. Objective assessment of risk maps of tick-borne encephalitis and Lyme borreliosis based on spatial patterns of located cases. *International Journal of Epidemiology*, 26(5):1121–1130, 1997. ISSN 03005771. doi: 10.1093/ije/26.5.1121.

P. Zeman, P. Pazdiora, and C. Benes. Spatio-temporal variation of tick-borne encephalitis (TBE) incidence in the Czech Republic: Is the current explanation of the disease's rise satisfactory? *Ticks and Tick-borne Diseases*, 1(3):129–140, 2010. ISSN 1877959X. doi: 10.1016/j.ttbdis.2010.05.003.

Y. Zhang and X. Zhao. A Reaction-Diffusion Lyme Disease Model with Seasonality. *SIAM Journal on Applied Mathematics*, 73(6):2077–2099, 2013. ISSN 0036-1399. doi: 10.1137/120875454.

All links correct as of the 22nd of September 2016.